



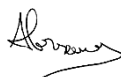
Copernicus DEMs Quality Assessment Summary

Author(s):



Kévin GROSS

VisioTerra Task 5 Mission Expert



Axel CORSEaux

VisioTerra Engineer

Approval:



Serge RIAZANOFF

VisioTerra Task 5 Lead

Accepted:

Clément ALBINET

ESA Technical Officer

AMENDMENT RECORD SHEET

The Amendment Record Sheet below records the history and issue status of this document.

ISSUE	DATE	REASON
1.0	22 December 2020	First issue with sections 1, 2, 3 and 4
1.1	19 May 2021	Quality assessment from ICESat-2 LiDAR
1.2	29 July 2021	Quality assessment from GEDI LiDAR

TABLE OF CONTENTS

1. INTRODUCTION.....	8
1.1 Reference document.....	8
1.1.1 Quality assessment	8
1.1.2 TerraSAR-X and TanDEM-X	8
1.1.3 Copernicus DEMs.....	9
1.1.4 ICESat-1	10
1.1.5 ICESat-2	11
1.1.6 GEDI	12
1.1.7 Vertical reference systems	13
1.1.8 Geocoding and orthorectification.....	13
1.1.9 Other studies	13
1.2 Glossary	15
1.3 Definitions.....	16
2. EXECUTIVE SUMMARY	18
2.1 Maturity Matrix.....	18
2.2 Summary of quality assessment	19
3. PRODUCT ASSESSMENT OVERVIEW	21
3.1 Overview of Copernicus DEMs generation and products	21
3.1.1 Short history of Copernicus DEMs	21
3.1.2 The TanDEM-X constellation.....	21
3.1.3 Produced by TanDEM-X constellation.....	22
3.1.4 Becoming an element of Copernicus programme	23
3.1.5 Formats of Copernicus DEMs	23
3.1.6 Copernicus DEMs product generation.....	24
3.2 EDAP standard tables	25
3.2.1 Product Information	25
3.2.2 Product Generation.....	27
3.2.3 Ancillary Information	29
3.2.4 Uncertainty Characterisation	29
3.2.5 Validation	30
4. DETAILED ASSESSMENT	34
4.1 DEMs intercomparison – Qualitative assessment	34
4.1.1 Global views	35
4.1.2 Lake Garda (Italy)	36
4.2 Elevation assessment from ICESat-1 / GLAS LiDAR – Quantitative assessment	37
4.2.1 History of ICESat-1	37
4.2.2 Technical specifications.....	37
4.2.3 Assessment of ICESat-1 / GLAS measurements reliability.....	39

4.2.3.1	GLAH14 Product.....	39
4.2.3.1.1	Product organisation	39
4.2.3.1.2	Data filtering	39
4.2.3.2	Sampling of ICESat-1 / GLAS data	40
4.2.3.3	Collocated measurements on the same orbit	40
4.2.3.3.1	Scope.....	40
4.2.3.3.2	Method	40
4.2.3.3.3	Results.....	43
4.2.3.4	Geographical distribution of ICESat-1 products	44
4.2.4	Assessment of Copernicus DEM EEA-10 from ICESat-1 / GLAS data.....	45
4.2.4.1	Spatial extent	45
4.2.4.2	Method and notations	45
4.2.4.2.1	Conversion from TOPEX / Poseidon to WGS84	45
4.2.4.2.2	From ICESat-1 longitude and latitude to the Copernicus DEM EEA-10 tile	47
4.2.4.2.3	From EGM2008 to WGS84	47
4.2.4.2.4	Computing the height difference.....	48
4.2.4.2.5	Overall algorithm.....	49
4.2.4.3	Results	50
4.2.4.4	Typical sources of elevation errors	51
4.2.4.4.1	ICESat-1 elevation errors	51
4.2.4.4.2	Geomorphological and land use / land cover context causing elevation errors	52
4.2.5	Assessment of Copernicus DEM GLO-30 from ICESat-1 / GLAS data	57
4.2.5.1	Spatial extent	57
4.2.5.2	Method and notations	57
4.2.5.3	Results	58
4.2.6	Assessment of Copernicus DEM GLO-90 from ICESat-1 / GLAS data	59
4.2.6.1	Spatial extent	59
4.2.6.2	Method and notations	59
4.2.6.3	Results	60
4.3	Elevation assessment from ICESat-2 / ATLAS LiDAR – Quantitative assessment.....	61
4.3.1	History of ICESat-2.....	61
4.3.2	Technical specifications.....	61
4.3.3	Assessment of ICESat-2 / ATLAS measurements reliability	63
4.3.3.1	ATL08 product	63
4.3.3.1.1	Product organisation	63
4.3.3.1.2	Data filtering.....	64
4.3.3.2	Sampling of ICESat-2 / ATLAS data.....	65
4.3.3.3	Collocated measurements on the same orbit	65
4.3.3.3.1	Scope.....	65
4.3.3.3.2	Method.....	65
4.3.3.3.3	Results.....	68
4.3.3.4	Geographical distribution of ICESat-2 products	72
4.3.4	Assessment of Copernicus DEM EEA-10 from ICESat-2 / ATLAS data.....	72
4.3.4.1	Method and notations	72
4.3.4.1.1	Summary of the methods used.....	72
4.3.4.1.2	Computing the height difference.....	73
4.3.4.2	Overall algorithm.....	74
4.3.4.3	Results	75
4.3.4.4	Typical sources of elevation errors	76
4.3.4.4.1	ICESat-2 elevation errors	76
4.3.4.4.2	Geomorphological and land use / land cover context causing elevation errors	77
4.3.5	Assessment of Copernicus DEM GLO-30 from ICESat-2 / ATLAS data	83
4.3.5.1	Spatial extent	83
4.3.5.2	Method and notations	83
4.3.5.3	Results	84
4.3.6	Assessment of Copernicus DEM GLO-90 from ICESat-2 / ATLAS data	86
4.3.6.1	Spatial extent	86
4.3.6.2	Method and notations	86
4.3.6.3	Results	87
4.4	Elevation assessment from GEDI LiDAR – Quantitative assessment.....	89
4.4.1	History of GEDI.....	89
4.4.2	Technical specifications.....	90
4.4.3	Assessment of GEDI measurement reliability	91

4.4.3.1	GEDI02_A product.....	91
4.4.3.1.1	Product organisation	91
4.4.3.1.2	Data filtering	94
4.4.3.2	Sampling of GEDI data	95
4.4.3.3	Height comparison with ICESat-1 and ICESat-2	96
4.4.3.3.1	Scope.....	96
4.4.3.3.2	Method	96
4.4.3.4	Geographical distribution of GEDI products	98
4.4.4	Assessment of Copernicus DEM EEA-10 from GEDI data	99
4.4.4.1	Method and notations	99
4.4.4.1.1	Summary of the methods used.....	99
4.4.4.1.2	Computing the height difference.....	100
4.4.4.2	Overall algorithm.....	101
4.4.4.3	Results	102
4.4.4.4	Typical sources of elevation errors	103
4.4.4.4.1	GEDI elevation errors.....	103
4.4.4.4.2	Geomorphological and land use / land cover context causing elevation errors	104
4.4.5	Assessment of Copernicus DEM GLO-30 from GEDI data	107
4.4.5.1	Spatial extent	107
4.4.5.2	Method and notations	107
4.4.5.3	Results	108
4.4.6	Assessment of Copernicus DEM GLO-90 from GEDI data.....	110
4.4.6.1	Spatial extent	110
4.4.6.2	Method and notations	110
4.4.6.3	Results	111
5.	CONCLUSIONS.....	113
5.1	Mission / product assessment overview	113
5.1.1	Comparing the “FAIR”	113
5.1.2	Features of Copernicus DEMs compared to other global DEMs	113
5.2	Detailed assessment.....	114
5.2.1	Intercomparison of DEMS (qualitative assessment)	114
5.2.2	Copernicus DEMs height comparison with ICESat-1, ICESat-2 and GEDI (quantitative assessment)	114
5.2.2.1	ICESat-1, ICESat-2 and GEDI: technical specifications.....	115
5.2.2.2	Results of the EEA-10, GLO-30 and GLO-90 quantitative assessments	116
5.2.2.3	Comparison of EEA-10, GLO-30 and GLO-90 over Europe	118
5.2.2.4	Comparison of GLO-30 vs. SRTM, ASTER-GDEM and ALOS World 3D	119

LIST OF FIGURES

Figure 1	- View of the close satellite formation (left) and the helix satellite formation (right).	22
Figure 2	- Data acquisition configurations: Pursuit monostatic (left), bistatic (middle), and alternating bistatic (right).	22
Figure 3	- Copernicus DEMs Generation Process Chart (See 1.1.3).	24
Figure 4	- Global views of the difference between “ALOS World 3D” and “Copernicus DEM GLO-30”.	35
Figure 5	- Anomaly of ALOS World 3D above Lake Garda (Italy).	36
Figure 6	- ICESat-1 3D representation. (https://www.csr.utexas.edu/glas/)	37
Figure 7	- GLAS instrument characteristics. (https://earth.esa.int/workshops/spaceandtheartic09/Zwally.pdf)	38
Figure 8	- Root of a GLAH14 product.	39
Figure 9	- Ground tracks considered for the ICESat-1 reliability study.	41
Figure 10	- ICESat-1 reliability study, interpolated heights over ground track 85.	43
Figure 11	- ICESat-1 reliability study, interpolated heights over ground track 351.	43
Figure 12	- Distribution of the 642 ICESat-1 products.	44
Figure 13	- Copernicus DEM EEA-10 coverage map.	45
Figure 14	- Latitude difference between WGS84 and TOPEX/Poseidon ellipsoids (in centimetres).	46
Figure 15	- EGM2008 map with reference to WGS84.	48
Figure 16	- Summary of the Copernicus DEM EEA-10 assessment method.	49
Figure 17	- Error histogram of the (Copernicus DEM EEA-10 – ICESat-1) comparison.	50
Figure 18	- ICESat-1 cloud outliers over France.	51
Figure 19	- EEA-10 - ICESat-1 height differences - Case of Życiński Las near Żytina (Poland).	52
Figure 20	- EEA-10 - ICESat-1 height differences – Case of Forêt de la Matte near Matemale (France).	53
Figure 21	- EEA-10 - ICESat-1 height differences – Evolution of the studied deforestation over two acquisition dates.	53
Figure 22	- EEA-10 - ICESat-1 height differences - Case of the Alps near the Breithorn (Switzerland).	54
Figure 23	- EEA-10 - ICESat-1 height differences - Case of the Alps near Andalo Valtellino (Italy).	54
Figure 24	- EEA-10 - ICESat-1 height differences - Case of Carrière de Marche-les-Dames near Namèche (Belgium).	55
Figure 25	- EEA-10 - ICESat-1 height differences – Evolution of the studied excavation over two acquisition dates.	55
Figure 26	- EEA-10 - ICESat-1 height differences - Case of an industrial building in Grenzach-Wyhlen (Germany).	56
Figure 27	- EEA-10 - ICESat-1 height differences – Demolition of an industrial building over two acquisition dates.	56
Figure 28	- Copernicus DEM GLO-30 coverage map.	57
Figure 29	- Error histogram of the (Copernicus DEM GLO-30 – ICESat-1) comparison.	58
Figure 30	- Copernicus DEM GLO-90 coverage map.	59
Figure 31	- Error histogram of the (Copernicus DEM GLO-90 – ICESat-1) comparison.	60
Figure 32	- 3D representation of ICESat-2. (https://svs.gsfc.nasa.gov/cgi-bin/details.cgi?aid=11712)	61
Figure 33	- Ground tracks of ICESat-2. (extracted from https://doi.org/10.5194/tc-2020-330)	62
Figure 34	- Root group of ATL08 products.	63
Figure 35	- Orientations of the ATLAS instrument, impact on the laser beams ground tracks labelling. (extracted from RD-22)	63
Figure 36	- Pairs of profiles considered for the ICESat-2 reliability study.	67
Figure 37	- Height difference statistics for every profile pair.	71
Figure 38	- Distribution of the 119 068 ATL08 products.	72
Figure 39	- Summary of the Copernicus DEM EEA-10 assessment method using ICESat-2 ATL08 as a vertical reference.	74
Figure 40	- Error histogram of the (Copernicus DEM EEA-10 – ICESat-2) study, comparison with previous results using ICESat-1 as vertical reference.	76
Figure 41	- Incorrect photon labelling in tropical forest (Brazil). (extracted from RD-26)	77
Figure 42	- EEA-10 - ICESat-2 height differences – Case of Bois de la Mare Chanteuil near Galluis (France).	78
Figure 43	- Reference picture of Bois de la Mare Chanteuil (France).	79
Figure 44	- EEA-10 - ICESat-2 height differences - Case of the vines of Léognan (France).	80

Figure 45	- EEA-10 - ICESat-2 height differences - Case of the Alps, near the Mont Blanc (Italy).	80
Figure 46	- EEA-10 - ICESat-2 height differences – Varying snow cover – Case of the Alps, near the Mont Blanc (Italy).	81
Figure 47	- EEA-10 - ICESat-2 height differences - Case of a building construction in Bergen op Zoom (Netherlands).	81
Figure 48	- EEA-10 - ICESat-2 height differences – Field before building construction in Bergen op Zoom (Netherlands).	82
Figure 49	- Error histogram of the (Copernicus DEM GLO-30 – ICESat-2) study, comparison with previous results using ICESat-1 as vertical reference.	85
Figure 50	- Error histogram of the (Copernicus DEM GLO-90 – ICESat-2) study, comparison with previous results using ICESat-1 as vertical reference.	88
Figure 51	- GEDI onboard the ISS. (https://gedi.umd.edu/instrument/instrument-overview/)	89
Figure 52	- GEDI lasers, beams and ground tracks. (https://gedi.umd.edu/instrument/specifications/)	90
Figure 53	- GEDI height profiles over Luxembourg (near Diekirch, 2019.04.18).	90
Figure 54	- Root group of GEDI02_A products.	91
Figure 55	- GEDI return waveform and footprint.	92
Figure 56	- Histogram of the difference between GEDI lowest mode and highest return, filtered using surface_flag.	93
Figure 57	- GEDI02_A BEAM0000 height filtering over Brazil (2019.04.19).	94
Figure 58	- Histogram of the difference between GEDI lowest mode and highest return, filtered using quality_flag and degrade_flag.	95
Figure 59	- Intersection of GEDI and ICESat-1 / ICESat-2 height profiles over Salar de Uyuni.	96
Figure 60	- Intersections between GEDI and ICESat-1 over Salar de Uyuni (left), outside of Salar de Uyuni (right).	97
Figure 61	- Intersections between GEDI and ICESat-2 over Salar de Uyuni.	97
Figure 62	- Intersections between GEDI and ICESat-2 around Salar de Uyuni.	98
Figure 63	- Distribution of the 1628 used GEDI02_A products.	99
Figure 64	- Summary of the Copernicus DEM EEA-10 assessment method using GEDI as a vertical reference.	101
Figure 65	- Error histogram of the (Copernicus DEM EEA-10 - GEDI) study, comparison with previous results using ICESat-1 and ICESat-2 as vertical references.	103
Figure 66	- EEA-10 - GEDI height differences – Case of dense forests near Chendrea (Romania).	104
Figure 67	- EEA-10 - GEDI height differences – Case of sparse canopy near fields of Centro Tre Denari (Italy).	105
Figure 68	- EEA-10 - GEDI height differences – Case of the Tagebau Nochten mine (Germany).	105
Figure 69	- EEA-10 - GEDI height differences – Evolution of the Tagebau Nochten mine (Germany).	106
Figure 70	- EEA-10 - GEDI height differences – Case of an industrial building in Striesa (Germany).	106
Figure 71	- Error histogram of the (Copernicus DEM GLO-30 - GEDI) study, comparison with previous results using ICESat-1 and ICESat-2 as vertical references.	109
Figure 72	- Error histogram of the (Copernicus DEM GLO-90 - GEDI) study, comparison with previous results using ICESat-1 and ICESat-2 as vertical references.	112
Figure 73	- Copernicus DEM EEA-10 height error histogram from -17 m to 17 m (left) – from -3 m to 3 m (right).	117
Figure 74	- Copernicus DEM GLO-30 height error histogram from -17 m to 17 m (left) – from -3 m to 3 m (right).	117
Figure 75	- Copernicus DEM GLO-90 height error histogram from -17 m to 17 m (left) – from -3 m to 3 m (right).	117
Figure 76	- Copernicus DEM EEA-10, GLO-30 and GLO-90 height errors histogram over Europe.	119
Figure 77	- Histogram of height differences between ICESat-1/ICESat-2 and global DEMs (LE95).	120

LIST OF TABLES

Table 1	- Copernicus DEMs Product Quality Evaluation Matrix.	18
Table 2	- Main features of TerraSAR-X and TanDEM-X.	21
Table 3	- Copernicus DEMs available formats.	23
Table 4	- GLAS instrument technical specifications.	38
Table 5	- Values of the sat_corr_flg in the GLAH14 product.	39
Table 6	- ICESat-1 GLAH14 ground tracks and products studied.	42
Table 7	- Statistics regarding standard deviation of interpolated heights at each latitude.	44
Table 8	- Difference between TOPEX/Poseidon and WGS84 ellipsoids.	46
Table 9	- Statistics of the (Copernicus DEM EEA-10 – ICESat-1) comparison.	50
Table 10	- Statistics of the (Copernicus DEM GLO-30 – ICESat-1) comparison.	58
Table 11	- Statistics of the (Copernicus DEM GLO-90 – ICESat-1) comparison.	60
Table 12	- Technical specifications of ICESat-1 and ICESat-2.	62
Table 13	- ATL08 sc_orient variable values.	64
Table 14	- ATLAS laser beam labelling.	64
Table 15	- ATL08 product terrain heights validity conditions.	65
Table 16	- ATL08 product canopy heights validity conditions.	65
Table 17	- ICESat-2 ATL08 profile pairs origin.	68
Table 18	- Statistics of the (Copernicus DEM EEA-10 - ICESat-2) comparison.	75
Table 19	- Statistics of the (Copernicus DEM GLO-30 – ICESat-2) comparison.	84
Table 20	- Statistics of the (Copernicus DEM GLO-90 – ICESat-2) comparison.	87
Table 21	- GEDI technical specifications.	91
Table 22	- GEDI02_A product height validity conditions.	95
Table 23	- Error statistics of the (Copernicus DEM EEA-10 - GEDI) study, comparison with previous results using ICESat-1 and ICESat-2 as vertical references.	102
Table 24	- Error statistics of the (Copernicus DEM GLO-30 - GEDI) study, comparison with previous results using ICESat-1 and ICESat-2 as vertical references.	108
Table 25	- Error statistics of the (Copernicus DEM GLO-90 - GEDI) study, comparison with previous results using ICESat-1 and ICESat-2 as vertical references.	111
Table 26	- Comparison of the detailed FAIR notations.	113
Table 27	- DEM features.	113
Table 28	- Technical specifications of ICESat-1, ICESat-2 and GEDI missions.	115
Table 29	- Copernicus DEM EEA-10, GLO-30 and GLO-90 LE95 height errors statistics.	116
Table 30	- Copernicus DEM EEA-10, GLO-30 and GLO-90 height errors statistics over Europe.	118
Table 31	- Quantitative assessment of GLO-30 compared to other global DEMs.	119

1. INTRODUCTION

1.1 Reference document

The following is a list of reference documents with a direct bearing on the content of this Technical Note. Where referenced in the text, these are identified as [RD-n], where 'n' is the number in the list below:

1.1.1 Quality assessment

- RD-1.** EDAP.REP.001 *EDAP Quality Assessment Guidelines*
issue 1.3, 16 October 2019
NPL
[..\management\20191120_Piro_EDAP.REP.001_1.3 - Mission Quality Assessment Guidelines.pdf](#)
- RD-2.** QA4ECV PUM *QA4ECV Documentation Guidance: Product User Manual*
Version 1.0, May 2017
QA4ECV
<http://www.qa4ecv.eu/sites/default/files/QA4ECV%20PUM%20Guidance.pdf>
[..\reference_documents\20170500_QA4ECV_Documentation_Guidance_Product_User_Manual.pdf](#)
- RD-3.** QA4ECV ATBD *QA4ECV Product Documentation Guidance: Algorithm Theoretical Basis Document*
Version 1.0, May 2017
QA4ECV
<http://www.qa4ecv.eu/sites/default/files/QA4ECV%20ATBD%20Guidance.pdf>
[..\reference_documents\20170500_QA4ECV_Product_Documentation_Guidance_Algorithm_Theoretical_Basis_Document.pdf](#)
- RD-4.** JCGM 100:2008 *Evaluation of measurement data – Guide to the expression of uncertainty in measurement*
First edition, September 2008
Joint Committee for Guides in Metrology
https://www.bipm.org/documents/20126/2071204/JCGM_100_2008_E.pdf
[..\reference_documents\20080900_JCGM_Evaluation_of_measurement_data_Guide_to_the_expression_of_uncertainty_in_measurement.pdf](#)

1.1.2 TerraSAR-X and TanDEM-X

- RD-5.** Krieger, 2012 *TanDEM-X: A radar interferometer with two formation flying satellites*
63rd International Astronautical Congress, Naples, Italy, International Astronautical Federation.
<https://doi.org/10.1016/j.actaastro.2013.03.008>
[..\reference_documents\20130406_Krieger_TanDEM-X_A_radar_Interferometer_with_two_formation-flying_satellites.pdf](#)

- RD-6.** Bachmann & al., 2009 *TerraSAR-X Antenna Calibration and Monitoring Based on a Precise Antenna Model*
IEEE Transactions on Geoscience and Remote Sensing, vol. 48, no. 2, pp. 690-701, Feb. 2010
<https://ieeexplore.ieee.org/document/5356173>
..\reference_documents\20090928_Bachmann_TerraSAR-X_Antenna_Calibration_and_Monitoring_Based_on_a_Precise_Antenna_Model.pdf
- RD-7.** Post-launch calibration *TerraSAR-X Calibration results*
July 2018
German Aerospace Center
https://www.researchgate.net/publication/224232741_TerraSAR-X_calibration_results
..\reference_documents\20080700_Schwerdt_TerraSAR-X_calibration_results.pdf
- RD-8.** González & al, 2008 *TanDEM-X DEM Calibration Concept and Height References*
7th European Conference on Synthetic Aperture Radar, 2008, pp. 1-4.
https://elib.dlr.de/53636/1/DEM_Calibration_Concept_hueso.pdf
..\reference_documents\20080600_Hueso_TanDEM_X_DEM_Calibration_Concept_and_Height_References.pdf
- RD-9.** González & al, 2012 *Bistatic system and baseline calibration in TanDEM-X to ensure the global digital elevation model quality*
ISPRS Journal of Photogrammetry and Remote Sensing, ISSN: 0924-2716, Vol: 73, Page: 3-11
<https://doi.org/10.1016/j.isprsjprs.2012.05.008>

1.1.3 Copernicus DEMs

- RD-10.** Data access *Data Discovery and Download*
Copernicus Space Component Data Access
<https://spacedata.copernicus.eu/fr/web/cscda/data-access/discovery-and-download>
- RD-11.** Product Handbook *Copernicus Digital Elevation Model Product Handbook version 3.0, 9 November 2020*
Airbus
https://spacedata.copernicus.eu/documents/20126/0/GEO1988-CopernicusDEM-SPE-002_ProductHandbook_I3.0.pdf
..\reference_documents\20201109_Airbus_Copernicus_DEM_Product_Handbook.pdf
- RD-12.** TD-GS-PS-0021 *TanDEM-X - Ground Segment - DEM Products Specification Document*
issue 3.1, 05.08.2016
DLR
https://elib.dlr.de/108014/1/TD-GS-PS-0021_DEM-Product-Specification_v3.1.pdf
..\reference_documents\20160805_DLR_TanDEM-X_Ground_Segment_DEM_Products_Specification_Document.pdf

- RD-13.** *WorldDEM™ Technical Product Specification - Digital Surface Model, Digital Terrain Model*
version 2.5, April 2019 - Airbus
https://www.intelligence-airbusds.com/automne/api/docs/v1.0/document/download/ZG9jdXRoZXF1ZS1kb2N1bWVudC01NTcyOQ==/ZG9jdXRoZXF1ZS1maWxILTU1NzI4/WorldDEM_TechnicalSpecificationsss_Version2.6-202012.pdf
..\reference_documents\20201200_Airbus_WorldDEM_Technical_Product_Specification.pdf
- RD-14.** P. Rizzoli & al., 2017 *Generation and performance assessment of the global TanDEM-X digital elevation model*
<http://dx.doi.org/10.1016/j.isprsjprs.2017.08.008>
..\reference_documents\20170913_Rizzoli_Generation_and_performance_assessment_of_the_global_TanDEM-X_digital_elevation_model.pdf
- RD-15.** Validation report *Copernicus DEM Validation Report*
version 3.0, 9 November 2020
Airbus
https://spacedata.copernicus.eu/documents/20126/0/GEO1988-CopernicusDEM-RP-001_ValidationReport_I3.0.pdf
..\reference_documents\20201109_Airbus_Copernicus_DEM_Validation_Report.pdf
- RD-16.** K. Becek & al., 2016 *Evaluation of Vertical Accuracy of the WorldDEM™ Using the Runway Method*
Remote Sens. 2016, 8(11), 934;
<https://doi.org/10.3390/rs8110934>
..\reference_documents\20161110_Becek_Evaluation_of_Vertical_Accuracy_of_the_WorldDEM™_Using_the_Runway_Method.pdf
- RD-17.** COPE-PMAN-EOPG-TN-15-0004 *Copernicus Space Component Data Access Portfolio: Data Warehouse 2014 – 2020*
issue/revision 2.7, 16/12/2019 - ESRIN
<https://spacedata.copernicus.eu/documents/20126/0/DAP+Document+--+current+%2810%29.pdf>
..\reference_documents\20210104_ESA_Copernicus_Space_Component_Data_Access_Portfolio_Data_Warehouse_2014_2022.pdf

1.1.4 ICESat-1

RD-18. User Guide



User guide GLAS/ICESat L2 Global Land Surface Altimetry Data
23 October 2014
National Snow and Ice Data Center
https://nsidc.org/data/GLAH14/versions/34?qt-data_set_tabs=3#qt-data_set_tabs
..\reference_documents\20141023_NSIDC_GLAS_ICESat_L2_Global_Land_Surface_Altimetry_Data_(HDF5)_Version_34_National_Snow_and_Ice_Data_Center.htm

- RD-19. Data Management Plan** *Science Data Management Plan*
Version 4.0
July 1999
Peggy L. Jester and David W. Hancock III
<https://glas.wff.nasa.gov/wp-content/uploads/sdmp.pdf>
[../reference_documents/19990700_Jester_Science_data_management_plan.pdf](https://reference_documents/19990700_Jester_Science_data_management_plan.pdf)
- RD-20. Cal/Val Plan** *GLAS Altimeter Post-Launch Calibration/Validation Plan*
Version 1.0, October 2001
Bob E. Schutz
http://www2.csr.utexas.edu/glas/pdf/plan/validation_plan_v1_oct2001.pdf
[../reference_documents/20011000_Schutz_GLAS_Altimeter_Post_Launch_Calibration_Validation_Plan.pdf](https://reference_documents/20011000_Schutz_GLAS_Altimeter_Post_Launch_Calibration_Validation_Plan.pdf)
- RD-21. Glas_laser_ops_attrib** *NSIDC Distributed ICESat GLAS Laser Operations Periods*
December 2014
National Snow and Ice Data Center
https://nsidc.org/sites/nsidc.org/files/files/glas_laser_ops_attrib.pdf
[../reference_documents/20141200_NSIDC_glas_laser_ops_attrib.pdf](https://reference_documents/20141200_NSIDC_glas_laser_ops_attrib.pdf)


1.1.5 ICESat-2

- RD-22. ATL08 User Guide** *ATLAS/ICESat-2 L3A Land and Vegetation Height, Version 3 - User Guide*
23 June 2020
National Snow and Ice Data Center
https://nsidc.org/data/atl08?qt-data_set_tabs=3
[../reference_documents/20200423_Neuenschwander_ATLAS_ICESat-2_L3A_Land_and_Vegetation_Height_Version_3_User_Guide.pdf](https://reference_documents/20200423_Neuenschwander_ATLAS_ICESat-2_L3A_Land_and_Vegetation_Height_Version_3_User_Guide.pdf)
- RD-23. ATL08 ATBD** *Ice, Cloud; and Land Elevation Satellite 2 (ICESat-2) Algorithm Theoretical Basis Document (ATBD) for Land - Vegetation Along-Track Products (ATL08)*
15 January 2020
Amy Neuenschwander and Katherine Pitts
https://nsidc.org/sites/nsidc.org/files/technical-references/ICESat2_ATL08_ATBD_r003.pdf
[../reference_documents/20200115_Neuenschwander_ICESat-2_Algorithm_Theoretical_Basis_Document_for_Land-Vegetation_Along-Track_Products.pdf](https://reference_documents/20200115_Neuenschwander_ICESat-2_Algorithm_Theoretical_Basis_Document_for_Land-Vegetation_Along-Track_Products.pdf)
- RD-24. Major Activities** *ICESat-2 Major Activities (includes yaw flips)*
13 January 2021
Kaitlin Harbeck
https://nsidc.org/sites/nsidc.org/files/technical-references/ICESat2_major_activities_01122021.xlsx
[../reference_documents/20211201_Harbeck_ICESat2_major_activities.xlsx](https://reference_documents/20211201_Harbeck_ICESat2_major_activities.xlsx)



- RD-25.** ATL08 Data Dictionary *ATL08 Data Dictionary (V03)*
03 February 2020
NASA/GSFC
https://nsidc.org/sites/nsidc.org/files/technical-references/ICESat2_ATL08_data_dict_v003.pdf
..\reference_documents\20200203_NASA_ATL08_Product_Data_Dictionary.pdf
- RD-26.** ATL08 Release 003 *ATL08 Land and Vegetation Data product – Release 003*
15 March 2020
Amy Neuenschwander and Ben Jelley
https://nsidc.org/sites/nsidc.org/files/technical-references/ICESat2_ATL08_Known_Issues_v003_Aug2020.pdf
..\reference_documents\20200315_Neuenschwander_ATL08_Land_and_Vegetation_Data_product_Release_003.pdf
- RD-27.** C. Carabaja & al., 2020 *ICESat-2 Altimetry as Geodetic Control*
Int. Arch. Photogramm. Remote Sens. Spatial Inf. Sci., XLIII-B3-2020, 1299–1306
<https://doi.org/10.5194/isprs-archives-XLIII-B3-2020-1299-2020>
..\reference_documents\20200822_Carabaja_ICESat-2_altimetry_as_geodetic_control.pdf

1.1.6 GEDI

- RD-28.** L2 User Guide *GLOBAL Ecosystem Dynamics Investigation (GEDI) Level 2 User Guide*
Version 2.1, April 2021
NASA, UMD

https://lpdaac.usgs.gov/documents/998/GEDI02_UserGuide_V21.pdf
..\reference_documents\20210400_GLOBAL_Ecosystem_Dynamics_Investigation_Level_2_User_Guide.pdf
- RD-29.** L2A Data Dictionary *GEDI L2A Product Data Dictionary*
NASA GSFC, UMD
https://lpdaac.usgs.gov/documents/982/gedi_l2a_dictionary_P003_v2.html
..\reference_documents\GEDI_L2A_Product_Data_Dictionary.html
- RD-30.** Waveform ATBD *Algorithm Theoretical Basis Document (ATBD) for GEDI Transmit and Receive Waveform Processing of L1 and L2 Products*
Version 1.0, 4 December 2019
NASA GSFC, UMD
https://doi.org/10.5067/DOC/GEDI/GEDI_WF_ATBD.001
..\reference_documents\20191204_Hoftern_Algorithm_Theoretical_Basis_Document_for_GEDI_Transmit_and_Receive_Waveform_Processing_for_L1_and_L2_Products.pdf

RD-31. Geolocation ATBD

Algorithm Theoretical Basis Document (ATBD) for GEDI Waveform Geolocation for L1 and L2 Products
Version 1.0, 5 December 2019
NASA GSFC, UMD
https://doi.org/10.5067/DOC/GEDI/GEDI_WFGEO_ATBD.001
..\reference_documents\20191205_Luthcke_Algorithm_Theoretical_Basis_Document_for_GEDI_Waveform_Geolocation_for_L1_and_L2_Products.pdf

RD-32. R. Dubayah & al., 2020

The Global Ecosystem Dynamics Investigation: High-resolution laser ranging of the Earth's forests and topography
<https://doi.org/10.1016/j.srs.2020.100002>
..\reference_documents\20200122_Dubayah_The_Global_Ecosystem_Dynamics_Investigation_High_resolution_laser_ranging_of_the_Earth_s_forests_and_topography.pdf

1.1.7 Vertical reference systems

RD-33. EGM2008

Office of Geomatics, *Earth Gravitational Model 2008 Data and Apps*
National Geospatial-Intelligence Agency
<https://earth-info.nga.mil/>

1.1.8 Geocoding and orthorectification

RD-34. SPOT Geom. HB

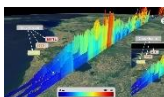
SPOT 123-4-5 Geometry Handbook
Issue 1, revision 4 - 20/08/2004
Serge RIAZANOFF, GAEL Consultant for CNES / SPOT IMAGE
<http://www-igm.univ-mlv.fr/~riazano/publications/GAEL-P135-DOC-001-01-04.pdf>

1.1.9 Other studies

RD-35. EDAP.REP.029

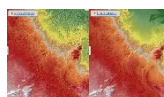
Global DEM quality assessment summary
Issue 1.2, 16/07/2020 – VisioTerra
https://visioterra.fr/telechargement/P317_ESA_EDAP/EDAP.REP.029_1.2_Global_DEM_Quality_Assessment_Summary.pdf

RD-36. HYP-087-VtWeb



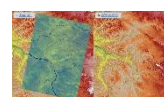
Presentation of ICESat-2 ATLAS
https://visioterra.fr/telechargement/A003_VISIOTERRA_COMMUNICATION/HYP-087-VtWeb-E_Presentation_of_ICESat-2_ATLAS.pdf

RD-37. HYP-089-VtWeb



Comparison of Digital Elevation Models (DEMs) in Chott Melghir (Algeria)
https://visioterra.fr/telechargement/A003_VISIOTERRA_COMMUNICATION/HYP-089-VtWeb_Comparison_of_DEMs_in_Chott_Melghir_Algeria.pdf

RD-38. HYP-093-VtWeb



Le MNT Copernicus en RDC
https://visioterra.fr/telechargement/A003_VISIOTERRA_COMMUNICATION/HYP-093-VtWeb-F_MNT_Copernicus_en_RDC.pdf

RD-39. HYP-094-VtWeb



Assessment of slopes in Alaska LiDAR DEM

https://visioterra.fr/telechargement/A003_VISIOTERRA_COMMUNICATION/HYP-094-VtWeb-E_Assessment_of_slopes_in_Alaska_LiDAR_DEM.pdf

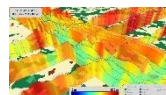
RD-40. HYP-095-VtWeb



Comparison of Copernicus DEM releases 2020 vs 2019

https://visioterra.fr/telechargement/A003_VISIOTERRA_COMMUNICATION/HYP-095-VtWeb-E_Comparison_of_Copernicus_DEM_releases_2020_vs_2019.pdf

RD-41. HYP-096-VtWeb



Comparison of LiDAR GEDI vs ICESat-1/ICESat-2

https://visioterra.fr/telechargement/A003_VISIOTERRA_COMMUNICATION/HYP-096-VtWeb-E_Comparison_of_LiDAR_GEDI_vs_ICESat-1_ICESat-2.pdf

1.2 Glossary

The following acronyms and abbreviations have been used in this Report.

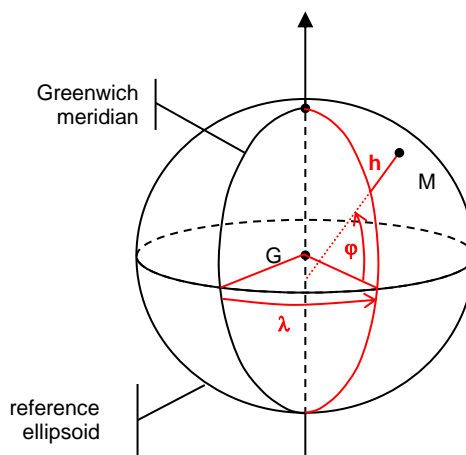
ALOS	Advanced Land Observing Satellite
ASTER	Advanced Spaceborne Thermal Emission and Reflection Radiometer
ATBD	Algorithm Theoretical Basis Document
ATLAS	Advanced Topographic Laser Altimeter System
AVNIR-2	Advanced Visible and Near Infrared Radiometer type 2
AW3D	ALOS World 3D
AW3D30	ALOS World 3D – 30 m
CRS	Coordinates Reference System
DEM	Digital Elevation Model
DGED	Defense Gridded Elevation Data
DLR	Deutsches Zentrum für Luft- und Raumfahrt
DSM	Digital Surface Model
DTED	Digital Terrain Elevation Data
DTM	Digital Terrain Model
EGM96	Earth Gravitational Model 1996
EGM2008	Earth Gravitational Model 2008
EPSG	European Petroleum Survey Group
GCP	Ground Control Point
GDEM	Global Digital Elevation Model
GeoTIFF	Geocoded TIFF
GL1	Global 1" arc
GLAS	Geoscience Laser Altimeter System
GPS	Global Positioning System
GSD	Ground Sampling Distance
HDF5	Hierarchical Data Format version 5
ICESat-1	Ice, Cloud and land Elevation Satellite 1
ICESat-2	Ice, Cloud and land Elevation Satellite 2
INSPIRE	INfrastructure for SPatial InfoRmation in Europe
JAXA	Japan Aerospace Exploration Agency
LiDAR	Light Detection and Ranging
LP DAAC	Land Processes Distributed Active Archive Center
KML	Keyhole Markup Language
METI	Ministry of Economy, Trade, and Industry (Japan)
NASA	National Aeronautics and Space Administration (USA)
NGA	National Geospatial-Intelligence Agency (USA, former NIMA)
NSIDC	National Snow and Ice Data Center
PALSAR	Phased Array L-band Synthetic Aperture Radar
PRISM	Panchromatic Remote-sensing Instrument for Stereo Mapping
RMSE	Root Mean Square Error
SIR-C	Shuttle Imaging Radar-C
SRTM	Shuttle Radar Topography Mission
SRTM-GL1	Shuttle Radar Topography Mission Global 1 arc second
STS-99	Space Transportation System 99 (Endeavour)
TIFF	Tagged Image File Format
UMD	University of Maryland
USGS	United States Geological Survey
VRS	Vertical Reference System
WGS84	World Geodetic System 1984

1.3 Definitions

The following definitions have been used in this Report.

coordinates
reference
system (CRS)

geographic

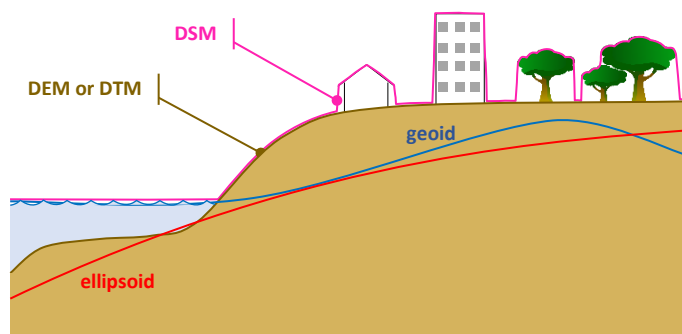


DTM
or
DEM
or
DSM

The “Digital Terrain Model” is also called “Digital Elevation Model” (DEM) or sometimes “Altimetry model”. A DEM is a raster data made of a georeferenced grid in which each cell gives an altitude with regard to a geoid (most frequent case) or a height above an ellipsoid.

In maritime parts, the altitudes or elevations may give the sea level (altitude equal to 0 metres above a geoid) or may give the ocean floor (negative values also called bathymetry).

The “Digital Surface Model” (DSM) gives altitudes or heights above overground: building roofs, top of canopy, sea level...



KML

The KML (Keyhole Markup Language) is a XML grammar describing the objects (points, lines, images, polygons) handled by Google Earth.

KML is based on the version 3.0 of the GML (Geographic Markup Language).

hyperlook

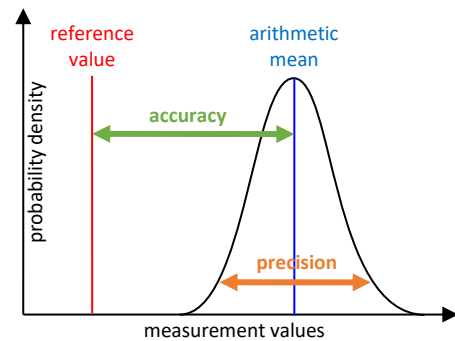
Rich URL containing the server address / product identifier / processing parameters / geometry of view) that readers may activate to achieve the same views in their usual Web browser (Internet Explorer, Firefox, Chrome, Safari...).

Metrology

accuracy vs. precision

Accuracy measures the closeness of agreement between a measured quantity value and a true quantity value. Distance between the arithmetic mean and the reference value is called the bias.

The precision measures the closeness of agreement between indications or measured quantity values obtained by replicate measurements on the same or similar objects under specified conditions.

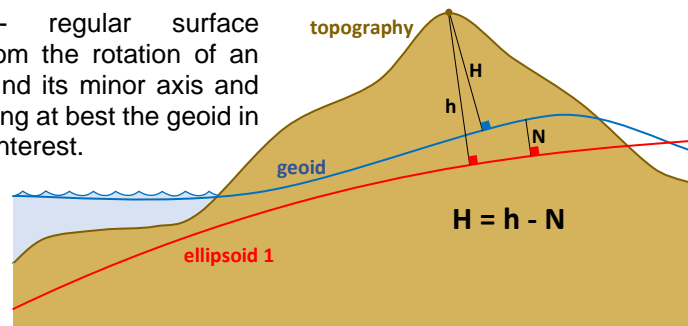


See https://www.bipm.org/utis/common/documents/jcgm/JCGM_200_2012.pdf

vertical reference system

There are three types of reference surface:

- topography - being the site of the interface between the solid phase and the gaseous and liquid phases of terrestrial matter;
- geoid - equipotential surface of the acceleration field of gravity (gravity + centrifugal force); the geoid is close to the mean surface of the sea;
- ellipsoid - regular surface resulting from the rotation of an ellipse around its minor axis and approximating at best the geoid in an area of interest.



The heights H with respect to the geoid (also called "altitude") are reference heights for the study of physical phenomena such as runoff. The altitude 0 metre corresponds to the mean sea level.

The heights h with respect to the ellipsoid (also called "elevation") are used for terrestrial modelling and in particular for orthorectification with respect to a reference ellipsoid (often WGS84).

2. EXECUTIVE SUMMARY

2.1 Maturity Matrix

Product Information	Product Generation	Ancillary Information	Uncertainty Characterisation	Validation
Product Details	Sensor Calibration & Characterisation Pre-Flight	Product Flags	Uncertainty Characterisation Method	Reference Data Representativeness
Availability & Accessibility	Sensor Calibration & Characterisation Post-Launch	Ancillary Data	Uncertainty Sources Included	Reference Data Quality
Product Format	Retrieval Algorithm Method		Uncertainty Values Provided	Validation Method
User Documentation	Retrieval Algorithm Tuning		Geolocation Uncertainty	Validation Results
Metrological Traceability Documentation	Additional Processing			

Key
Not Assessed
Not Assessable
Basic
Intermediate
Good
Excellent



Information Not Public

Table 1 - Copernicus DEMs Product Quality Evaluation Matrix.

2.2 Summary of quality assessment

This document presents the quality assessment of the three Copernicus DEMs: Copernicus DEM EEA-10, Copernicus DEM GLO-30 and Copernicus DEM GLO-90. A first major section focuses on evaluating the maturity of the Copernicus DEMs (see section 3), with respect to the EDAP Quality Assessment Guidelines (see RD-1). The second major section of the document encompasses two quality assessment methods (see section 4):

- **Qualitative assessments** - the VisioTerra VtWeb tool is used to compute the difference between Copernicus DEM GLO-30 and ALOS World 3D. This tool allows to compute the difference between two DEMs at any scale, immediately highlighting their anomalies (see section 4.1).
- **Quantitative assessments** - Copernicus DEM EEA-10, GLO-30 and GLO-90 are compared to ICESat-1 / GLAS, ICESat-2 / ATLAS and GEDI LiDAR reference data. Five quantitative studies are followed per DEM, respectively using ICESat-1, ICESat-2 terrain, ICESat-2 terrain with canopy, GEDI lowest mode (ground) and GEDI highest return (top of canopy) heights as vertical references (see sections 4.2 and 4.3).

Illustrations and results of the qualitative assessment, consisting of comparing ALOS World 3D to Copernicus DEM GLO-30, are available in section 4.1. This section provides both global views of this comparison and a case study of the Lake Garda in Italy, highlighting an anomaly of ALOS World 3D.

Regarding the quantitative assessment, this technical note aims to answer to the following questions:

- Considering ICESat-1, ICESat-2 and GEDI products, which reference data is the most suitable for DEM quantitative assessments?
- Which instance (among EEA-10, GLO-30 and GLO-90) of the Copernicus DEM has the best overall height error statistics?
- Taking into account results of previous quantitative assessments of ALOS World 3D, ASTER GDEM and SRTMGL1 (RD-35), and the results of the quantitative assessment of Copernicus DEM GLO-30, which global DEM at 1" is the most accurate?

The quantitative studies show that the best results are achieved with **ICESat-1**, retrieving an arithmetical mean of 0.033 metres and a RMSE of 0.628 metres among all height differences for the assessment of Copernicus DEM GLO-30 (LE95 statistics). Similar results are achieved with **ICESat-2 terrain height only**, with an arithmetical mean of 0.195 metres and a RMSE of 0.999 metres. Worse results are obtained using **ICESat-2 terrain with canopy height** as a vertical reference, retrieving an arithmetical mean of -1.124 m and a RMSE of 2.907 m. Considering **GEDI lowest mode** reference data gives an arithmetical mean of 1.088 m, but a high RMSE of 3.639 m. The worst statistics are obtained considering **GEDI highest return**, retrieving an arithmetical mean of -5.840 m and a RMSE of 6.710 m. According to these studies, ICESat-1 seems to be the best vertical reference for DEM quantitative assessments. ICESat-2 terrain heights give similar results and is still recommended for DEM quantitative assessments. ICESat-2 terrain with canopy heights is not recommended, as the canopy height is only an estimation and not the actual canopy height retrieved at each geolocation indicated in the ICESat-2 products. GEDI lowest mode and highest return are not recommended as the statistics show very high error arithmetic mean and RMSE.

Among **Copernicus DEM EEA-10, GLO-30 and GLO-90**, the **Copernicus DEM GLO-30** obtains the best height error statistics. Considering ICESat-1 reference data, a mean of 0.033 metres, a standard deviation of 0.627 metres and a RMSE of 0.628 m are obtained for the height errors of Copernicus DEM GLO-30 (see section 4.2.5.3). Copernicus DEM GLO-90 height error statistics show similar results, with a mean of 0.066 metres, a standard deviation of 0.706 metres and a RMSE of 0.709 metres (see section 4.2.6.3). Copernicus DEM EEA-

10 height error statistics are the worse, considering a mean of 0.276 metres, a standard deviation of 1.389 metres and a RMSE of 1.415 metres (see section 4.2.4.3).

The quality of **ALOS World 3D**, **ASTER GDEM**, **SRTMGL1** and **Copernicus DEM GLO-30** was assessed using **ICESat-1** reference data. These DEMs are available at global scale and share the same spatial resolution of 1". In previous quantitative studies, ALOS World 3D was assessed to be the best DEM, as opposed to SRTMGL1 and ASTER GDEM (see RD-35). According to the quantitative studies of this technical note, **Copernicus DEM GLO-30 is assessed to be the best DEM**, showing a significative improvement with regard to the three other global DEMs. The height error statistics of Copernicus DEM GLO-30 are even better than those of ALOS World 3D, retrieving a mean of 0.033 metres, a standard deviation of 0.627 metres and a RMSE of 0.628 metres, as opposed to ALOS World 3D, which obtained a mean of -0.151 m, a standard deviation of 1.660 metres and a RMSE of 1.653 metres (LE95 statistics, see section 5.2.2.4).

3. PRODUCT ASSESSMENT OVERVIEW

3.1 Overview of Copernicus DEMs generation and products

3.1.1 Short history of Copernicus DEMs

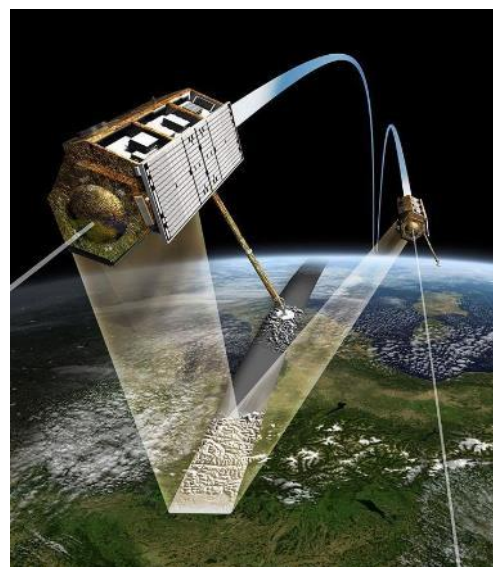
The German Space Agency (DLR) has developed great skills in the field of X-band Radar imaging. Its first successes were achieved in the 1990s by developing the "SRTM-XSAR" instrument within the framework of the famous [SRTM mission](#) in partnership with the United States Space Agency (NASA).

During the 2000s, the DLR developed an ambitious X-band acquisition program involving two identical satellites: TerraSAR-X and then TanDEM-X whose very close orbits make it possible to calculate centimetric vertical displacements of the ground by interferometry and a digital model of all the Earth with a sampling step (12m) and an unrivalled vertical accuracy.

3.1.2 The TanDEM-X constellation

A new era in radar remote sensing began 10 years ago, on 21 June 2010, when the radar satellite TanDEM-X was launched. Since then, it has been orbiting Earth in close formation flight with TerraSAR-X, its three-year-older 'twin'. The distance between the satellites varies between several kilometres and sometimes only 120 metres. This enables the radar sensors to obtain a 3D view of Earth. This is referred to as a bistatic interferometer in space, which allows the terrain structure to be recorded in three dimensions in just one pass. This space mission continues to be globally unique.

The primary mission objective – the creation of a highly accurate global elevation model of Earth's entire landmass – was achieved as early as mid-2016 with the completion of the TanDEM-X DEM (Digital Elevation Model). The digital elevation model provides precise topographic information and sets a new standard due to its high accuracy and global homogeneity. The DEM product is available in three different resolution variants. Depending on the quality requirements, elevation measurements were calculated for a grid of 12, 30 or 90 metres. The absolute height error, the inaccuracy of each measurement – only 1.3 metres – is extremely small and far exceeds the original requirement of 10 metres. (extracted from https://www.dlr.de/content/en/articles/news/2020/02/20200625_congratulations-tandem-x-ten-years-of-3d-mapping-from-space.html).



	TerraSAR-X (TSX)	TanDEM-X (TDX)
Launch date	15.06.2007	21.06.2010
Orbital altitude	514.8 km	514 km
Revisit time (orbit repeat cycle)	11 days	11 days
Radar frequency	9.65 GHz	9.65 GHz
Radar wavelength	3.1 cm (X band)	3.1 cm (X band)
Orbital plan inclination	97.4° (Sun synchronous)	97.4° (Sun synchronous)
Polarizations	HH, VH, HV, VV	HH, VH, HV, VV

Table 2 - Main features of TerraSAR-X and TanDEM-X.

One may find an accurate description of the two satellites formation in RD-5.

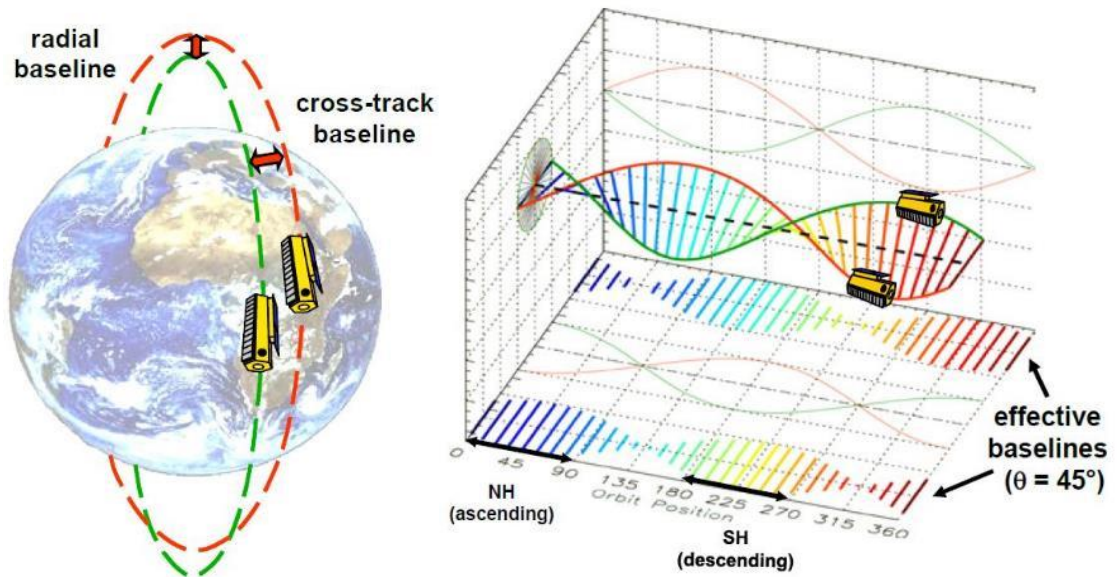


Figure 1 - View of the close satellite formation (left) and the helix satellite formation (right).

This precise configuration enables each one of the two satellites to receive the backscattered energy from the pulse sent by it-self (monostatic) or sent by the other satellite and received by both satellites (bistatic).

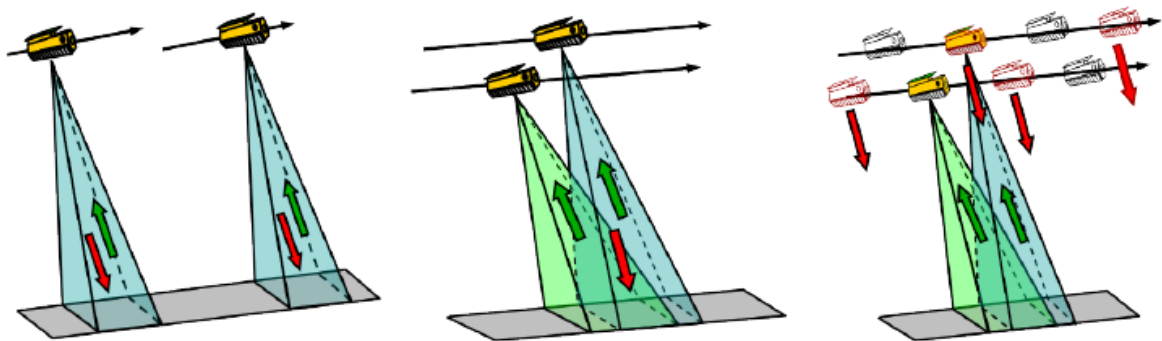


Figure 2- Data acquisition configurations: Pursuit monostatic (left), bistatic (middle), and alternating bistatic (right).

3.1.3 Produced by TanDEM-X constellation

Elevations expressed in the Copernicus DEMs were acquired by two satellites: TerraSAR-X and TanDEM-X. Some confusions are made between those terms, because the name TanDEM-X refers both as the satellite name and the constellation of both satellites.

The main goal of the TanDEM-X constellation was to create a global DEM using both the TerraSAR-X and TanDEM-X satellites. This DEM, TerraSAR-X DEM, was the source DEM used to create WorldDEM™ which is the basis of the three Copernicus DEMs.

3.1.4 Becoming an element of Copernicus programme

The global instances of the Copernicus DEM are available cost-free (Copernicus DEM GLO-30 and Copernicus DEM GLO-90). Only Copernicus DEM EEA-10 and some countries of Copernicus DEM GLO-30 have a restricted access to public. The current licensing can be found at the following link:

https://spacedata.copernicus.eu/documents/20126/0/CSCDA_ESA_Mission-specific+Annex.pdf/5308d1e7-17de-b55b-2be8-8a3a286aa88b?t=1581077110498

3.1.5 Formats of Copernicus DEMs

The Copernicus DEM instances are available in three different formats depending on the product resolution:

- **DGED** (Defence Gridded Elevation Data) – This is the main format of the Copernicus DEMs. It is available for the three products resolutions and provides elevation data as 32-bit floating data within GeoTIFF image format. The associated metadata are given as XML files and the quality data as GeoTIFF images.
- **DTED** (Digital Terrain Elevation Data) – This format is available for the GLO-30 and GLO-90 products. It provides elevation data as 16-bit integer data.
- **INSPIRE** – This format is available for the EEA-10 product only. It provides the elevation as a 32-bit floating data with a slightly better spatial resolution (0.3" arc second instead of 0.4" arc second).

The table here below sums up the available formats.

	INSPIRE	DGED	DTED
EEA-10	X	X	
GLO-30		X	X
GLO-90		X	X

Table 3 - Copernicus DEMs available formats.

The DGED format has been selected for this study as well as for the import of the Copernicus DEMs in the VtWeb platform for, at least, the following reasons: -the format is the same for the three products, -it provides elevation data with great accuracy and -the GeoTIFF format is widely supported.

3.1.6 Copernicus DEMs product generation

This section gathers technical information about the three Copernicus DEMs: **Copernicus DEM EEA-10**, **Copernicus DEM GLO-30** and **Copernicus DEM GLO-90**, as the three DEMs are described in the same technical documents and share many common features.

As the Copernicus DEMs are derived from the WorldDEM™ and the TanDEM-X DEM, some of the next references (such as the ATBD) are not directly referring to the Copernicus DEMs. The following figure (see 1.1.3) summarizes the generation process of the Copernicus DEMs:

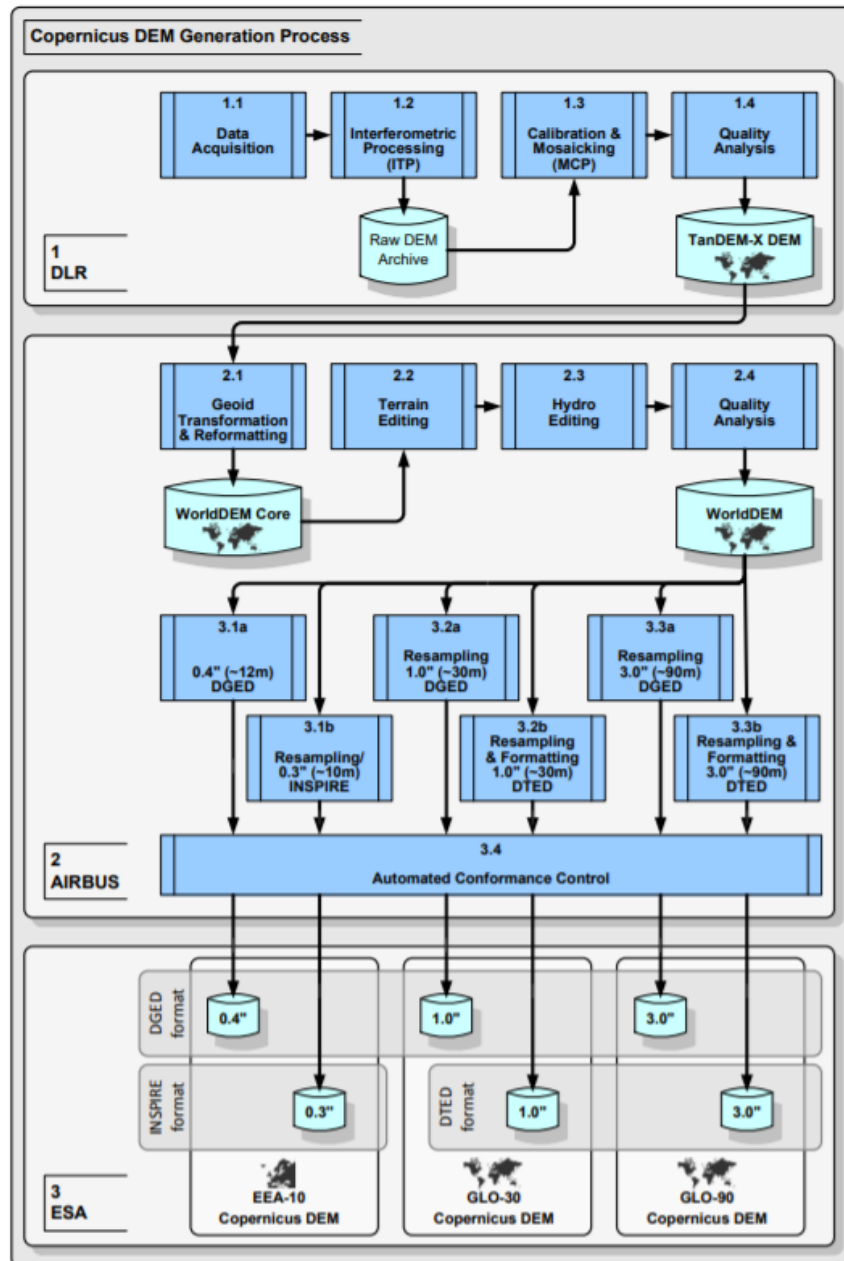


Figure 3 – Copernicus DEMs Generation Process Chart (See 1.1.3).

3.2 EDAP standard tables

3.2.1 Product Information

All the required information has been found: the Copernicus DEMs have been given the Excellent grade for Product Details.

Product Details	
Product Names	<i>Copernicus DEM EEA-10 Copernicus DEM GLO-30 Copernicus DEM GLO-90</i>
Sensor Name	<i>SAR-X (both satellites)</i>
Sensor Type	<i>X-band SAR (both sensors)</i>
Mission Type	<i>TanDEM-X mission (TanDEM-X/TerraSAR-X satellites)</i>
Mission Orbit	<i>Sun synchronous, 97.44 degrees of inclination</i>
Product Version Number	<i>2019_1 (not explicitly given but deduced from the data directory name). The present study is based on this version. 2020_1 is a second version that has been notified in January 2021 and integrated recently in VtWeb (RD-40).</i>
Product IDs	<i>COP-DEM_EEA-10-DGED short-named EEA-10 COP-DEM_GLO-30-DGED short-named GLO-30 COP-DEM_GLO-90-DGED short named GLO-90</i>
Processing level of product	<i>Level 3</i>
Measured Quantity Name	<i>Elevation</i>
Measured Quantity Units	<i>metres</i>
Stated Measurement Quality	Absolute vertical accuracy: < 4m (90% linear error) Relative vertical accuracy: < 2m for slopes below or equal 20%, < 4m for slopes above 20% (90% linear point-to-point error within an area of 1° x 1°)
Spatial Resolution	<i>1 arc second in latitude, variable in longitude (0.4 to 4.0 arc seconds depending on the latitude)</i>
Spatial Coverages	<i>Copernicus DEM GLO-30, GLO-90: Global Copernicus DEM EEA-10: European Economic Area</i>
Temporal Resolution	<i>11 days (TanDEM-X orbit repeat cycle)</i>
Temporal Coverage	<i>2010 to 2015 (TanDEM-X acquisitions)</i>
Point of Contact	Copernicus Services Coordinated Interface (SCI) ESA - European Space Agency EOSupport@Copernicus.esa.int
Product locator (DOI/URL)	https://spacedata.copernicus.eu/web/cscda/dataset-details?articleId=394198
Conditions for access and use	https://spacedata.copernicus.eu/documents/20126/0/CSCDA_ESA_Mission-specific+Annex.pdf/5308d1e7-17de-b55b-2be8-8a3a286aa88b?t=1581077110498
Limitations on public access	<i>Restricted access for the EEA-10 instances, public release for the GLO-30 and GLO-90 instances (Armenia and Azerbaijan have limited access to GLO-30 as specified in https://spacedata.copernicus.eu/fr/web/cscda/explore-more/news-archive/-/asset_publisher/Ye8eqYeRPLEs/blog/id/434960 and the Excel table at https://spacedata.copernicus.eu/documents/20126/0/Non-released-</i>

	tiles_GLO-30_PUBLIC_Dec.xlsx/bcdd6cef-6379-4890-de8f-788daf41dce8?t=1608549440765
Product Abstract	<i>The Copernicus DEM is a Digital Surface Model (DSM) which represents the surface of the Earth including buildings, infrastructure and vegetation. This DEM is derived from an edited DSM named WorldDEM™. The Copernicus DEM is provided in 3 different instances named EEA-10, GLO-30 and GLO-90. The Copernicus DEM instances have varying geographical extent (European and global) and varying format (INSPIRE, DGED, DTED).</i>

To discriminate between the four FAIR principles and to assess a global notation more traceable, four notations have been given over 4 (Findable), 3 (Accessible), 3 (Interoperable) and 4 (Reusable) leading to a total notation over 14.

Copernicus DEM instances fully meet the FAIR principles and have an associated Data Management Plan, which gives an Excellent grade to Copernicus DEMs for the Availability & Accessibility section.

Availability & Accessibility	
Compliant with FAIR principles	<i>Yes (14/14)</i>
Data Management Plan	<i>CSC data access (RD-17)</i>
Availability Status	<i>Available via HTTP/FTP (registered users only, see RD-10)</i>

As the Copernicus DEM instances are available in the GeoTIFF format and follow a specific metadata convention, an Excellent grade has been given for Product Format.

Product Format	
Product File Format	<i>GeoTIFF</i>
Metadata Conventions	<i>ISO 19115 Geographic Information – Metadata (First edition, 2003-05-01)</i>
Analysis Ready Data?	<i>Yes</i>

As a product user guide is available (but not QA4EVC compliant, see RD-2 for product user guide assessment guidelines) and a physical description has been found, but no ATBD, the Intermediate grade has been given for User Documentation.

User Documentation		
<i>Document</i>	<i>Reference</i>	<i>QA4ECV Compliant</i>
Product User Guide	<i>See 1.1.3</i>	<i>No case studies given</i>
ATBD	<i>See RD-14</i>	<i>No specific ATBD but a good physical description found in RD-14</i>

As no proper metrological traceability has been found (except for a first elevation budget), but as a traceability chain is present in the user guide, identifying most of the important processing steps of the Copernicus DEM instances, the Intermediate grade has been given for Metrological Traceability Documentation.

Metrological Traceability Documentation	
Document Reference	<i>A first elevation error budget of WorldDEM™ (Copernicus DEM is a successor of WorldDEM™ as shown in Figure 3) is given in RD-16.</i>
Traceability Chain / Uncertainty Tree Diagram Available	<i>Yes, but not strictly following the QA4ECV (see 1.1.3, figure 19)</i>

3.2.2 Product Generation

The RD-6 document gives a complete overview of the TerraSAR-X calibration procedures, especially giving information about the pre-flight calibration. Based on a mathematical antenna model, methods and results of the pre-flight validation are given in section V. A Good grade has been given for Sensor Calibration & Characterisation – Pre-Flight, as the pre-flight calibration methods and results are rigorously described, and as no reference have been found concerning the impact of uncertainties on the final product.

Sensor Calibration & Characterisation – Pre-Flight	
Summary	<i>Sections III, IV and V of the reference document provide information about the antenna model used to calibrate the TerraSAR-X instrument before launch, as well as the methods and results of the pre-launch validation. The pre-launch validation results successfully fulfil the requirements of the TerraSAR-X instrument.</i>
References	<i>See RD-6 under sections III, IV and V.</i>

The 5 tasks described in the reference document cover the major aspects of the post-launch calibration. As a consequence, the Good grade has been given for Sensor Calibration & Characterisation – Post launch.

Sensor Calibration & Characterisation – Post-Launch	
Summary	<i>Post-Launch calibration has been divided into 5 tasks: Geometric Calibration, Antenna Pointing Determination, Antenna Model Verification, Relative Radiometric Calibration, Absolute Radiometric Calibration. These 5 tasks are described in the reference document below.</i>
References	<i>See RD-7</i>

The reference document gives an overview of the generation of the TanDEM-X DEM, which includes the height retrieval method for this DEM. As the height retrieval methods are richly described and as the accuracy of the generated DEM is evaluated (using ICESat-1 data), an Excellent grade has been given to the Retrieval Algorithm Method.

Retrieval Algorithm Method	
Summary	<i>Sections 2.3 and 2.6 of the reference document describes the algorithms used to retrieve heights from multiple TerraSAR-X and TanDEM-X acquisitions.</i>
References	<i>See RD-14 under section 2.3: Processing single-pass interferometric data and 2.6: Global DEM generation process: from single scenes to DEM mosaic.</i>

The retrieval algorithm involves global DEMs and ICESat-1 reference data. ICESat-1 data is accurate and available at global scale. However, the mentioned DEMs are not fully representative of the TanDEM-X DEM, both in terms of geographical extent (SRTM C-band DEM), and resolution (GLOBE DEM). As a consequence, the Intermediate grade has been given for Retrieval Algorithm Tuning.

Retrieval Algorithm Tuning	
Summary	<i>Section 2.6 of the reference document describes the parameters used in order to enhance the quality of TanDEM-X acquisitions, also covering external data sources used in the tuning process.</i>
References	<i>See RD-14 under section 2.6: Global DEM generation process: from single scenes to DEM mosaic.</i>

The Copernicus DEM instances are generated from the WorldDEM™ / WorldDEM Core, which are generated from the TanDEM-X DEM. As a consequence, the additional processing steps referenced in the following tables can be relative to the WorldDEM Core, the WorldDEM™ and the Copernicus DEMs. Hereafter, the additional processing steps are

described respecting the order of the processing chain when available (see Figure 3). As there are numerous additional processing steps which are fully documented, providing a rich set of quality layers, the Excellent grade has been given to Additional Processing.

Additional Processing	
<i>Additional Processing 1 – Geoid transformation</i>	
Description	<i>The TanDEM-X DEM ellipsoidal heights, relative to the WGS84-G1150 ellipsoid, are converted to geoid heights, relative to the EGM2008 geoid. This processing step generates the WorldDEM Core, which is the basis of the WorldDEM™ generation.</i>
Reference	<i>See RD-13, under section 3.1.</i>
<i>Additional Processing 2 – Terrain editing</i>	
Description	<i>Terrain editing is applied to the WorldDEM Core, and consists of editing the following features: spikes / wells, voids, noise and negative elevations nearby ocean shorelines. Further explanations concerning the conditions of edition are given in the reference document.</i>
Reference	<i>See RD-13 under section 4.2.1</i>
<i>Additional Processing 3 – Hydrology editing</i>	
Description	<i>Hydrology editing is applied to the WorldDEM Core, and consists of classifying water body pixels into oceans, lakes and rivers, and to edit the elevation of each water body pixel according to its classification. Further explanations concerning the conditions of edition are given in the reference document.</i>
Reference	<i>See RD-13, under section 4.2.2</i>
<i>Additional Processing 4 – Airport editing</i>	
Description	<i>Airport editing is applied to the WorldDEM Core, and consists of modifying bad height values acquired over airports. Further explanations concerning the conditions of edition are given in the reference document.</i>
Reference	<i>See RD-13, under section 4.2.3</i>
<i>Additional Processing 5 – Quality layers</i>	
Description	<i>The following quality layers are generated from the previous processing steps:</i> <ul style="list-style-type: none"> - <i>Filling Mask (FLM): indicating the sources of elevations used to fill data voids,</i> - <i>Editing Mask (EDM): indicating if a pixel has been edited, and which editing has been applied,</i> - <i>Water Body Mask (WBM): indicating the classification of a water body pixel</i> <i>Further explanations concerning the generation of these quality layers are given in the reference document.</i>
Reference	<i>See RD-13, under section 4.2.3</i>
<i>Additional Processing 6 – Resampling and reformatting</i>	
Description	<i>The WorldDEM™ is resampled and reformatted to generate the three Copernicus DEM instances (EEA-10, GLO-30, GLO-90).</i>
Reference	<i>See RD-13, under section 4.2.3</i>

3.2.3 Ancillary Information

As product flags are available at pixel level and as their gradation is well documented, an Excellent grade has been given for Product Flags.

Product Flags	
Product Flag Documentation	<i>See 1.1.3 under section 1.2.5: Quality Layers</i>
Comprehensiveness of Flags	<i>Excellent</i>

As both an accuracy layer and a source data layer are available, an Excellent grade has been given for Ancillary Data.

Ancillary Data	
Ancillary Data Documentation	<i>See 1.1.3 under section 1.2.5: Quality Layers, subsections 1.2.5.5 and 1.2.5.6)</i>
Comprehensiveness of Data	<i>Excellent</i>
Uncertainty Quantified	<i>Yes (section 2 and 1.2.5.5)</i>

3.2.4 Uncertainty Characterisation

The Copernicus DEM instances are compared to ICESat-1 reference data. As this assessment seems to follow a limited part of the Type A uncertainty classification method (as described in the Guide to the Expression of Uncertainty in Measurement, see RD-4 under section 4.2), an Intermediate grade has been given for Uncertainty Characterisation Method.

Uncertainty Characterisation Method	
Summary	<i>The methods used to characterize the uncertainty of the Copernicus DEMs are details in section 2 of the reference document (Data and Methodology)</i>
Reference	<i>See RD-15 under section 2: Data and Methodology</i>

As a short summary of each error source is available, the Good grade has been given for Uncertainty Sources Included.

Uncertainty Sources Included	
Summary	<i>The section 2.4 of the reference document covers the different error sources affecting the quality of SAR acquisitions (in this case, SAR-X acquisitions).</i>
Reference	<i>see RD-14 under section 2.4: DEM Error Sources</i>

As a height error mask is available at pixel level, but no error-covariance is given, the Good grade has been given for Uncertainty Values Provided.

Uncertainty Values Provided	
Summary	<i>A height error mask is provided. Figure 5 and figure 8 of the reference document respectively show height error maps over the European Economic Area and worldwide.</i>
Reference	<i>See RD-15, figure 5 and figure 8</i>
Analysis Ready Data?	<i>Yes</i>

As a circular error is only given for the whole product, the Basic grade have been given for Geolocation Uncertainty.

Geolocation Uncertainty	
Summary	<i>The section 2.3 of the reference document gives the absolute horizontal accuracy of every Copernicus DEM instance, stated as a circular error of less than 6 metres (90% confidence level).</i>
Reference	<i>See 1.1.3 under section 2.3: Absolute Horizontal Accuracy</i>

3.2.5 Validation

This section presents the validation report of the Copernicus DEMs prepared by Airbus (Validation Activity #1), as well as the validation activities performed in this document (Validation Activities #2, #3 and #4). The grades given in this section only refer to the Validation Activity #1, as it is the validation report of reference for the Copernicus DEM instances.

The Copernicus DEM instances are assessed using ICESat-1 data, which is reliable and available at global scale. However, the assessment concerns tiles with at least 200 valid ICESat-1 elevations, which excludes a significant number of tiles (see RD-15, figures 5 and 8). As a consequence; an Intermediate grade has been given to the Reference Data Representativeness.

As the reference ICESat-1 data used only comes with a global estimation of the uncertainty, an Intermediate grade has been given for Reference Data Quality.

Vertical accuracies of the Copernicus DEM instances are given in the validation report, but this document does not include any validation activity performed on the reference ICESat-1 data. As a consequence, an Intermediate grade has been given for Validation Method.

As stated in the validation report, "The mission goal of TerraSAR-X and TanDEM-X was the generation of a global DEM with an accuracy better than 10m". The validation results show that only a small number of Copernicus DEM tiles do not reach this accuracy. Even if the results are good, as the validation is not independently assessed, the Intermediate grade has been given for Validation Results.

Validation Activity #1 (Airbus)	
Independently Assessed?	<i>No</i>
Reference Data Representativeness	
Summary	<i>The ICESat-1 GLAS reference dataset used in this validation report is available at a global scale.</i>
Reference	<i>see RD-15 under section 2.2: ICESat-1 GLAS Reference Data</i>
Reference Data Quality & Suitability	
Summary	<i>Reference data has been filtered in order to remove outliers (see section 2.3); the vertical accuracy of the reference data is more than three times higher than the vertical accuracy of each Copernicus DEM instance (see section 2.5.1)</i>
Reference	<i>See RD-15 under sections 2.3 and 2.5.1</i>
Validation Method	
Summary	<i>The reference data elevations are converted from the Topex/Poseidon ellipsoid to the EGM2008 geoid. Reference data is filtered by taking into account the slope of the terrain and waveform of the returning signal.</i>

	<i>Erroneous data taken over water surfaces is filtered using the Copernicus DEM Water Body Mask. Acquisitions in mountainous terrain are also filtered (see section 2.3).</i>
Reference	<i>See RD-15 under sections 2.3 to 2.5.2</i>
Validation Results	
Summary	<i>Vertical accuracy is assessed relative to the WorldDEM™ product, which is the source DEM used to generate all Copernicus DEM instances. WorldDEM™ has been assessed both on the European Economic Area and globally. A vertical accuracy of 2.03 metres has been assessed for the European Economic Area (90% linear error). Globally, a vertical accuracy of 2.17m has been assessed.</i>
Reference	<i>see RD-15 under section 3: Results</i>

Validation Activity #2 (VisioTerra)	
Independently Assessed?	Yes
Reference Data Representativeness	
Summary	<i>The quality assessment of the three Copernicus DEM instances is assessed using all the terrain acquisitions of the GLAS instrument, which are available at global scale (GLAH14 product). The number of compared heights may vary from one DEM study to another, as bad quality data is filtered both on the DEM products and ICESat-1 products.</i>
Reference	<i>see section 4.2 of this document</i>
Reference Data Quality & Suitability	
Summary	<i>GLAS acquisitions are analysed on the same orbit on multiple periods to ensure the consistency of the retrieved heights. A particularly flat area has been chosen for this assessment: The Salt Lake Salar de Uyuni in Bolivia. The results of this study highlight the accuracy and constancy of GLAS acquisitions.</i>
Reference	<i>see section 4.2.3 of this document</i>
Validation Method	
Summary	<i>Copernicus DEMs heights are compared to ICESat-1 acquisitions to assess their accuracy. The ICESat-1 data is filtered using the provided quality flags. At each ICESat-1 footprint location, an interpolated height is processed from each Copernicus DEM. Both ICESat-1 and Copernicus DEMs heights are converted from their original vertical reference system to the WGS84 ellipsoid, from which every ICESat-1 height is subtracted to its corresponding Copernicus DEM instance interpolated height.</i>
Reference	<i>see section 4.2.4.2 of this document</i>
Validation Results	
Summary	<i>The results show an average difference between the height value in ICESat-1 and Copernicus DEM GLO-30 of 0.025 metres with a RMSE of 0.457 metres. Other results are available in the referenced sections below.</i>
Reference	<i>see sections 4.2.4.3, 4.2.5.3 and 4.2.6.3 of this document</i>

Validation Activity #3 (VisioTerra)	
Independently Assessed?	Yes
Reference Data Representativeness	
Summary	<i>The quality assessment of the three Copernicus DEM instances is assessed using all the terrain and canopy acquisitions of the ATLAS instrument (ATL08 product, 9 orbit cycles of acquisition). The number of compared heights may vary from one DEM study to another, as bad quality data is filtered both on the DEM products and ICESat-2 products. Results of this study are compared to results obtained taking ICESat-1 / GLAH14 data as a vertical reference (Validation Activity #2).</i>
Reference	<i>see section 4.3 of this document</i>
Reference Data Quality & Suitability	
Summary	<i>ATLAS acquisitions are analysed on the same orbit on multiple periods to ensure the consistency of the retrieved heights. A particularly flat area has been chosen for this assessment: The Salt Lake Salar de Uyuni in Bolivia. The results of this study highlight the accuracy and constancy of ATLAS acquisitions.</i>
Reference	<i>see section 4.3.3 of this document</i>
Validation Method	
Summary	<i>Copernicus DEMs heights are compared to ICESat-2 / ATL08 terrain and canopy height estimations to assess their accuracy. The ICESat-2 data is filtered using the provided quality flags. At each ICESat-2 estimated terrain and canopy height's location, an interpolated height is processed from each Copernicus DEM. Copernicus DEMs heights are converted from their original vertical reference system to the WGS84 ellipsoid, from which every ICESat-2 height (terrain only and terrain with canopy) is subtracted to its corresponding Copernicus DEM instance interpolated height.</i>
Reference	<i>see section 4.3.4.1 of this document</i>
Validation Results	
Summary	<i>The results show a mean difference between the height values of the Copernicus DEM EEA-10 and ICESat-2 of 0.822 metres with a standard deviation of 1.944 metres for terrain heights only, and a mean difference of -5.477 metres with a standard deviation of 4.838 metres considering canopy heights (LE95). These results show that the Copernicus DEM EEA-10 heights are closer to the terrain than to the canopy. Considering terrain heights only, the statistics show that the Copernicus DEM EEA-10 is really accurate. These statements are also true for the GLO-30 and GLO-90 instances. Other results are available in the referenced sections below.</i>
Reference	<i>see sections 4.3.4.3, 4.3.5.3 and 4.3.6.3 of this document</i>

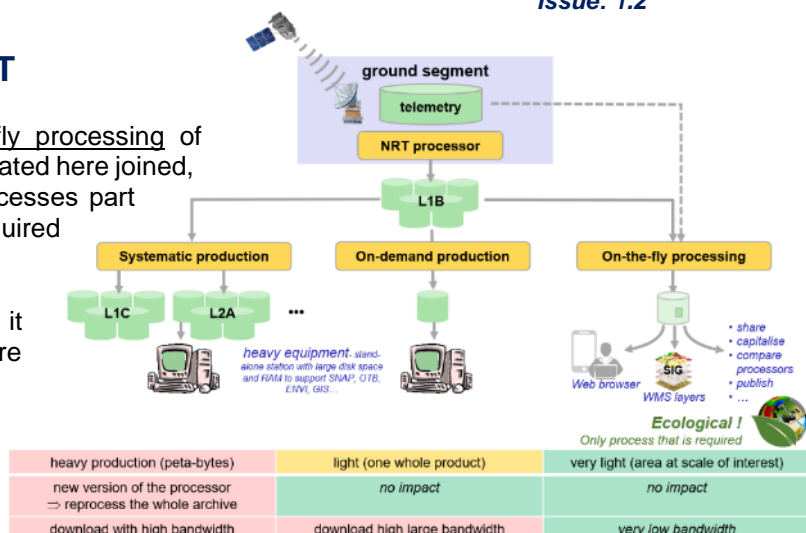
Validation Activity #4 (VisioTerra)	
Independently Assessed?	Yes
Reference Data Representativeness	
Summary	<i>The quality assessment of the three Copernicus DEM instances is assessed using one month of GEDI acquisitions (GEDI02_A product). The number of compared heights may vary from one DEM study to another, as bad quality data is filtered both on the DEM products and GEDI products. Results of this</i>

	<i>study are compared to results obtained taking ICESat-1 / GLAH14 and ICESat-2 / ATL08 data as vertical references (Validation Activity #2 and #3).</i>
Reference	<i>see section 4.4 of this document</i>
Reference Data Quality & Suitability	
Summary	<i>GED102_A heights are compared to ICESat-1 and ICESat-2 heights on a few samples over a particularly flat area: the Salar de Uyuni in Bolivia. This study is just an example of comparison between multiple LiDARs and is not representative of the overall GED102_A product quality.</i>
Reference	<i>see section 4.4.3.3 of this document</i>
Validation Method	
Summary	<i>Copernicus DEMs heights are compared to GEDI lowest mode (ground) and highest return (top of canopy) heights to assess their accuracy. The GEDI data is filtered using the provided quality flags. At each GEDI lowest mode and highest return location, an interpolated height is processed from each Copernicus DEM. Copernicus DEMs heights are converted from their original vertical reference system to the WGS84 ellipsoid, from which every GEDI height (lowest mode and highest return) is subtracted to its corresponding Copernicus DEM instance interpolated height.</i>
Reference	<i>see section 4.4.4.1 of this document</i>
Validation Results	
Summary	<i>The results show a mean difference between the height values of the Copernicus DEM EEA-10 and GEDI of 2.363 metres with a standard deviation of 5.277 metres for lowest mode, and a mean difference of -6.916 metres with a standard deviation of 3.968 metres considering highest return (LE95). These results show that the Copernicus DEM EEA-10 heights are closer to GEDI lowest mode (terrain) than to GEDI highest return (top of canopy). Other results are available in the referenced sections below.</i>
Reference	<i>see sections 4.4.4.3, 4.4.5.3 and 4.4.6.3 of this document</i>

4. DETAILED ASSESSMENT

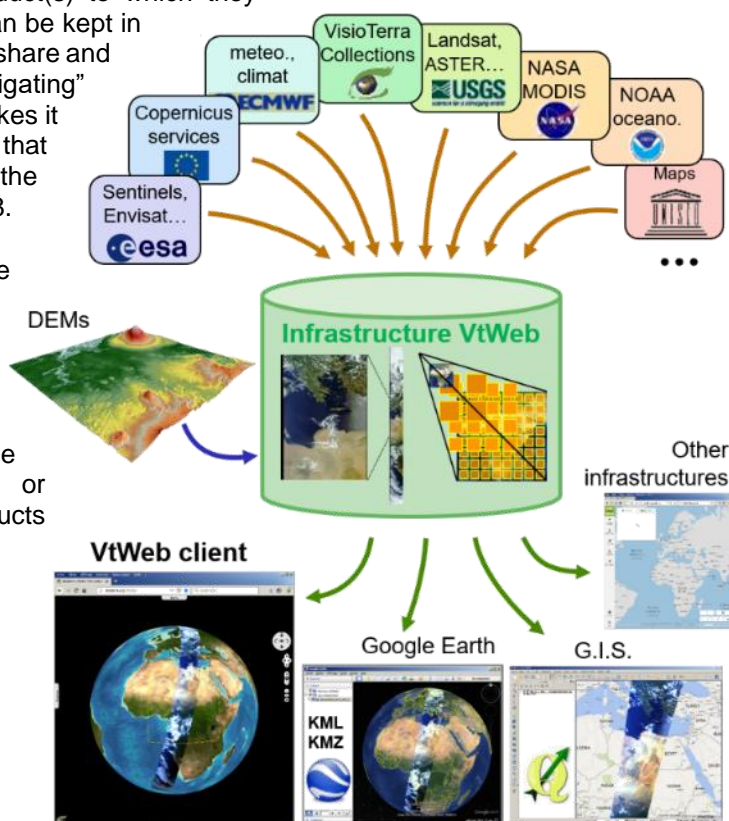
VisioTerra promotes the on-the-fly processing of data required by the user. As illustrated here joined, this “ecological process” only processes part of the products and on the required scale.

This processing strategy makes it possible to interactively configure the functions and to tune the rendering parameters according to the range of values and/or the features of the landscape.



These processing parameters, the product(s) to which they apply as well as the viewing geometry can be kept in a hyperlook, a rich URL that the user can share and that other users will replay by “navigating” interactively in the data. This process makes it possible to design galleries of use cases that can be kept. See for example, the hyperlooks documents RD-37 and RD-38.

These new possibilities require the maintenance of a server called “Data Processing Relay (DPR)” capable here of -viewing DEMs with different restitution styles (for example different shading directions), -calculating on-the-fly derived measurements (for example slope, azimuth, curvatures), or even -orthorectifying on-the-fly products previously prepared, i.e. downloaded from ESA servers (or other data providers) and organized in quadrees without modifying their geometry neither their radiometry.

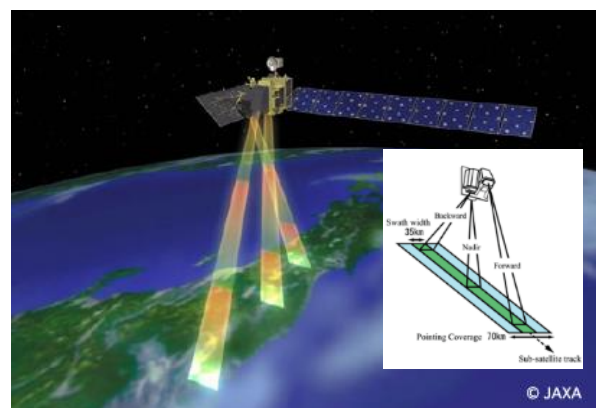


4.1 DEMs intercomparison – Qualitative assessment

The previous study (RD-35) showed that the “ALOS World 3D” DEM is clearly superior to the other two DEMs SRTM and ASTER-GDEM.

These good results are certainly due to the tri-stereo (forward, nadir and backward) acquisition technique of the PRISM instrument on board the “DAICHI” satellite (ALOS), more stringent quality assurance procedures performed by the Japanese Space Agency (JAXA) and the experience gained through the production of ASTER GDEM.

For more information about ALOS World 3D, please refer to <https://www.aw3d.jp/en/technology/>.



In this section, we qualitatively assess the differences between ALOS World 3D and Copernicus DEM GLO-30 (considered to be the reference). These two DEMs are at the same 1" arc ground sampling distance, i.e. 30 meters at the equator. All the results of this section can be found in the layer stack pointed to by the hyperlook

<https://visioterra.org/VtWeb/hyperlook/1de9b1899f7f48cb8df59a45db05ea15>

4.1.1 Global views

Before performing the subtraction between the two DEMs, the elevations of "ALOS World 3D" initially above the gravity model EGM96 are transformed into elevations above the WGS-84 ellipsoid. In the same way we transform the elevations of "Copernicus DEM GLO-30" initially above the gravimetric model EGM2008 in elevations above the ellipsoid WGS-84.

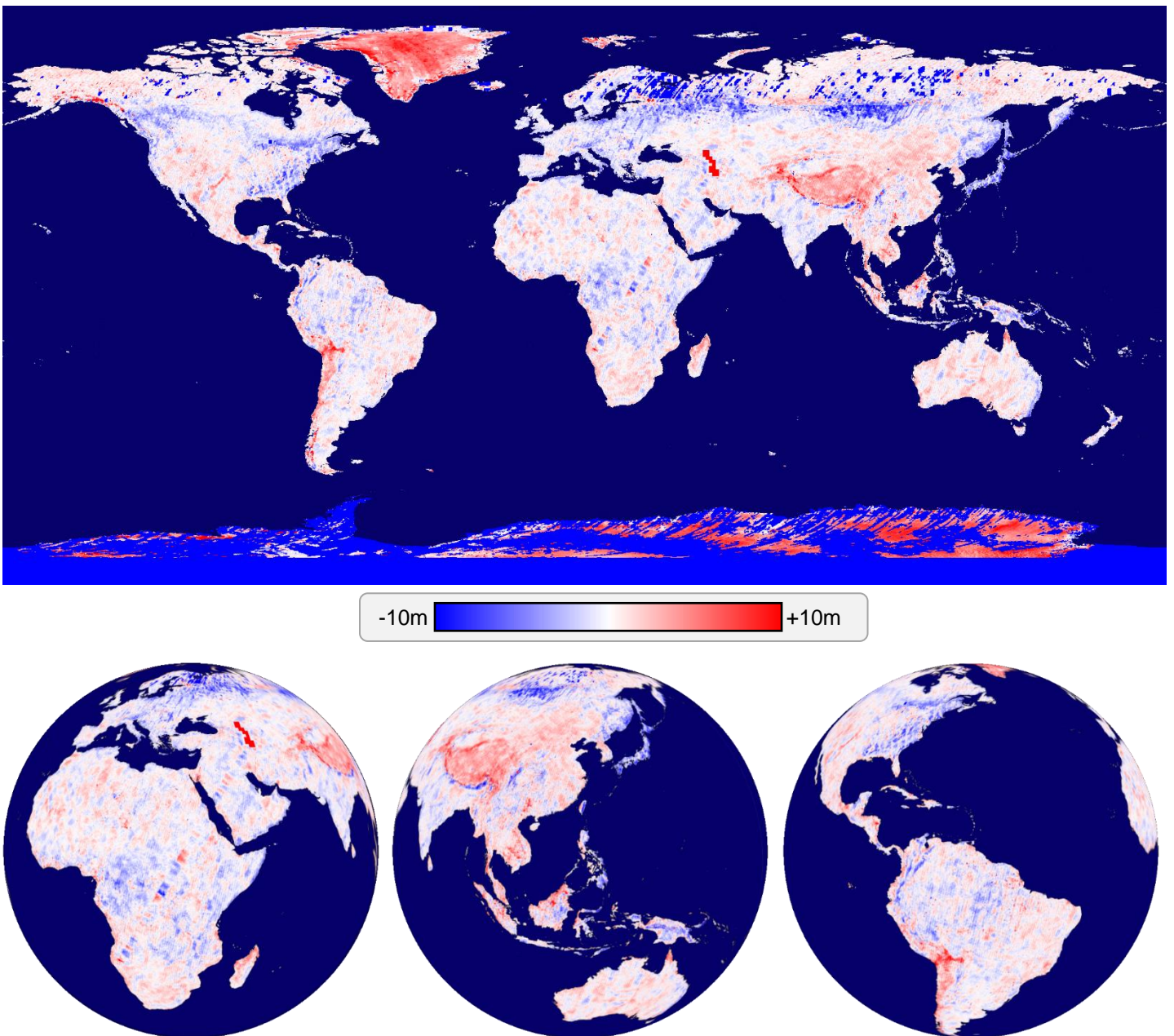


Figure 4 - **Global views of the difference between “ALOS World 3D” and “Copernicus DEM GLO-30”.**

In these 2D (geographic coordinate reference system) and 3D (vertical perspective) views, the colour chart indicates:

- **blue** that the elevations of Copernicus DEM GLO-30 are the highest,
- **white** that the elevations of ALOS World 3D and Copernicus GLO-30 are approximately equal,
- **red** that the elevations of ALOS World 3D are the highest.

More important differences will be noted at high latitudes. During the previous study (RD-35), we had already noted the weakest performances of "ALOS World 3D" outside the latitude interval $[-60^{\circ}; +60^{\circ}]$. We note in particular higher values of "ALOS World 3D" above the Antarctic, while segments of acquisitions of ALOS seem to render lower elevations in Siberia. Without being able to attribute paternity to one of the two DEMs, one observes a long segment showing differences by higher values interlaced with differences by lower values.

4.1.2 Lake Garda (Italy)

In this example, we observe an anomaly of "ALOS World 3D" on the water surface of Lake Garda. The animation <https://visioterra.org/VtWeb/hyperlook/cab3faa2c47742fba0faa271196e46e1> highlights this flaw.

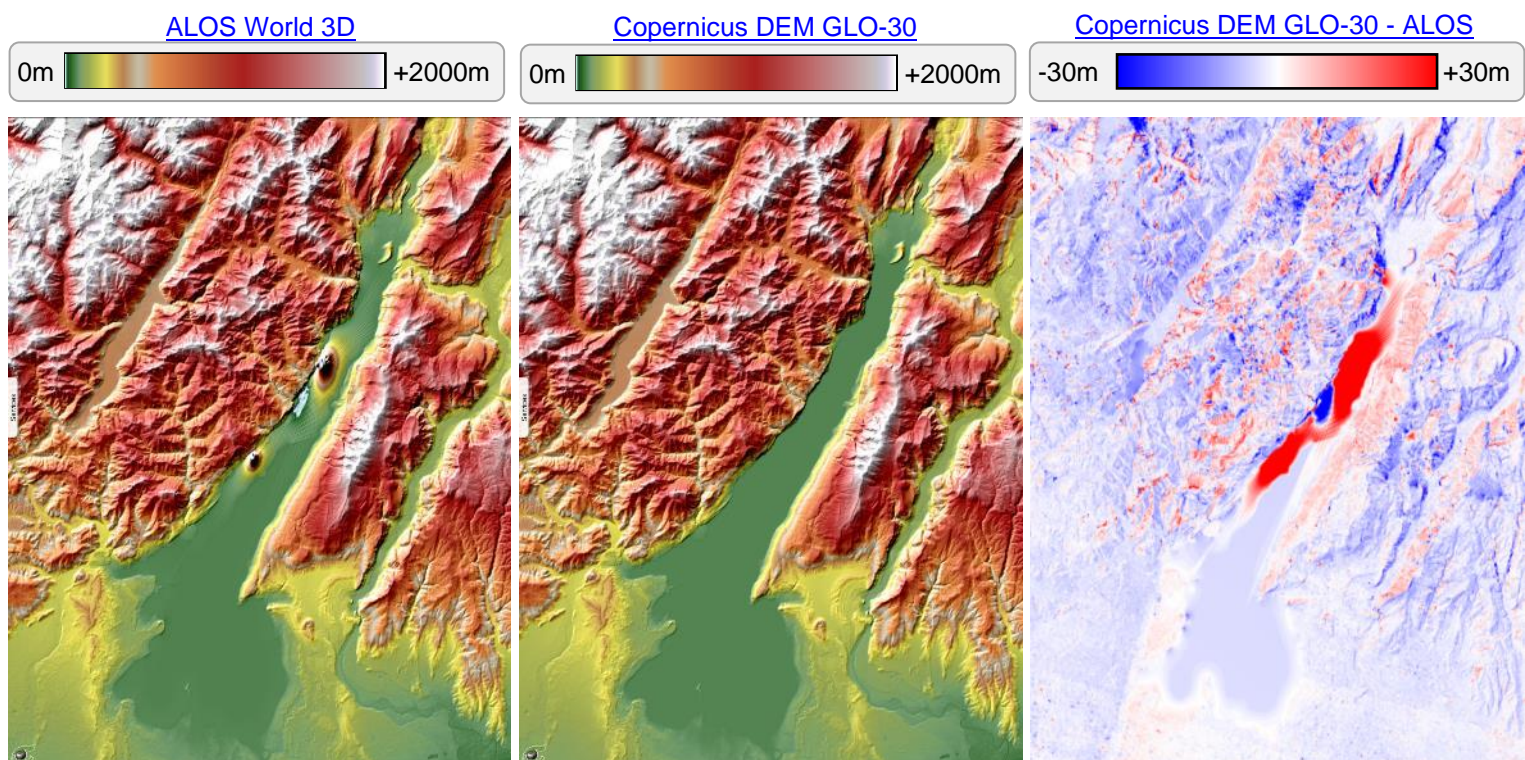


Figure 5 - Anomaly of ALOS World 3D above Lake Garda (Italy).

4.2 Elevation assessment from ICESat-1 / GLAS LiDAR – Quantitative assessment

This section 4.2 presents the quantitative evaluation of the vertical accuracy of Copernicus DEM EEA-10, Copernicus DEM GLO-30 and Copernicus DEM GLO-90 data using reference data from the ICESat-1 / GLAS LiDAR.

Unlike the previous section 4.1, the following evaluation is quantitative, consisting of the comparison between each valid elevation given in ICESat-1 products to its homologous point to be interpolated from the DEM to be verified.

4.2.1 History of ICESat-1

ICESat-1 was a mission led by the NASA Goddard Space Flight Center (GSFC). The purpose of this mission was to measure ice sheet mass balance, cloud and aerosol heights, as well as land topography and vegetation characteristics. The Geoscience Laser Altimeter System, which is a LiDAR, was developed to satisfy the needs of this mission. ICESat-1 was launched on the 13th of January 2003 and decommissioned on the 14th of August 2010, due to a laser failure that occurred on the 11th of October 2009. From February 2003 to October 2009, the GLAS instrument fired nearly 2 billion laser pulses all over the world.

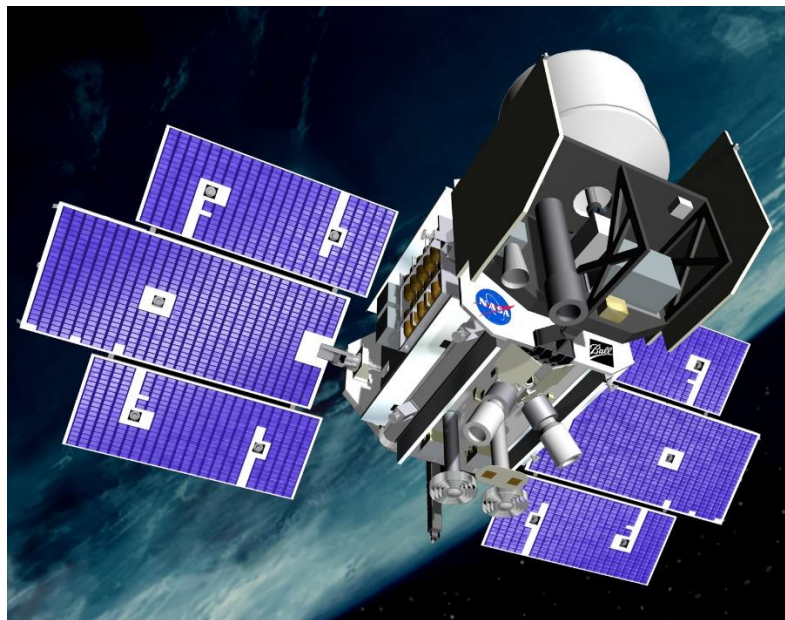


Figure 6 - ICESat-1 3D representation.
(<https://www.csr.utexas.edu/glas/>)

4.2.2 Technical specifications

Onboard ICESat-1, the Geoscience Laser Altimeter System (**GLAS**) sends laser pulses at the frequency of **40 Hz**, which approximates to an acquisition every 170 metres along track. The GLAS instrument emits laser pulses at both 532 nm and 1064 nm of wavelength.

The following figure illustrates the functioning of the GLAS instrument:

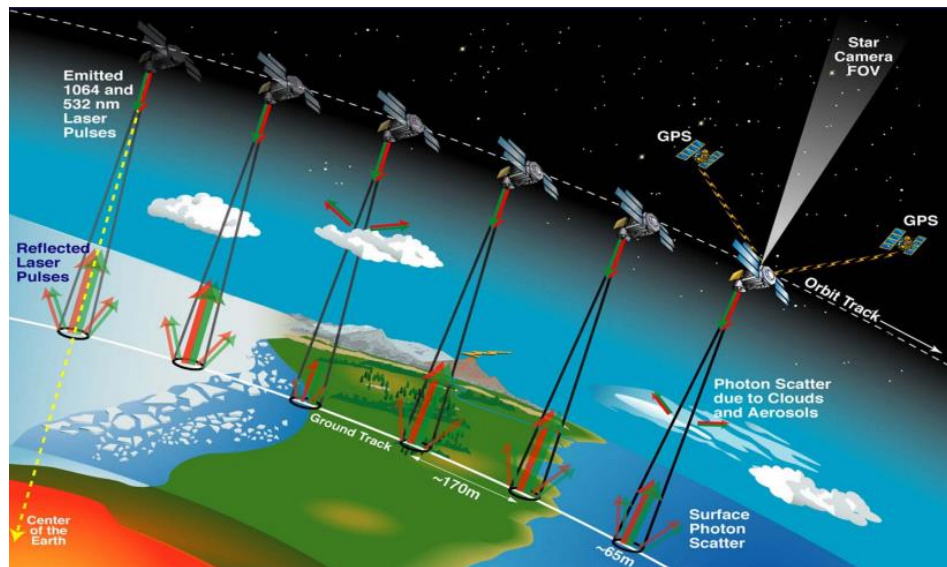


Figure 7 - GLAS instrument characteristics.
(<https://earth.esa.int/workshops/spaceandthearctic09/Zwally.pdf>)

The following table summarizes the characteristics of the ICESat-1 mission and the GLAS instrument:

Technical specification	Value
Instrument name	Geoscience Laser Altimeter System (GLAS)
First acquisition date	02.20.2003
Last acquisition date	11.10.2009
Acquisition frequency	40 Hz
Ground sampling distance	~170 m
Central wavelength	532 nm (green) / 1064 nm (near infrared)
Number of beams	1
Repeat cycle	Phase 1 – 8 days – [20/02/2003; 04/10/2003] Phase 2 – 91 days – [04/10/2003; 11/10/2009]
Footprint diameter	~70 m

Table 4 – GLAS instrument technical specifications

4.2.3 Assessment of ICESat-1 / GLAS measurements reliability

4.2.3.1 GLAH14 Product

4.2.3.1.1 Product organisation

Land altimetry data is available in the GLAH14 product. Each product is delivered in the HDF5 format and contains variables concerning location, elevation and quality of the data (in both 1 Hz and 40 Hz frequencies). The HDF5 format is a hierarchical format, organised in groups of variables. The following figure illustrates the root group of a GLAH14 product.

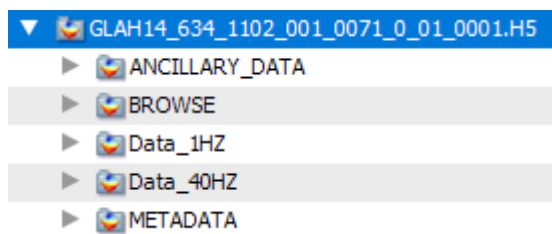


Figure 8 - Root of a GLAH14 product.

4.2.3.1.2 Data filtering

Each GLAH14 product used is filtered using these quality flags:

- **elev_use_flg** indicating whether the elevations on the record should be used (0 = true, 1 = false)
- **sat_corr_flg** indicating if a saturation correction needs to be applied (between 0 and 4, values meaning is detailed below)
- **elv_cloud_flg** indicating probable cloud contamination (0 = false, 1 = true)

The following table summarizes the meaning of each **sat_corr_flg** value (<https://insdc.org/icesat/saturation-correction>):

Value	Meaning
0	Not saturated or no signal (no correction needed)
1	Inconsequential
2	Applicable
3	Not computable
4	Not applicable

Table 5 - Values of the **sat_corr_flg** in the GLAH14 product.

Elevations having a **sat_corr_flg** value over 2 are excluded, as they can't be corrected. Saturation correction is added to the elevation values where **sat_corr_flg** equals 1 or 2. Potentially cloud contaminated elevations are removed from all the measures (where **elv_cloud_flg** equals 1).

The variable **d_satElevCorr** contains the saturation correction applied to elevations. Another correction, **d_ElevBiasCorr**, is applied to the data: this correction was determined by the GSFC on post flight analysis.

4.2.3.2 Sampling of ICESat-1 / GLAS data

This section defines the equations used in the sampling of ICESat-1 data. The following equation is used to process linear interpolation:

$$h_i = h_1 + (h_2 - h_1) * \frac{(l_1 - L_i)}{(l_2 - l_1)} \quad (\text{eq. 1})$$

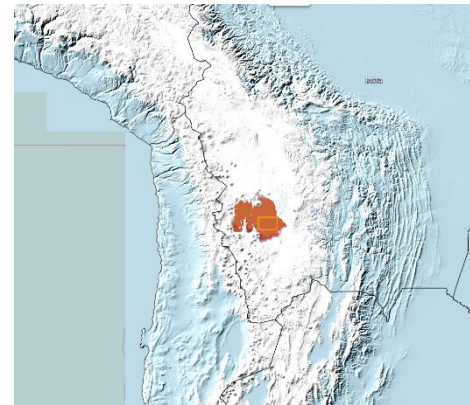
Where:

- L_i is the latitude of the height to be interpolated
- h_i is the interpolated height at L_i
- l_1 is the highest latitude $< L_i$ from the reference acquisition points
- l_2 is the lowest latitude $> L_i$ from the reference acquisition points
- h_1 is the height of the point of latitude l_1
- h_2 is the height of the point of latitude l_2

4.2.3.3 Collocated measurements on the same orbit

4.2.3.3.1 Scope

Multiple measurements are analysed on the same orbit to assess ICESat-1's instrument reliability. A particularly flat area is chosen for this assessment: The Salt Lake Salar de Uyuni in Bolivia (see attached figure).



4.2.3.3.2 Method

Definitions

The following terminology is used in this study:

- **Measurement:** height measured by ICESat-1/GLAS at a given geolocation (longitude, latitude). The geolocation of a measurement corresponds to the geolocation of the GLAS instrument's laser footprint centre during acquisition,
- **Ground track:** segment of orbit identified by an id, which remains identical from one revolution to another,
- **Profile:** set of measurements acquired contiguously along-track.

Reliability assessment

The goal of this study is to ensure ICESat-1/GLAS heights acquired over multiple revolutions on a common ground track do not largely differ. This study aims to evaluate the **constancy** of ICESat-1/GLAS height acquisitions over multiple revolutions.

For this study, measurements are extracted among the 642 products of the ICESat-1 GLAH14 dataset. Only valid measurements acquired over the study area are considered (see

4.2.3.1 for GLAH14 measurement filtering method). The following illustration shows the measurements considered for this study:

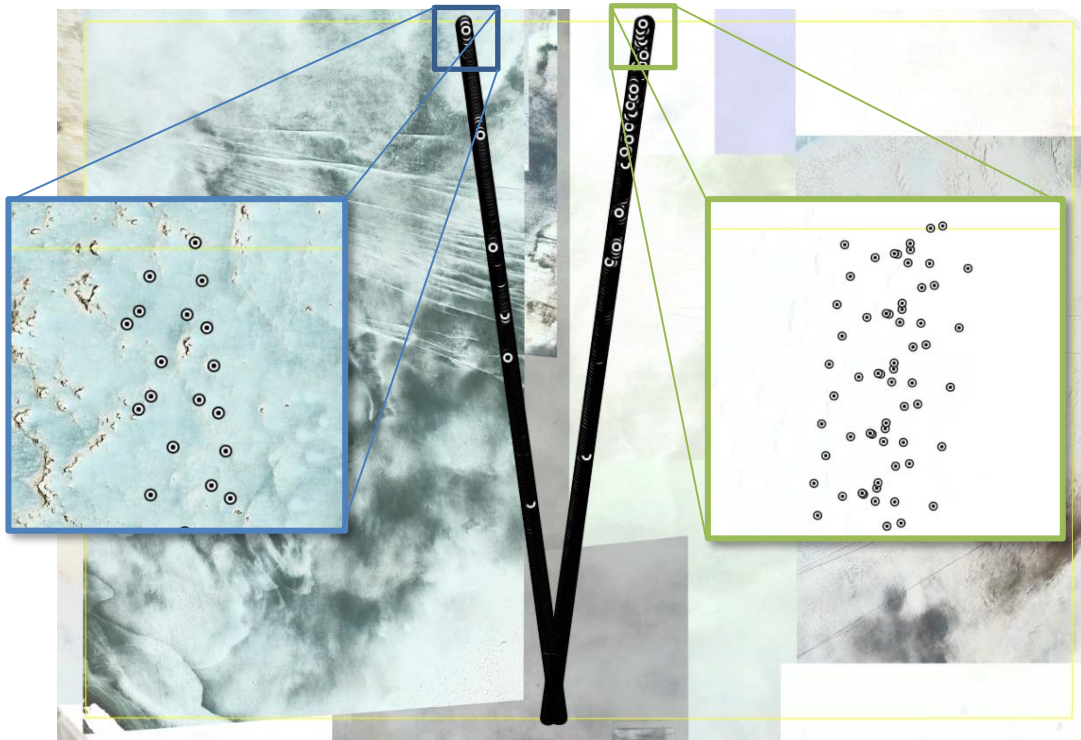


Figure 9 - Ground tracks considered for the ICESat-1 reliability study.

The following table gives an exhaustive list of GLAH14 products used in this study:

Ground track	Product identifier
351	GLAH14_634_2107_002_0351_0_01_0001.H5
	GLAH14_634_2109_002_0351_0_01_0001.H5
	GLAH14_634_2115_002_0351_0_01_0001.H5
	GLAH14_634_2113_002_0351_0_01_0001.H5
	GLAH14_634_2121_002_0351_0_01_0001.H5
	GLAH14_634_2111_003_0351_0_01_0001.H5
85	GLAH14_634_2123_002_0085_0_01_0001.H5
	GLAH14_634_2125_002_0085_0_01_0001.H5
	GLAH14_634_2107_003_0085_0_01_0001.H5

Ground track	Product identifier
	GLAH14_634_2113_002_0085_0_01_0001.H5
	GLAH14_634_2119_002_0085_0_01_0001.H5
	GLAH14_634_2103_002_0085_0_01_0001.H5
	GLAH14_634_2111_003_0085_0_01_0001.H5
	GLAH14_634_2121_002_0085_0_01_0001.H5
	GLAH14_634_2107_002_0085_0_01_0001.H5
	GLAH14_634_2115_002_0085_0_01_0001.H5
	GLAH14_634_2109_002_0085_0_01_0001.H5
	GLAH14_634_2115_003_0085_0_01_0001.H5

Table 6 – ICESat-1 GLAH14 ground tracks and products studied.

As shown in Figure 9, from one revolution to another, horizontal shifts may occur between the acquired profiles. These shifts may lead to important differences in height between measurements acquired over multiple revolutions on the same ground track. The choice of a particularly flat area for this study minimizes these height differences, but the horizontal shift prevents from comparing heights of multiple profiles over a same ground track directly: heights need to be interpolated at a fixed step on each profile.

ICESat-1/GLAS acquires measurements at 40Hz, which approximates to a ground sampling distance of 170 metres along-track near equator. Starting from the top of the study area, heights are interpolated linearly every 170 metres (fixed step in latitude) for each profile (see 4.2.3.2 for the equation of the linear interpolation). An interpolated height is only valid if the following conditions are true:

- Considering measurements with latitudes lower than the interpolated height latitude, the measurement with the highest latitude should be located at less than 170 metres of the interpolated height in latitude,
- Considering measurements with latitudes higher than the interpolated height latitude, the measurement with the lowest latitude should be located at less than 170 metres of the interpolated height in latitude,
- Along-track measurements from which the height is interpolated should be contained in the study area.

Given interpolated heights at a fixed step in latitude, standard deviation of the computed heights is calculated at each step, considering every profile of a ground track. Statistics are calculated based on these standard deviation calculations.

4.2.3.3.3 Results

The following figures show, for the two studied ground tracks, the evolution of the interpolated heights of each profile according to the latitude:

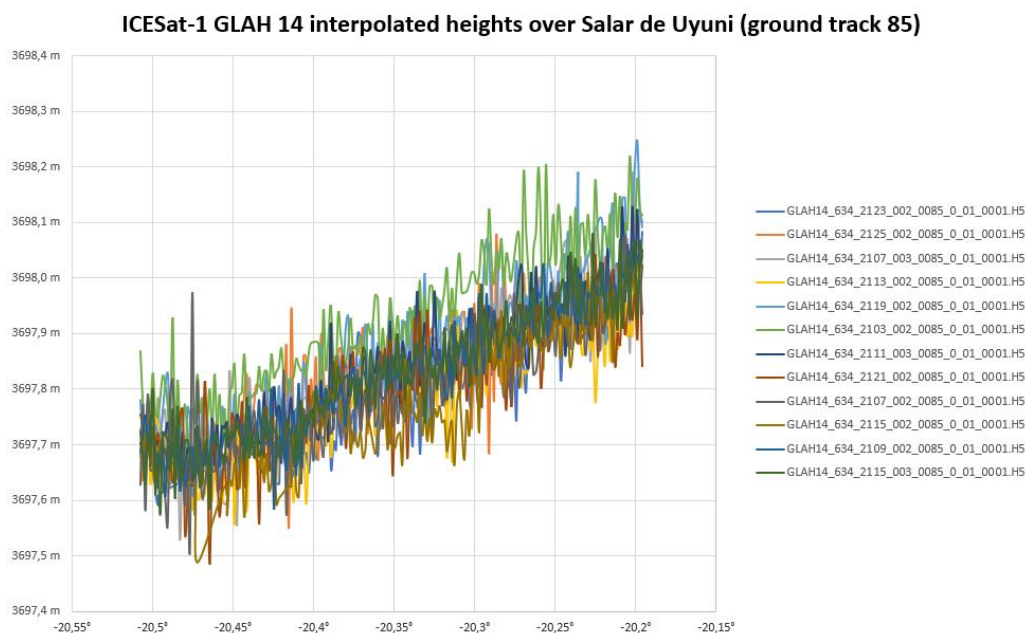


Figure 10– ICESat-1 reliability study, interpolated heights over ground track 85.

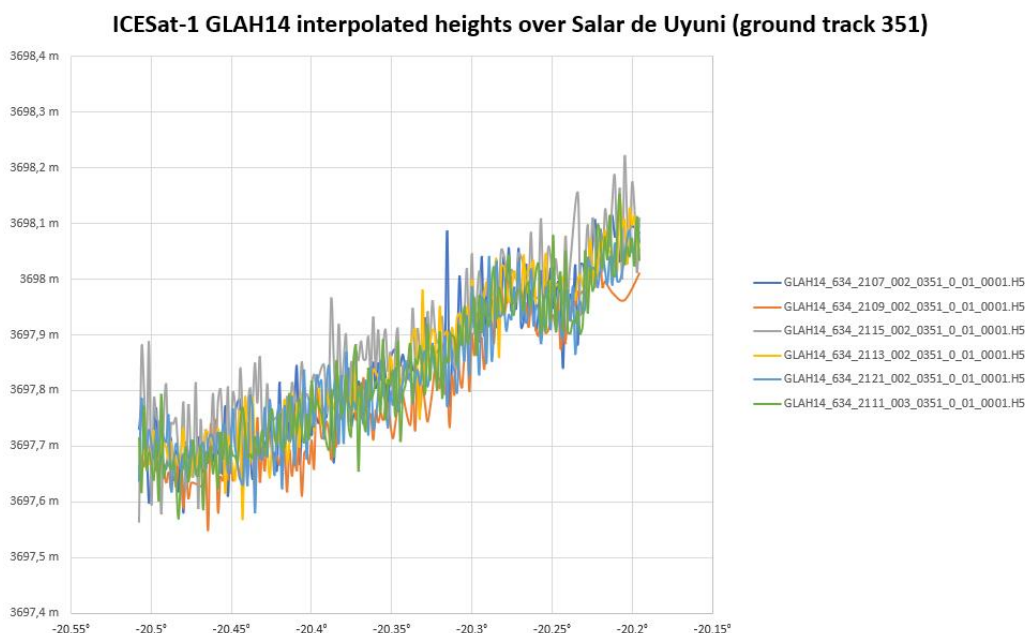


Figure 11 – ICESat-1 reliability study, interpolated heights over ground track 351.

Ground track 85 interpolated heights approximately range from 3697,5 metres to 3698,25 metres, whereas ground track 315 interpolated heights approximately range from 3697,55 metres to 3698,25 metres among all profiles.

The following table gives the statistics calculated for this study. These statistics are calculated at every latitude step, regarding the standard deviation of the interpolated heights of every profile among a ground track:

Per latitude step statistics					
Ground track	Count	Min	Max	Arithmetic Mean	Standard Deviation
85	204	0,029 m	0,112 m	0,064 m	0,016 m
351	204	0,013 m	0,115 m	0,049 m	0,017 m

Table 7 – Statistics regarding standard deviation of interpolated heights at each latitude.

The statistics show that the constancy of ICESat-1/GLAS measurements is really good, considering a maximal arithmetic mean of 0,064 metres and standard deviation of 0,017 metres.

4.2.3.4 Geographical distribution of ICESat-1 products

The assessments performed in this document are based on the **642 products** of ICESat-1 mission. Most of the products contain one day acquisition over 14 revolutions. These products are distributed all over the world as shown in the following figures.

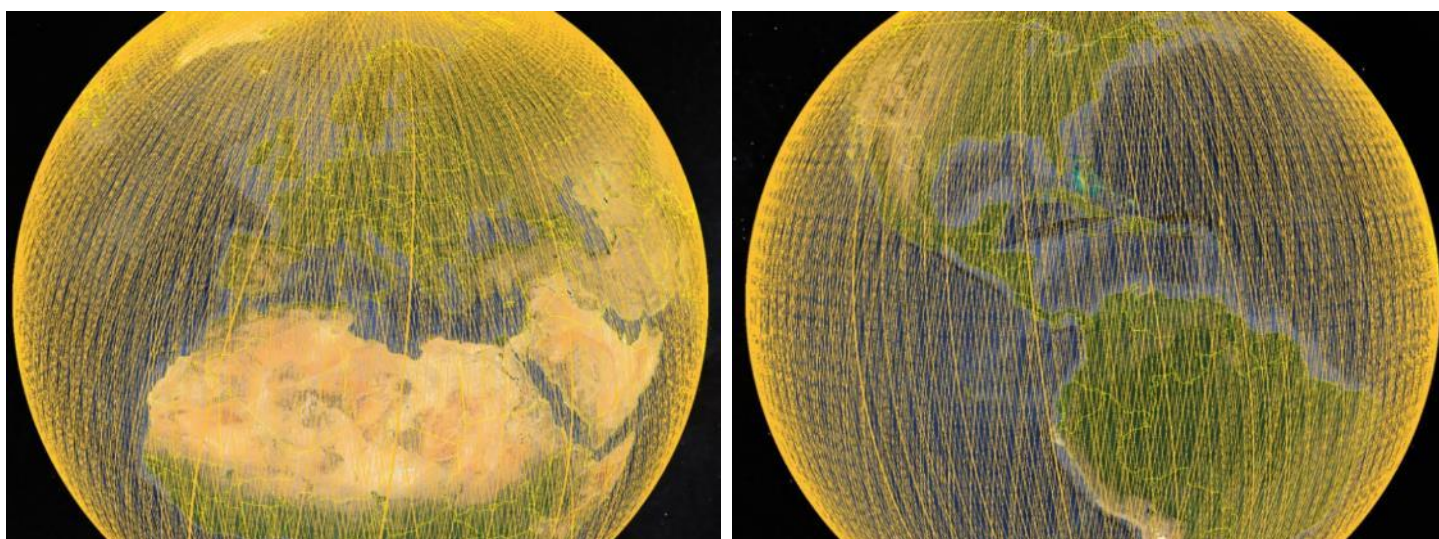


Figure 12 - Distribution of the 642 ICESat-1 products.

4.2.4 Assessment of Copernicus DEM EEA-10 from ICESat-1 / GLAS data

This section 4.2.4 presents the quantitative evaluation of the vertical accuracy of Copernicus DEM EEA-10 using reference data from the ICESat-1 / GLAS LiDAR. The method and the notations of the next subsection 4.2.4.2 are detailed here after. The same methods will apply for the evaluation of Copernicus DEM GLO-30 (section 4.2.5) and Copernicus DEM GLO-90 (section 4.2.6) and will not be repeated.

4.2.4.1 Spatial extent

As opposed to the global spatial extent of Copernicus DEM GLO-30 and Copernicus DEM GLO-90, Copernicus DEM EEA-10 is spatially restricted to the European Economic Area. The following figure (hyperlink

<https://visioterra.org/VtWeb/hyperlook/be0edefce6cd410686fe647deeed2529>) shows the coverage map of Copernicus DEM EEA-10:

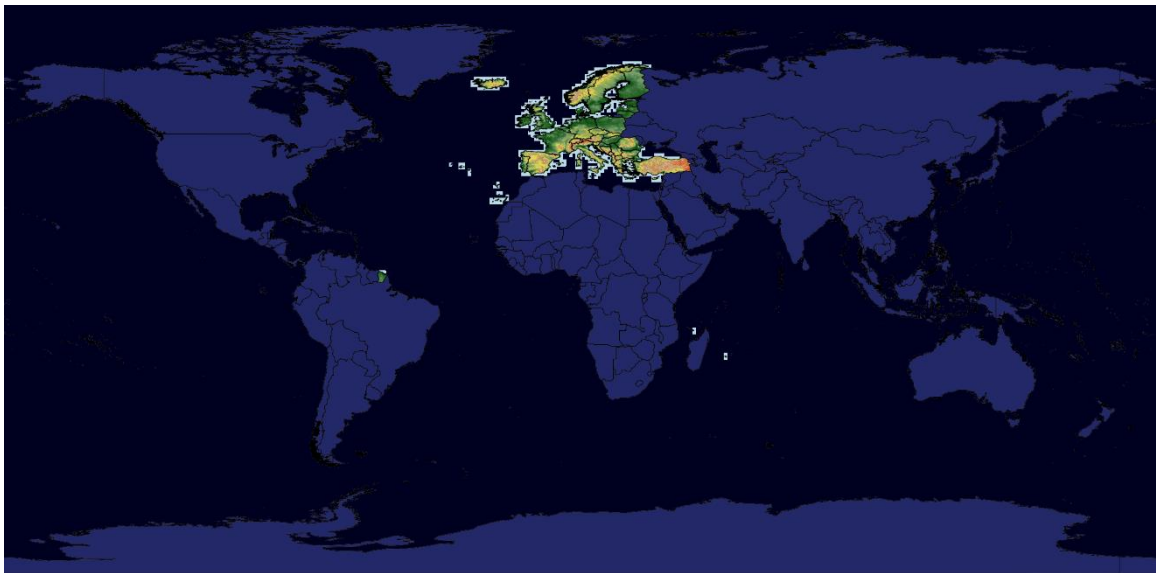


Figure 13 - Copernicus DEM EEA-10 coverage map.

4.2.4.2 Method and notations

Scope of the numerical analysis is to process height error statistics concerning Copernicus DEM EEA-10, given ICESat-1 GLAH14 products as a vertical reference.

4.2.4.2.1 Conversion from TOPEX / Poseidon to WGS84

ICESat-1 elevations are relative to the TOPEX/Poseidon ellipsoid and shall be converted to the WGS84 ellipsoid using the following formula (see <https://www.mdpi.com/2072-4292/10/2/297/htm>):

$$\Delta h = \frac{a'(1 - e'^2)}{\sqrt{1 - e'^2 \sin^2 \phi}} - \frac{a(1 - e^2)}{\sqrt{1 - e^2 \sin^2 \phi}} \quad (\text{eq. 2})$$

Where:

- a is the semi-major axis of the WGS84 ellipsoid,
- e is the eccentricity of the WGS84 ellipsoid,
- a' is the semi-major axis of the TOPEX/Poseidon ellipsoid,
- e' is the eccentricity of the TOPEX/Poseidon ellipsoid,
- ϕ is the latitude of the elevation (relative to the TOPEX/Poseidon ellipsoid),

Δh is the difference in elevation between the TOPEX/Poseidon and WGS84 ellipsoids.

This formula gives the difference in elevation between the WGS84 and TOPEX/Poseidon ellipsoids. This difference has to be subtracted from the TOPEX/Poseidon referenced elevations, as the TOPEX/Poseidon ellipsoid is smaller than WGS84. The following table (found at <https://nsidc.org/data/icesat/faq.html#alt7>) summarizes the differences between the WGS84 and TOPEX/Poseidon ellipsoids:

	TOPEX/Poseidon	WGS84
Equatorial radius (a)	6 378 136.3 metres	6 378 137.0 metres
Polar radius (b)	6 356 751.600 563 metres	6 356 752.314 245 metres
Reciprocal flattening (1/f)	298.25700000	298.25722356
Eccentricity (e)	0.081819221456	0.081819190843

Table 8 - Difference between TOPEX/Poseidon and WGS84 ellipsoids.

The differences in latitudes between these two ellipsoids are small (up to +/-1.5 cm), as illustrated by the following graph (see data in <ftp://sidacs.colorado.edu/pub/DATASETS/icesat/tools/idl/ellipsoid/>):

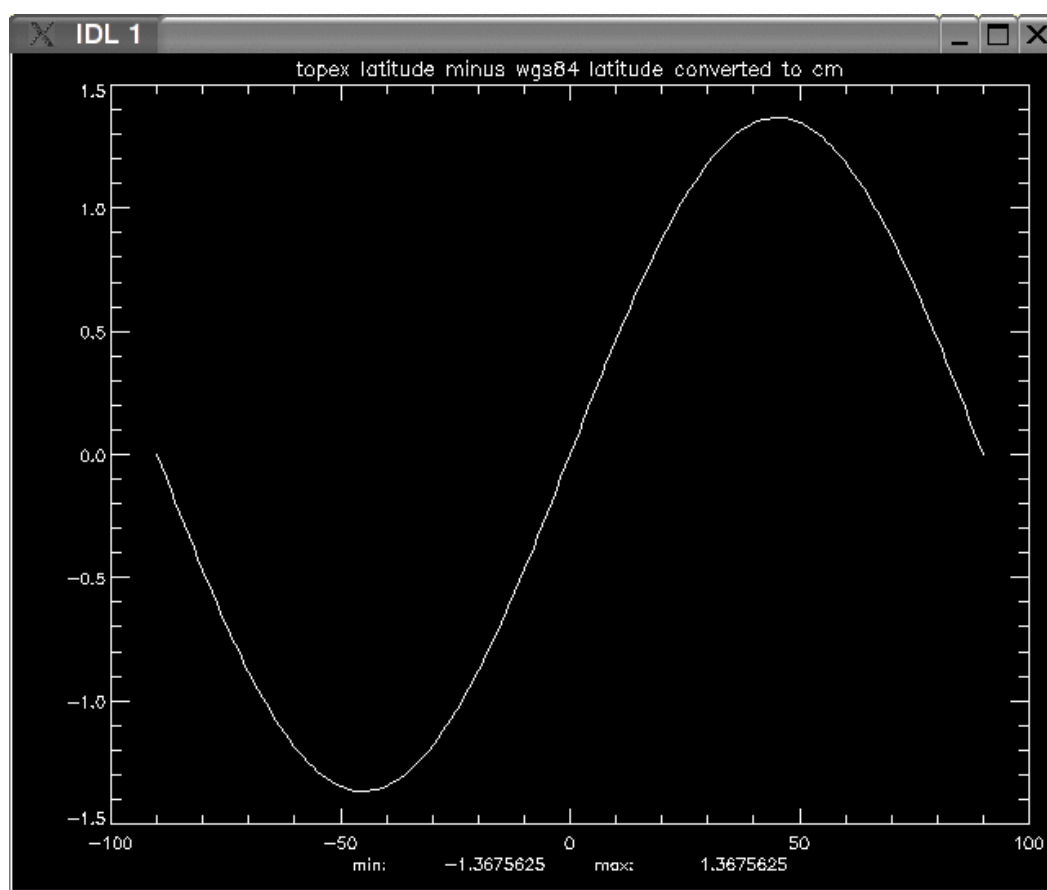


Figure 14 - Latitude difference between WGS84 and TOPEX/Poseidon ellipsoids (in centimetres).

Latitudes can be considered as equal from TOPEX/Poseidon to WGS84, as the maximum difference in latitude between the two ellipsoids is far below the horizontal accuracy of

ICESat-1. On average, horizontal accuracy ranges from 0.0 to 4.63 metres, with a minimal standard deviation of 2.22 metres.

4.2.4.2.2 From ICESat-1 longitude and latitude to the Copernicus DEM EEA-10 tile

The longitude and latitude ranges of each product are the following:

- ICESat-1: longitude $\in [0^\circ, 360^\circ]$, latitude $\in [-90^\circ, +90^\circ]$
- Copernicus DEM EEA-10: longitude $\in [-180^\circ, 180^\circ]$, latitude $\in [-90^\circ, +90^\circ]$

To match Copernicus DEM EEA-10 with ICESat-1 longitudes, 360° are subtracted from all ICESat-1 longitudes values greater than 180° .

To compare ICESat-1 to Copernicus DEM EEA-10 elevations, a corresponding Copernicus DEM EEA-10 tile is found for each ICESat-1 footprint, and the exact cell of the DEM containing it. The Copernicus DEM EEA-10 tile name pattern is the following:

Copernicus_DSM_10_<c><l>_00_<C><L>_00_DEM.tif

Where:

- | | |
|---|---|
| c | corresponds to the latitude's cardinal (S for South or N for North) |
| l | is the latitude in degrees ranging from 00 to 90 |
| C | corresponds to the longitude's cardinal (E for East or W for West) |
| L | is the longitude in degrees ranging from 000 to 180 |

Example: For ICESat-1_longitude = -96.051 and ICESat-1_latitude = 42.472, the corresponding Copernicus DEM EEA-10 tile is entitled:

"Copernicus_DSM_10_N42_00_W097_00_DEM.tif"

A Copernicus DEM EEA-10 tile is composed of 3601 rows and a varying number of columns (depending on the latitude). The bottom left value of the file corresponds to the smallest longitude and latitude. The following equation gives the position of the corresponding sample in the file:

$$p = |C - C \times y| \times L + |L \times x| \quad (\text{eq. 3})$$

Where:

- | | |
|-----|--|
| p | is the position of the sample |
| L | is the line size in bytes |
| C | is the column size |
| x | corresponds to ICESat-1 longitude's digits |
| y | corresponds to ICESat-1 latitude's digits |

Interpolating ICESat-1 footprints on the Copernicus DEM EEA-10 grid is necessary, as the location of ICESat-1 acquisitions are punctual, in opposite to regularly gridded elevation sources, such as DEMs. Bilinear interpolation is used on the Copernicus DEM EEA-10 grid to obtain elevations at each ICESat-1 footprint location.

4.2.4.2.3 From EGM2008 to WGS84

The EGM2008 geoid is the vertical reference system of Copernicus DEM EEA-10, longitudes and latitudes referring to the WGS4 ellipsoid. As a result, only elevations need to be converted from EGM2008 to the WGS84 ellipsoid, which is done considering EGM2008's geoid undulations. EGM2008 is distributed by the [NGA/NASA](#) as a grid, with respect to the WGS84 ellipsoid (see RD-33). At each Copernicus DEM EEA-10/ICESat-1 height comparison location, bilinear interpolation is used on the EGM96 undulation grid to retrieve heights relative to the WGS84 ellipsoid.

In this case, EGM2008 undulation values are added to the interpolated Copernicus DEM EEA-10 heights, retrieving Copernicus DEM EEA-10 heights relative to WGS84.

Figure here after shows the EGM2008 undulations over the WGS84 ellipsoid.

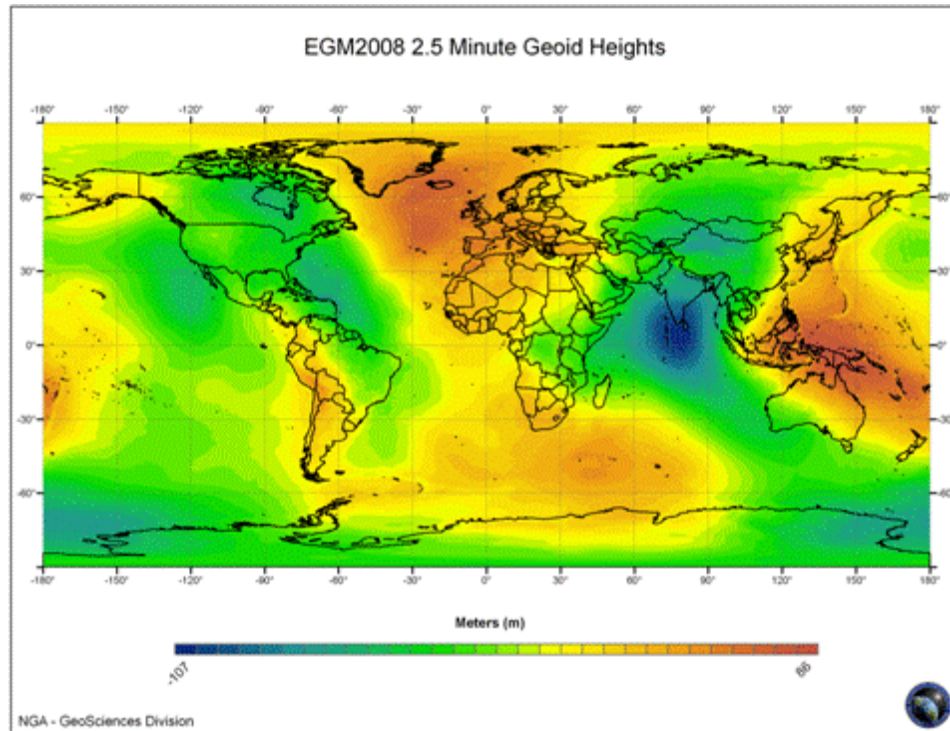


Figure 15 - **EGM2008 map with reference to WGS84.**

4.2.4.2.4 Computing the height difference

Height difference between Copernicus DEM EEA-10 and ICESat-1 is finally calculated:

$$\Delta h = h_{DEM} - h_{ICESat-1} \quad (\text{eq. 4})$$

Where:

- Δh is the height difference between Copernicus DEM EEA-10 and ICESat-1,
- $h_{ICESat-1}$ is the ICESat-1 height (with respect to the WGS84 ellipsoid),
- h_{DEM} is the Copernicus DEM EEA-10 height (with respect to the WGS84 ellipsoid).

4.2.4.2.5 Overall algorithm

The following diagram summarizes all the steps of the ICESat-1/Copernicus DEM EEA-10 height comparison:

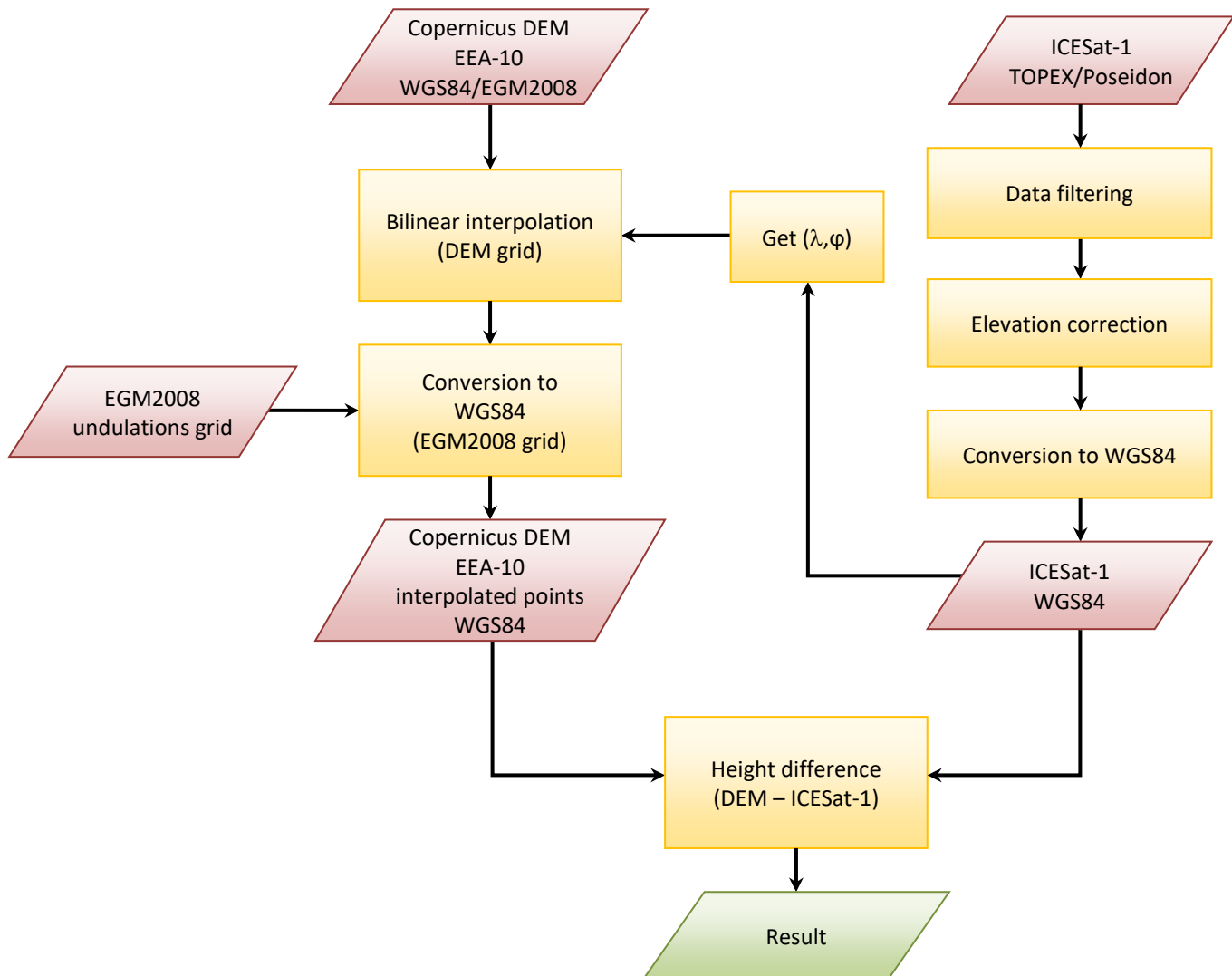


Figure 16 - Summary of the Copernicus DEM EEA-10 assessment method.

4.2.4.3 Results

Here are the results of this study. All the statistics refer to the differences between Copernicus DEM EEA-10 and ICESat-1 heights (Copernicus DEM EEA-10 – ICESat-1):

	Raw	LE95	LE90
Number of ICESat-1 products	642		
Number of compared heights	1 898 474	1 818 857	1 723 128
Min	-2641.975 m	-5.924 m	-3.422 m
Max	119.259 m	5.924 m	3.422 m
Mean (metres)	0.539 m	0.270 m	0.111 m
RMSE (metres)	9.535 m	1.415 m	0.983 m
Standard deviation (metres)	9.520 m	1.389 m	0.976 m
Median (metres)	0.03 m	0.00 m	-0.01 m
Skewness	1.436	1.091	0.679
Kurtosis	146.872	3.797	1.894

Table 9 - Statistics of the (Copernicus DEM EEA-10 – ICESat-1) comparison.

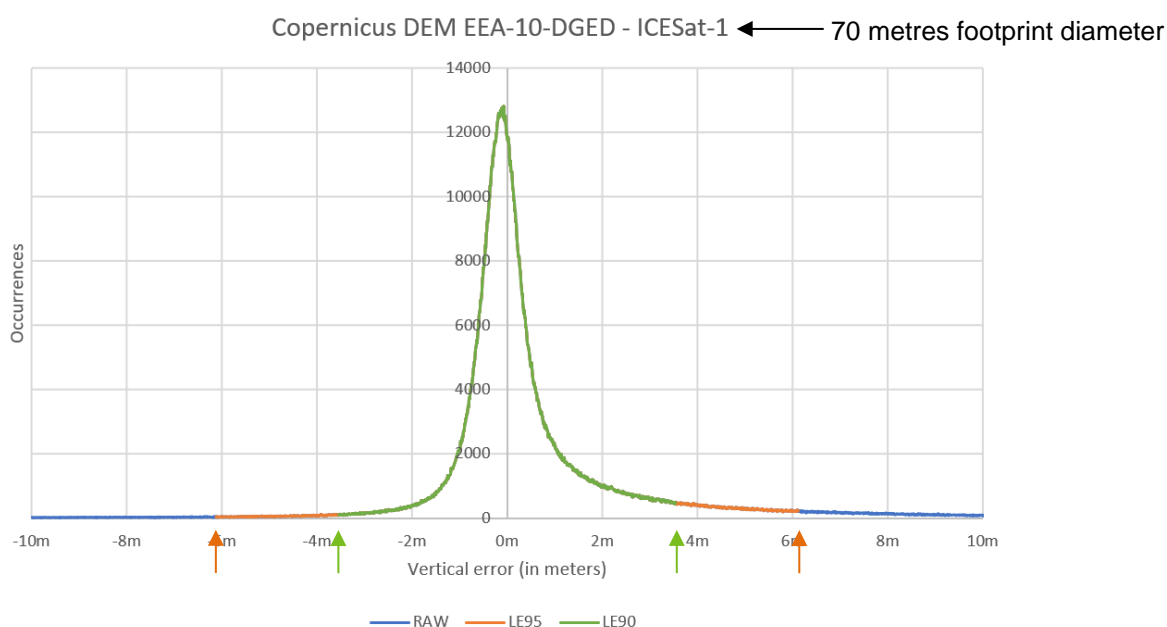


Figure 17 - Error histogram of the (Copernicus DEM EEA-10 – ICESat-1) comparison.

Arithmetic mean (0.270 m, 95% linear error) gives the systematic bias between Copernicus DEM EEA-10 and ICESat-1 heights. Root Mean Square Error or RMSE (1.415 m, 95% linear error) is the quadratic mean of the errors including the bias. Standard deviation (1.389 m, 95% linear error) gives the distribution of the errors around the mean out of the bias. The median error m is the one for which 50% of the pixels have an error less than m and 50% have an error greater than m.

This histogram looks like the Normal distribution (Gaussian) with a small positive bias.

4.2.4.4 Typical sources of elevation errors

4.2.4.4.1 ICESat-1 elevation errors

ICESat-1 data is reliable and precise, however, after filtering, a small percentage of outliers remain in the reference data. The main cause of outliers is the presence of clouds during the data acquisition. Most of the clouds are filtered by using product quality flags (see 4.2.3.1) but a small percentage of acquisitions still don't correspond to the terrain height but to the top of clouds height.

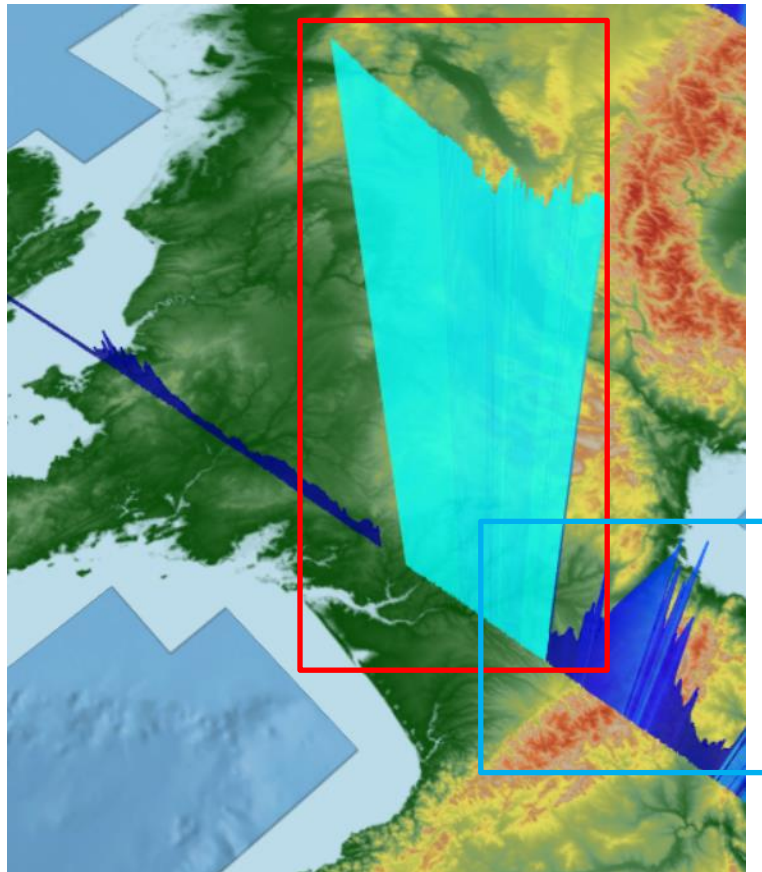


Figure 18 - **ICESat-1 cloud outliers over France.**

In Figure 18, a 3D profile corresponds to multiple ICESat-1 height acquisitions over the same orbit taken over France. Copernicus DEM GLO-30 has been used as a background map to distinguish good and bad ICESat-1 acquisitions: green areas represent relatively low elevations whereas intermediate or high elevations are coloured in yellow/red. In this case, an example of good elevation acquisition is delimited by the blue rectangle: the ICESat-1 acquired heights increase and decrease progressively, following the height colour gradient of the Copernicus DEM GLO-30. An example of bad ICESat-1 acquisition is delimited by the red rectangle: an abrupt change of height is detected by ICESat-1 (multiple kilometres), which is not highlighted by the DEM background map. In this case, the most probable explanation is that these acquisitions correspond to the top of clouds that were not filtered by the cloud mask of the ICESat-1 product concerned.

4.2.4.4.2 Geomorphological and land use / land cover context causing elevation errors

This section aims to provide a better understanding of the sources of elevation errors by observing their repartition all over the geographical extent of Copernicus DEM EEA-10. In the figures of this section, negative height errors are depicted in blue (Copernicus DEM EEA-10 height is lower than the ICESat-1 reference height) whereas positive height errors are depicted in red (Copernicus DEM EEA-10 height is greater than the ICESat-1 reference height). The labelling associated with each elevation error geolocation corresponds to the value of the height error in metres (value of Δh). The following subsections present potential causes of these elevation errors.

Sparse canopy

Assessing a Digital Surface Model (DSM) from LiDAR data can cause high elevation errors in case of sparse canopy. A gridded elevation model such as a DSM cannot highlight drastic height changes, which can punctually be highlighted by LiDAR data.

This type of error is highlighted in the case study of Figure 19. In this case study of Życiński Las near Żytina in Poland, a high elevation error is retrieved (+14.939 m). This height error is certainly due to the sparse canopy of this area, for which the acquired height of ICESat-1 is relative to the ground, whereas the Copernicus DEM EEA-10 height is relative to the canopy.

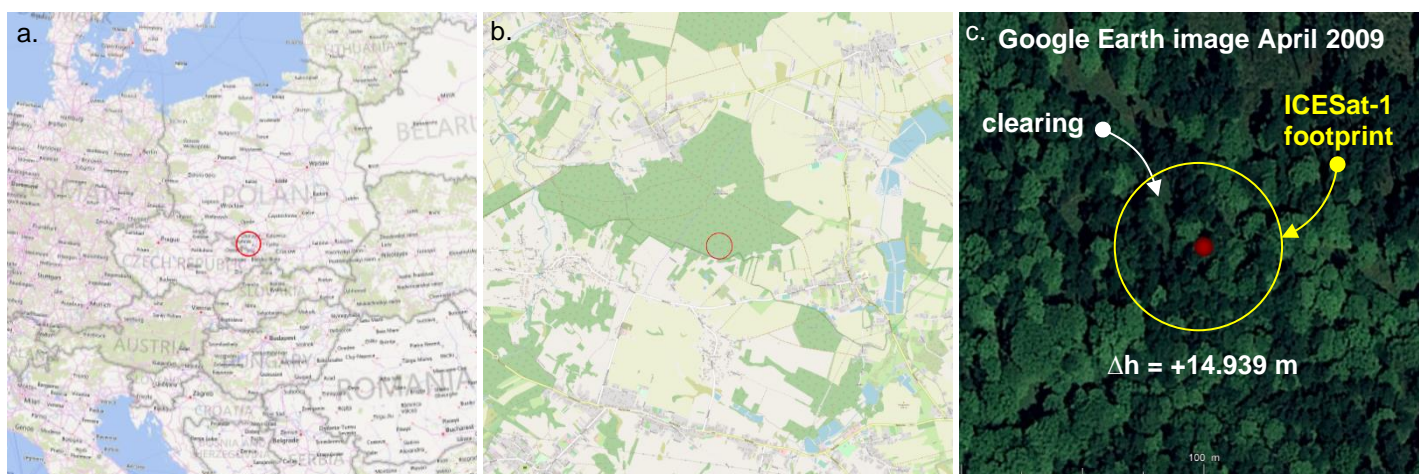


Figure 19 - EEA-10 - ICESat-1 height differences - Case of Życiński Las near Żytina (Poland).

Deforestation

Deforestation occurring between the ICESat-1 and TanDEM-X missions may cause errors, as these missions had two distinct temporal acquisition intervals (2003 to 2009 for ICESat-1, 2010 to 2015 for TanDEM-X). This type of error is highlighted by the case study of Figure 19, subfigure c, which shows an example of height error linked to deforestation in Forêt de la Matte near Matemale in France.

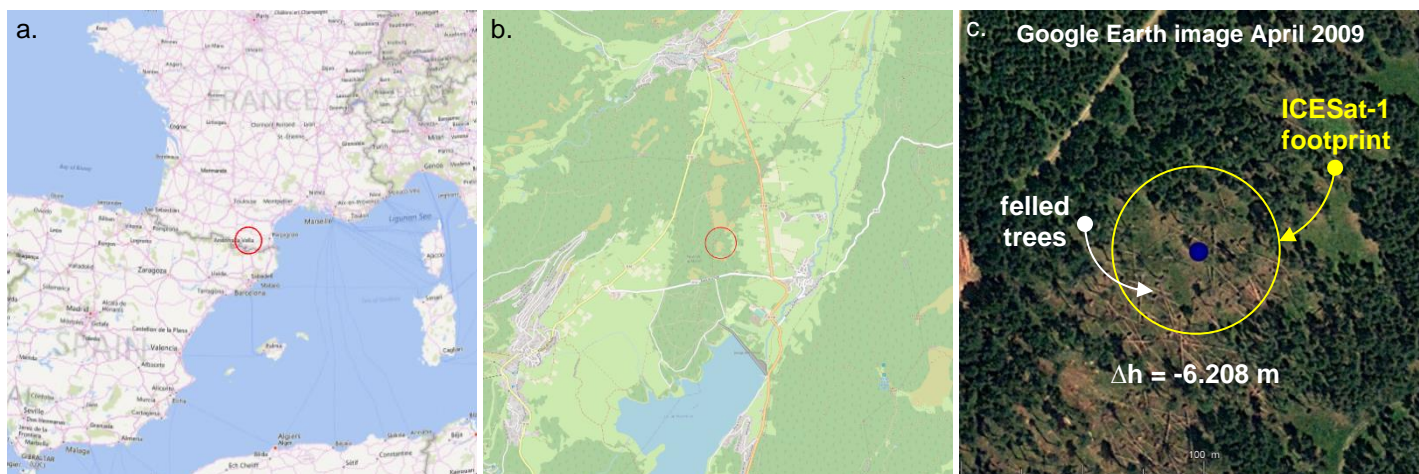


Figure 20 - EEA-10 - ICESat-1 height differences – Case of Forêt de la Matte near Matemale (France).

The case study of Figure 20 shows a height error geolocated over an area which was deforested. This area was observed on two dates, for which the acquisitions are shown in Figure 21.

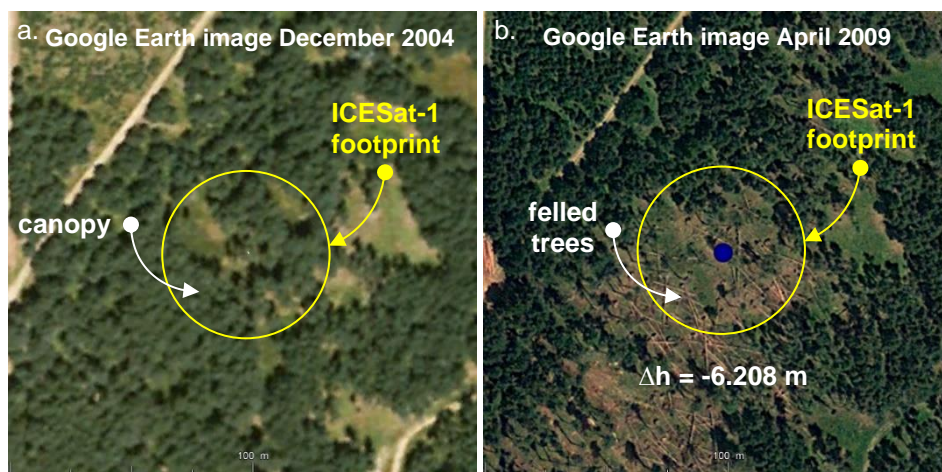


Figure 21 - EEA-10 - ICESat-1 height differences – Evolution of the studied deforestation over two acquisition dates.

The first acquisition of Figure 21 (subfigure a) was taken in December 2004 and shows no sign of deforestation. The second acquisition (subfigure b), acquired in April 2009, shows the same study area but deforested. As ICESat-1 height acquisitions range from 2003 to 2009, the deforestation occurring in this area is certainly the cause of this negative elevation error, ICESat-1 heights acquired before the deforestation of this area being relative to the canopy. As a consequence, Copernicus DEM EEA-10 heights relative to the ground may be compared to ICESat-1 heights relative to the canopy.

Deep valleys

Deep valleys related height errors are not the most widespread errors of this study, but they can reach tens of meters. A first case study is depicted in Figure 22, which shows a really high positive error (+48.522 m) in the Alps, near the Breithorn, in Switzerland.

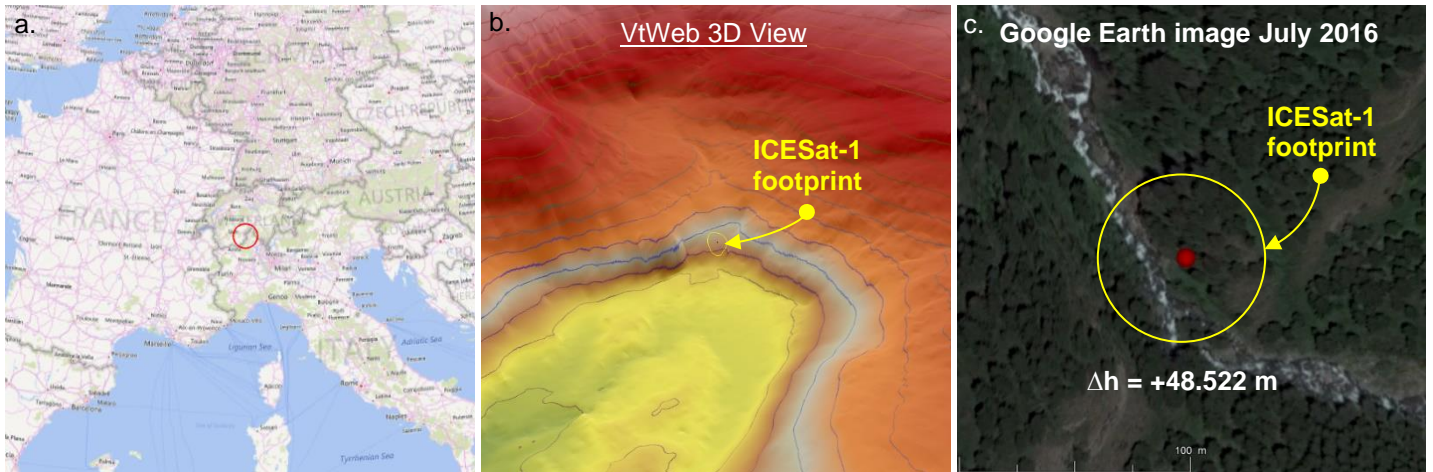


Figure 22 - EEA-10 - ICESat-1 height differences - Case of the Alps near the Breithorn (Switzerland).

A second case study, depicted in Figure 23, shows a similar height error (+43.638 m) in the Alps, near Andalo Valtellino, in Italy.

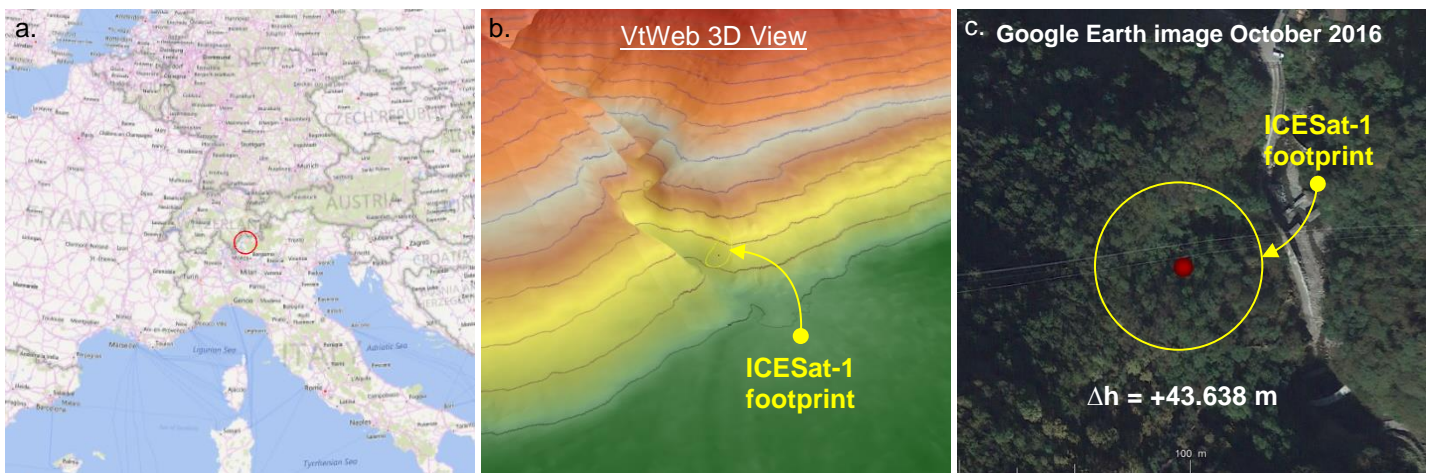


Figure 23 - EEA-10 - ICESat-1 height differences - Case of the Alps near Andalo Valtellino (Italy).

In subfigure b of Figure 22 and Figure 23, isocurves are set to 50 metres showing steep slopes over the study area.

Excavations

Excavations can lead to important height changes from one acquisition to another. Figure 24 highlights the case of Carrière de Marche-les-Dames, an excavation located near Namèche in Belgium.

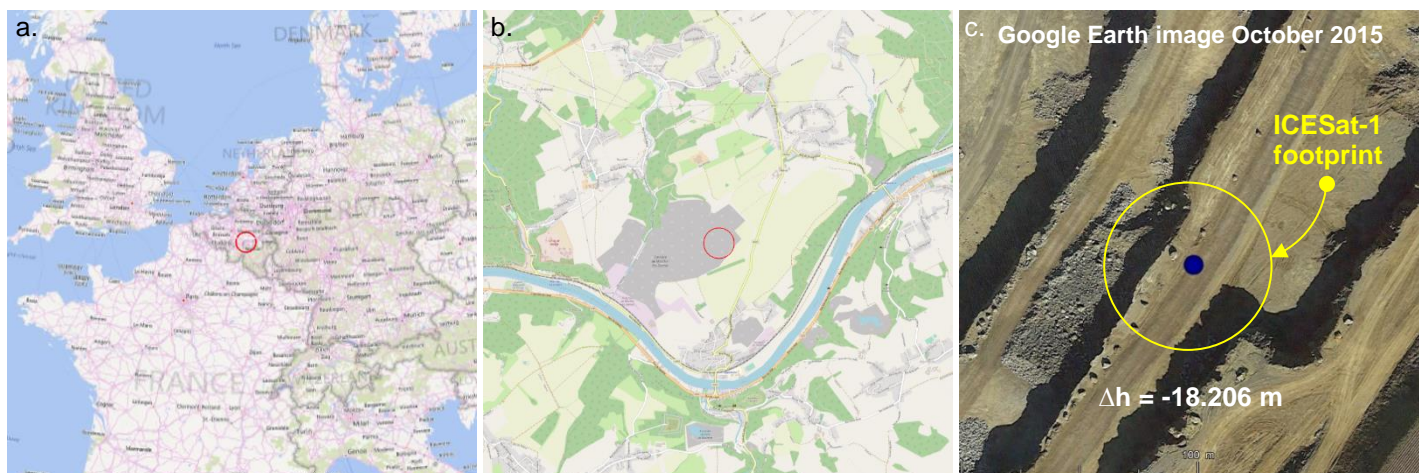


Figure 24 - EEA-10 - ICESat-1 height differences - Case of Carrière de Marche-les-Dames near Namèche (Belgium).

In this case study, an important negative error is calculated (-18.206 m), which occurs over Carrière de Marche-les-Dames. To ensure the depicted height error is linked to this excavation, two acquisitions of this area on different dates are compared in Figure 25.

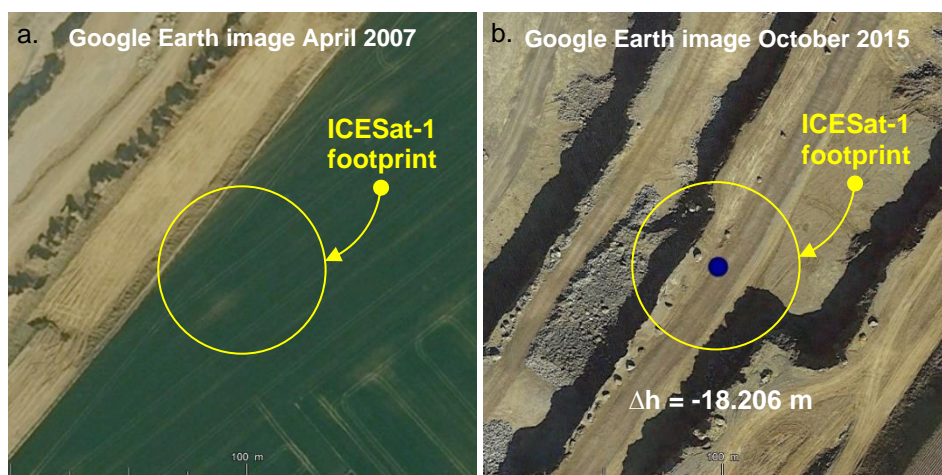


Figure 25 - EEA-10 - ICESat-1 height differences – Evolution of the studied excavation over two acquisition dates.

Figure 25 shows that the excavation of this case study was active from April 2007, date of acquisition of subfigure a, to October 2015, date of acquisition of subfigure b. As the first picture (subfigure a) was acquired on the acquisition period of ICESat-1, and as the second picture (subfigure b) was acquired on the acquisition period of TanDEM-X, the depicted height error is certainly due to the excavation expanding over the years.

Buildings

The construction and the demolition of buildings can cause height errors, as ICESat-1 and TanDEM-X acquired heights over different acquisition periods. Figure 26 highlights a case of industrial building demolition in Grenzach-Wyhlen, in Germany.

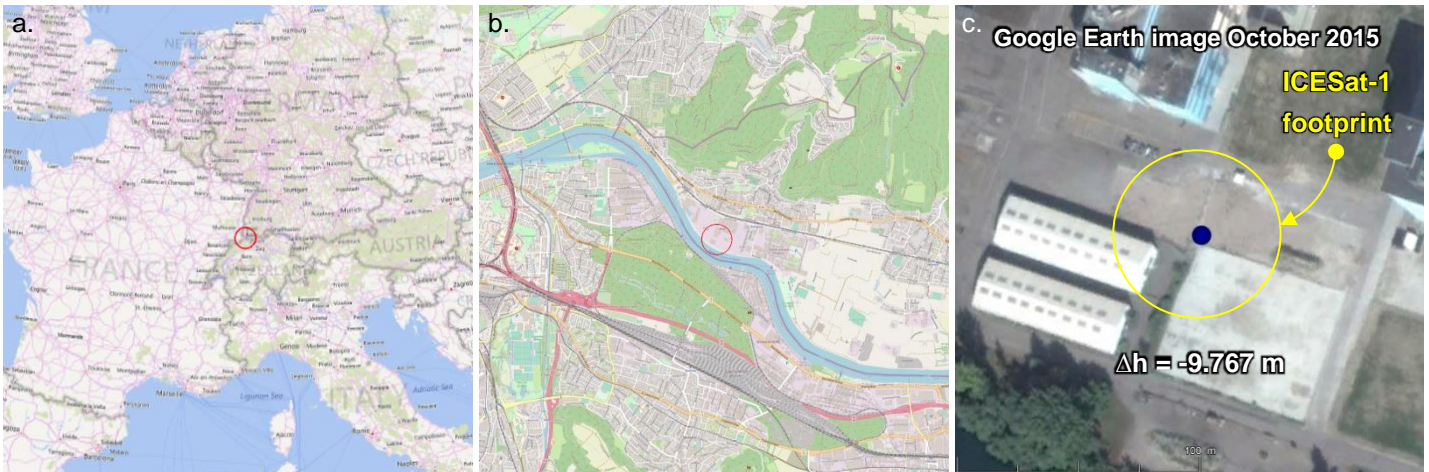


Figure 26 - EEA-10 - ICESat-1 height differences - Case of an industrial building in Grenzach-Wyhlen (Germany).

Figure 26 shows a height error over the foundations of a demolished industrial building. To ensure the depicted height error is caused by the demolition of a building, two pictures of the study area acquired on different dates are compared in Figure 27.



Figure 27 - EEA-10 - ICESat-1 height differences – Demolition of an industrial building over two acquisition dates.

The subfigure a of Figure 27 shows the presence of an industrial building over the study area in October 2009, whereas the building is demolished in the second picture dated from October 2015. As a consequence, the height error of this study area is probably due to the demolition of this building, especially considering the acquisition period of ICESat-1 (2003 to 2009) and TanDEM-X (2010 to 2015).

4.2.5 Assessment of Copernicus DEM GLO-30 from ICESat-1 / GLAS data

4.2.5.1 Spatial extent

The following figure (hyperlook <https://visioterra.org/VtWeb/hyperlook/dbe8a529cd2d4844b70f1008fa77b07e>) shows the coverage map of Copernicus DEM GLO-30.

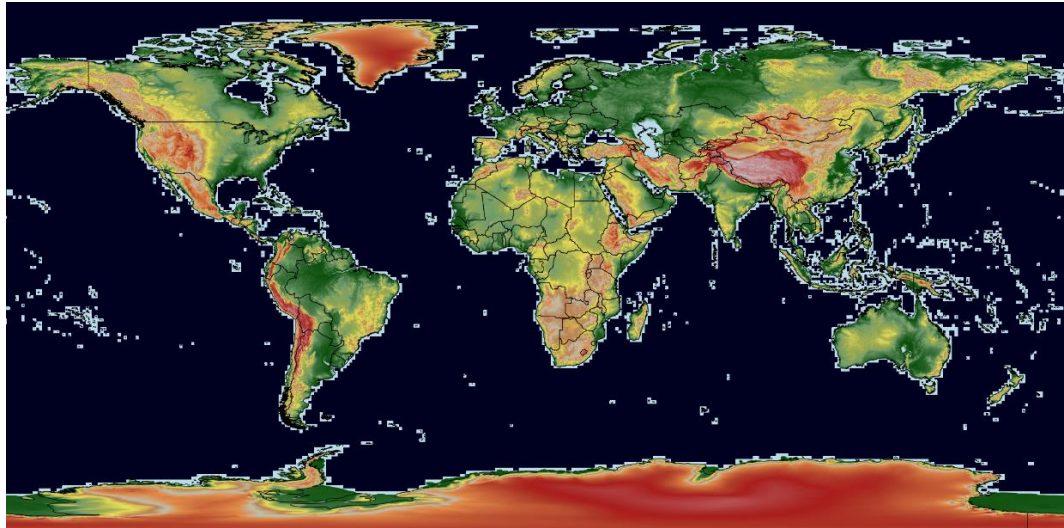


Figure 28 - Copernicus DEM GLO-30 coverage map.

However, Copernicus DEM GLO-30 is only assessed in the $[-60, 60]$ latitude interval in order to compare its results with SRTM-GL1, ASTER GDEM and ALOS World 3D. This limitation has been chosen considering the latitude limitation of SRTM-GL1 and the voids of ALOS World 3D.

4.2.5.2 Method and notations

The methodology used is the same as the one for the assessment of Copernicus DEM EEA-10 from ICESat-1 (see section 4.2.4).

4.2.5.3 Results

Here are the results of this study. All the statistics refer to the differences between ICESat-1 and Copernicus DEM GLO-30 heights (Copernicus DEM GLO-30 – ICESat-1):

	Raw	LE95	LE90
Number of ICESat-1 products	642		
Number of compared heights	62 441 346	59 319 279	56 197 212
Min	-4144.059 m	-2.725 m	-1.415 m
Max	3871.810 m	2.725 m	1.415 m
Mean (metres)	0.276 m	0.033 m	-0.027 m
RMSE (metres)	3.810 m	0.628 m	0.449 m
Standard deviation (metres)	3.800 m	0.627 m	0.449 m
Median (metres)	-0.01 m	-0.03 m	-0.04 m
Skewness	1.629	0.943	0.345
Kurtosis	190.349	3.594	1.033

Table 10 - **Statistics of the (Copernicus DEM GLO-30 – ICESat-1) comparison.**

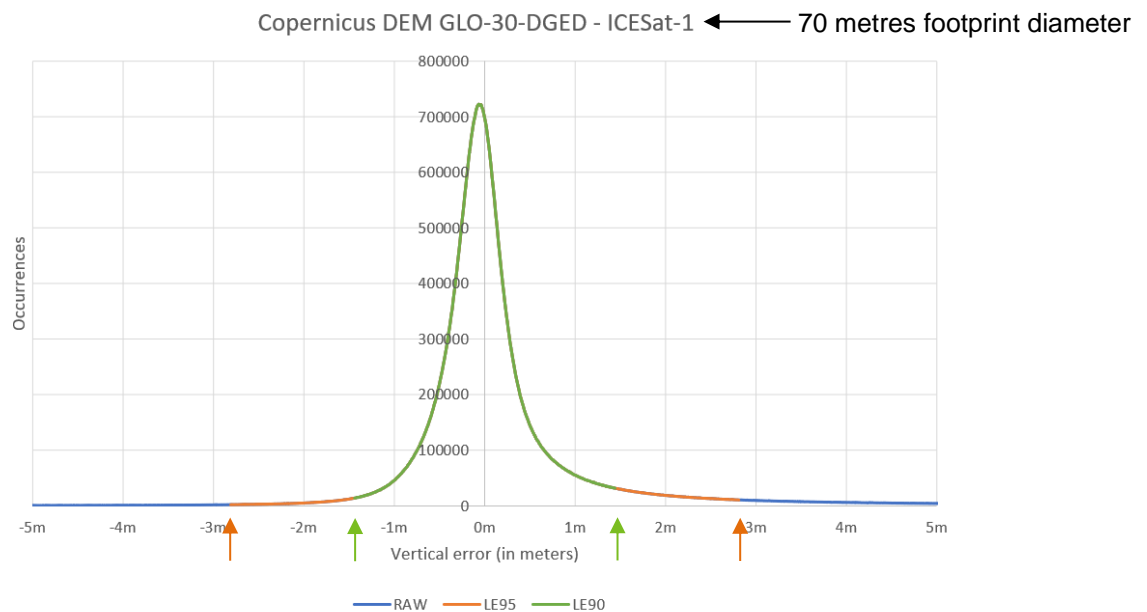


Figure 29 - **Error histogram of the (Copernicus DEM GLO-30 – ICESat-1) comparison.**

Arithmetic mean (0.033 m, 95% linear error) gives the systematic bias between Copernicus DEM GLO-30 and ICESat-1 heights. Root Mean Square Error or RMSE (0.628 m, 95% linear error) is the quadratic mean of the errors including the bias. Standard deviation (0.627 m, 95% linear error) gives the distribution of the errors around the mean out of the bias. The median error m is the one for which 50% of the pixels have an error less than m and 50% have an error greater than m.

4.2.6 Assessment of Copernicus DEM GLO-90 from ICESat-1 / GLAS data

4.2.6.1 Spatial extent

The following figure (hyperlook <https://visioterra.org/VtWeb/hyperlook/2083868e1ab84b27891ed8c5b8f21617>) shows the coverage map of Copernicus DEM GLO-90.

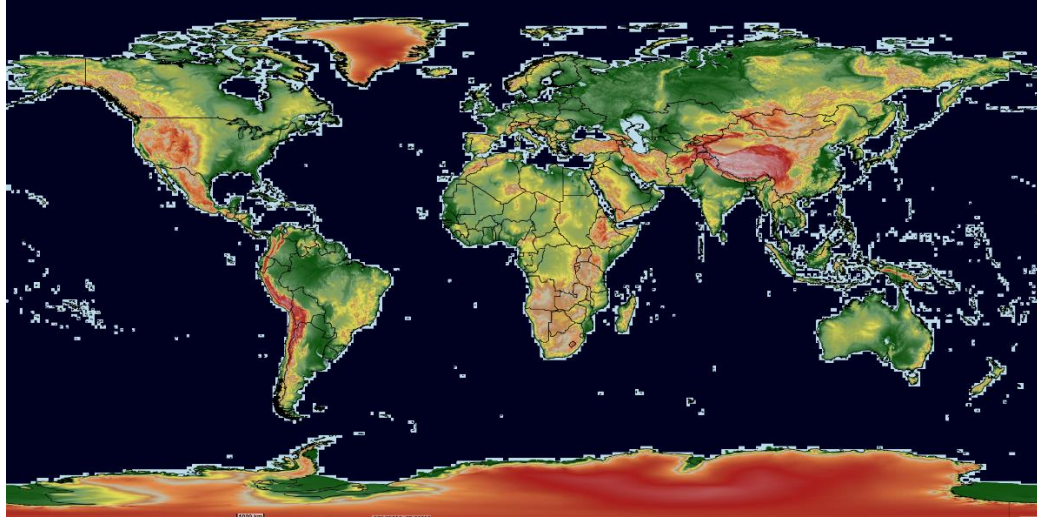


Figure 30- Copernicus DEM GLO-90 coverage map.

However, Copernicus DEM GLO-90 is only assessed in the $[-60, 60]$ latitude interval in order to compare its results with SRTM-GL1, ASTER GDEM and ALOS World 3D. This limitation has been chosen considering the latitude limitation of SRTM-GL1 and the voids of ALOS World 3D.

4.2.6.2 Method and notations

The methodology used is the same as the one for the assessment of Copernicus DEM EEA-10 from ICESat-1 (see section 4.2.4).

4.2.6.3 Results

Here are the results of this study. All the statistics refer to the differences between Copernicus DEM GLO-90 and ICESat-1 heights (Copernicus DEM GLO-90 – ICESat-1):

	Raw	LE95	LE90
Number of ICESat-1 products	642		
Number of compared heights	62 522 183	59 396 074	56 269 965
Min	-4144.069 m	-3.015 m	-1.636 m
Max	3871.787 m	3.015 m	1.636 m
Mean (metres)	0.278 m	0.066 m	0.006 m
RMSE (metres)	3.818 m	0.709 m	0.505 m
Standard deviation (metres)	3.808 m	0.706 m	0.505 m
Median (metres)	0.001 m	-0.001 m	-0.001 m
Skewness	0.823	0.793	0.364
Kurtosis	180.141	3.600	1.257

Table 11 - Statistics of the (Copernicus DEM GLO-90 – ICESat-1) comparison.

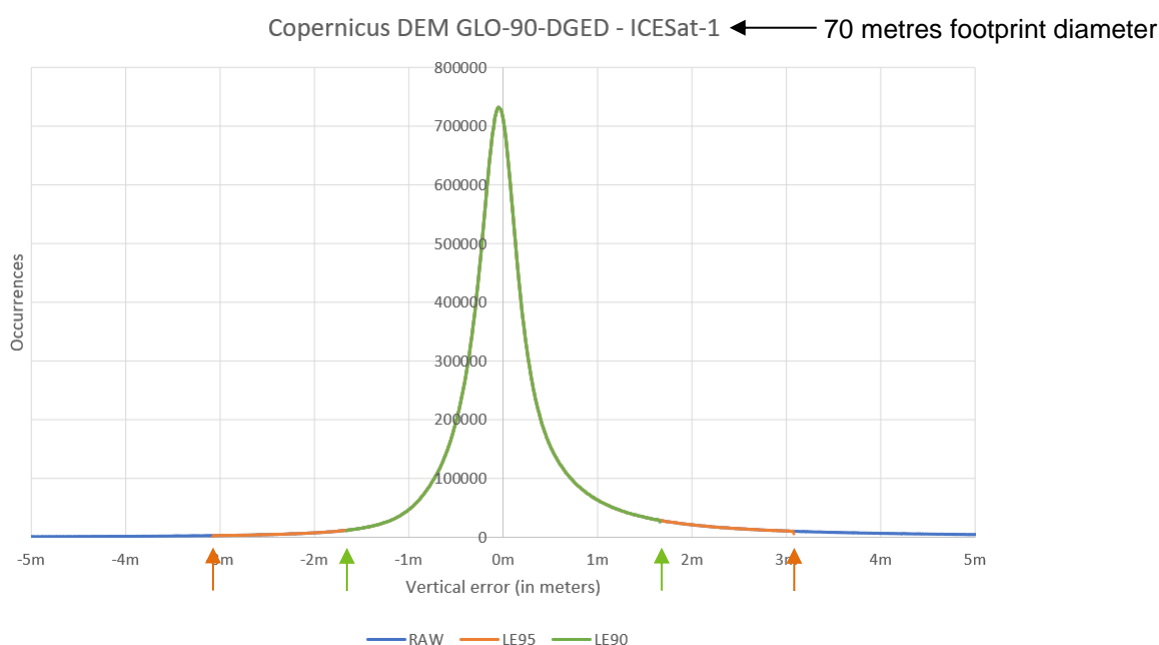


Figure 31 - Error histogram of the (Copernicus DEM GLO-90 – ICESat-1) comparison.

Arithmetic mean (0.066 m, 95% linear error) gives the systematic bias between ICESat-1 and Copernicus DEM GLO-90 heights. Root Mean Square Error or RMSE (0.709 m, 95% linear error) is the quadratic mean of the errors including the bias. Standard deviation (0.706 m, 95% linear error) gives the distribution of the errors around the mean out of the bias. The median error m is the one for which 50% of the pixels have an error less than m and 50% have an error greater than m.

4.3 Elevation assessment from ICESat-2 / ATLAS LiDAR – Quantitative assessment

This section presents the quantitative evaluation of the vertical accuracy of Copernicus DEM EEA-10, Copernicus DEM GLO-30 and Copernicus DEM GLO-90 data using reference data from the ICESat-2 / ATLAS LiDAR.

As described in the previous section 4.2, this assessment is quantitative, consisting of comparing each valid elevation given in LiDAR products to its homologous point to be interpolated from each assessed DEM.

As this study follows the same principles as the previous quantitative study (see section 4.2), this section focuses on the processing of ICESat-2 products used as a vertical reference. Information about the processing of the three Copernicus DEMs will not be repeated.

4.3.1 History of ICESat-2

Ice, Cloud and Land Elevation Satellite (ICESat-2) is an ongoing mission launched on the 15th of September 2018. This mission succeeds the ICESat-1 mission, which acquired heights from the 13th of January 2003 to the 11th of October 2009. The main goal of this mission is to precisely measure the elevation of ice sheets, sea ice, canopy and terrain surface. The ATLAS instrument, carried by ICESat-2, is a photon counting LiDAR. This instrument, by means of its unprecedented accuracy and measurement frequency, has already acquired terabytes of data in less than ten cycles of acquisition.

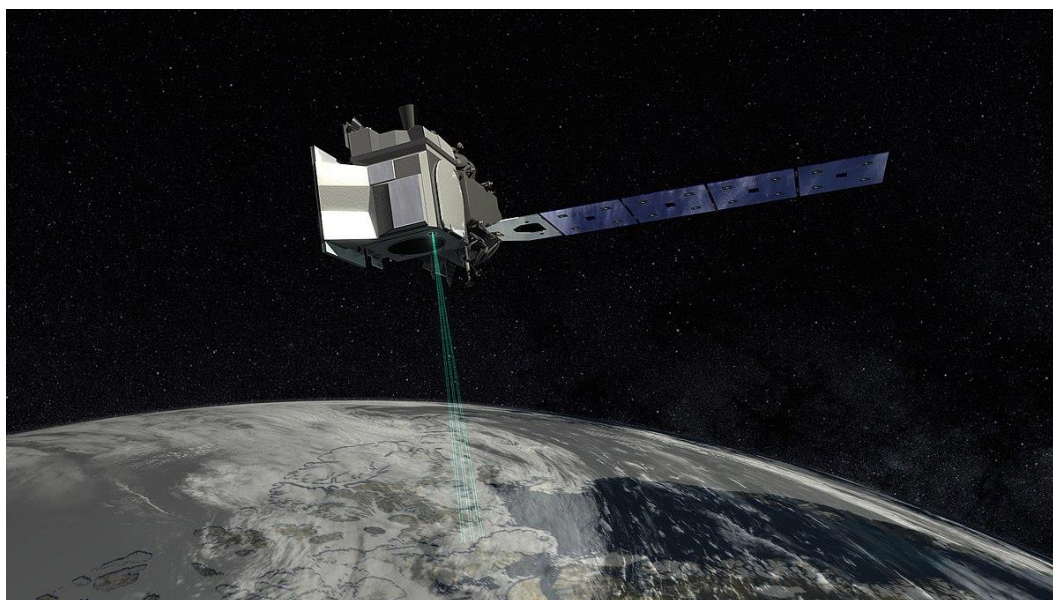


Figure 32 – 3D representation of ICESat-2.
(<https://svs.gsfc.nasa.gov/cgi-bin/details.cgi?aid=11712>)

4.3.2 Technical specifications

Onboard ICESat-2, the Advanced Topographic Laser Altimeter System (**ATLAS**) sends laser pulses at the very high frequency of **10Khz**, which is 250 times greater than the 40Hz acquisition frequency of the Geoscience Laser Altimeter System (GLAS instrument, carried by ICESat-1). Moreover, the **ATLAS** instrument acquires elevations over **six ground tracks**: three strong beams and three weak beams. The following figure illustrates the ground tracks of the ATLAS instrument:

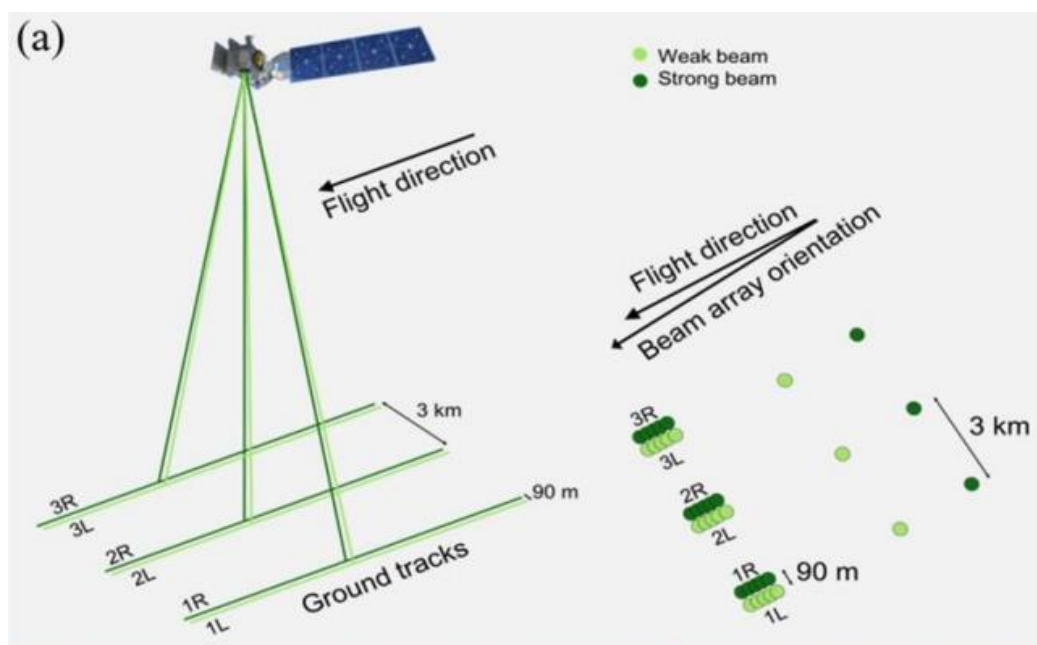


Figure 33 – Ground tracks of ICESat-2.
(extracted from <https://doi.org/10.5194/tc-2020-330>)

The following table summarizes the characteristics of the ICESat-2 mission and the ATLAS instrument:

Technical specification	Value
Instrument name	Advanced Topographic Laser Altimeter System (ATLAS)
First acquisition date	13.10.2018
Last acquisition date	Ongoing
Acquisition frequency	10 KHz
Ground sampling distance	~0.7 m
Central wavelength	532 nm (green)
Number of beams	6
Repeat cycle	91 days
Footprint diameter	13 m

Table 12 – Technical specifications of ICESat-1 and ICESat-2.

4.3.3 Assessment of ICESat-2 / ATLAS measurements reliability

4.3.3.1 ATL08 product

4.3.3.1.1 Product organisation

The ATL08 product, distributed by the NSIDC, contains terrain and canopy height above the WGS84 ellipsoid. This product is available in the HDF5 format. This format consists of a hierarchical data structure, composed of groups and variables. For instance, the root group of the ATL08 products contain the following groups and variables:

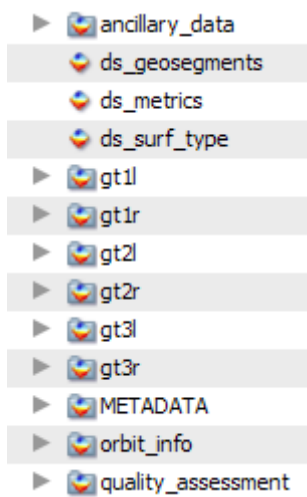


Figure 34 – Root group of ATL08 products.

The groups **ancillary_data**, **METADATA**, **orbit_info**, **quality_assessment** and the variables **ds_geosegments**, **ds_metrics** and **ds_surf_type** give information and data at product level, whereas the groups **gt1l**, **gt1r**, **gt2l**, **gt2r**, **gt3l** and **gt3r** contain height measurements, ancillary data and quality flags at a fixed step of 100 metres.

The **gt1l**, **gt1r**, **gt2l**, **gt2r**, **gt3l** and **gt3r** groups consist of the data acquired by each laser beam at a specified ground track. It is important to note that these ground track labels may refer to different actual laser beams from one product to another, as the orientation of ICESat-2 changes over the time. The following figure illustrates the two possible orientations of the ATLAS instrument:

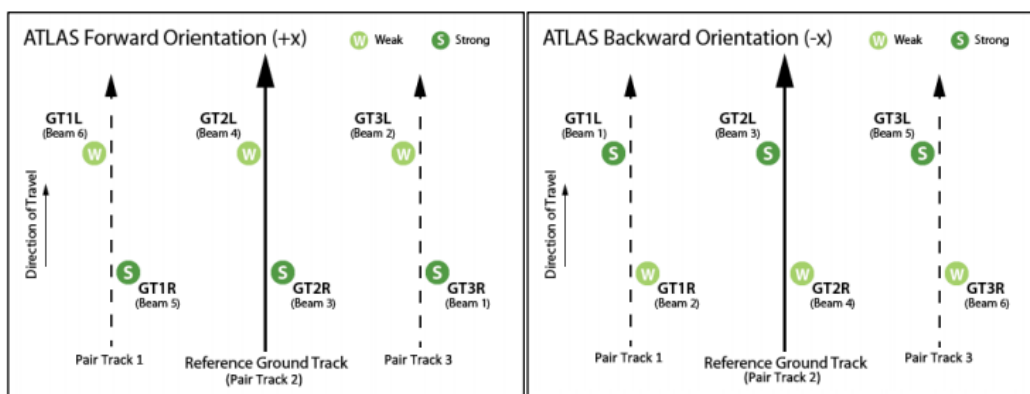


Figure 35 – Orientations of the ATLAS instrument,
impact on the laser beams ground tracks labelling.
(extracted from RD-22)

4.3.3.1.2 Data filtering

As illustrated in Figure 35, depending on the orientation of ICESat-2, a ground track label may refer to a weak laser beam or a strong laser beam. For the following studies, only strong laser beams acquisitions are considered to avoid potential biases, as the weak laser beams acquisitions are not suitable for determining both terrain and canopy height (see RD-23, under section 1). Such filtering depends on the orientation of the ATLAS instrument, which is obtained by reading the **sc_orient** variable of each ATL08 product, which can be equal to the following values:

sc_orient flag value	meaning
0	backward orientation
1	forward orientation
2	In transition between orientations

Table 13 – ATL08 sc_orient variable values.

Heights acquired in transition mode are not considered, as a transition between two orientations may lead to degraded acquisitions (see RD-25, under sc_orient variable description).

The following table summarizes the methods used to discriminate between strong and weak laser beams:

Type of beam	Forward orientation beam labels	Backward orientation beam labels
Strong	GT1R GT2R GT3R	GT1L GT2L GT3L
Weak	GT1L GT2L GT3L	GT1R GT2R GT3R

Table 14 – ATLAS laser beam labelling.

Terrain height acquisitions correspond to the **h_te_best_fit** attribute. ATL08 elevations are not retrieved at instrument measurement frequency, but at a fixed step of 100 metres based on photon data of the ATL03 product (see RD-22; under section 1.3.2).

Quality flags are available for each acquisition of each beam. Consequently, each beam acquisitions are filtered individually with the methods described here after. Acquisitions of each beam are filtered using the following flags:

- **segment_watermask:** inland water mask, equals 1 if inland water is detected, 0 otherwise,
- **n_te_photon:** number of photons classified as terrain in acquisition segment (100 metres segments of multiple acquisitions),
- **h_te_uncertainty:** uncertainty of mean terrain height for the current segment (100 metres segments of multiple acquisitions).

The following flag conditions have been applied in order to keep only valid terrain heights:

Flag	Condition	Meaning
segment_watermask	= 0	No inland water detected
n_te_photon	> 100	More than 100 photons return from terrain surface
h_te_uncertainty	< 7.5 m	Terrain height uncertainty is lower than 7.5 metres

Table 15 – ATL08 product terrain heights validity conditions.

Canopy height is retrieved using the **h_canopy** variable of each ATL08 product. This variable corresponds to the height of canopy above the estimated terrain surface (see RD-25, under the h_canopy variable description). Canopy height is only considered when the variable **canopy_flag** indicates the presence of canopy.

Invalid values of h_canopy have been filtered considering the filling values indicated in the ATL08 product (see RD-25, under the h_canopy variable description). The following table summarizes the criteria used to consider only valid canopy heights:

Variable	Condition	Meaning
canopy_flag	= 1	canopy is present
h_canopy	≠ 3.4028235E38f	canopy height is valid

Table 16 – ATL08 product canopy heights validity conditions.

As only strong beam acquisitions are taken into account, and as terrain and canopy heights have been filtered, the remaining terrain heights are considered as valid. These valid terrain heights are both used to assess the constancy of ICESat-2 height acquisitions (see section 4.3.3.3) and to assess the quality of Copernicus DEM EEA-10 (see section 4.3.4), Copernicus DEM GLO-30 (see section 4.3.5) and Copernicus DEM GLO-90 (see section 4.3.6).

4.3.3.2 Sampling of ICESat-2 / ATLAS data

Sampling equations used for ICESat-2 / ATLAS do not differ from equations used in the ICESat-1 / GLAS study. Please refer to section 4.2.3.2 for further details.

4.3.3.3 Collocated measurements on the same orbit

4.3.3.3.1 Scope

Multiple heights retrieved from the ATL08 product are analysed on the same orbit over multiple revolutions to assess ICESat-2's instrument reliability. This study has the same geographical extent than the study of ICESat-1's instrument reliability, over the Salt Lake of Salar de Uyuni (see section 4.2.3.3 and attached figure).



4.3.3.3.2 Method

Definitions

The following terminology is used in this study:

- **Terrain height:** terrain height given in the ATL08 product (identified as the h_te_best_fit variable) retrieved at a given geolocation (longitude, latitude). The terrain height is

estimated over 100 m segments worth of terrain photons along-track, taken from the ATL03 product. The terrain height is estimated at the mid-point location of each 100 m segment (see RD-23 for further explanation),

- **Reference ground track:** segment of orbit identified by an id, which remains identical from one revolution to another. Given an ATL08 product, the reference ground track remains identical for every terrain height, only the laser ground track changes (see definition below),
- **Laser track #n:** track of acquisition of a specific laser beam emitted from the ATLAS instrument. An ATL08 product typically contains 6 laser ground tracks sharing the same reference ground track.
- **Profile:** set of terrain heights acquired contiguously along-track, sharing the same reference ground track and laser ground track.

Reliability assessment

The goal of this study is to ensure ICESat-2/ATLAS heights acquired over multiple revolutions on a common reference ground track do not largely differ (especially, the terrain heights retrieved in the ATL08 product). This study aims to evaluate the **constancy** of ICESat-2/ATLAS terrain height estimations over multiple revolutions.

Considering the large amount of reference ground tracks, and therefore, the large amount of data, a strict filtering procedure has been applied in order to keep the best terrain height estimations from ATL08 products. The following list summarizes the steps of filtering ICESat-2 ATL08 products:

1. Only terrain heights contained in the defined bounding box are considered,
2. Terrain heights flagged as invalid are excluded (see section 4.3.3.1 for filtering procedures),
3. Profiles containing invalid data due to the terrain height filtering are excluded, avoiding potential biases linked to different numbers of terrain heights among reference ground tracks,
4. Profiles not beginning (respectively ending) at the top (respectively bottom) of the bounding box are excluded, for the same reasons as explained in step 3,
5. Profiles not sharing a common reference ground track with any other close enough profile is excluded (< 500 metres between profiles), as the constancy of ICESat-2 ATL08 heights cannot be estimated from only one profile.

The results of this filtering are 10 pairs of profiles, in which the two profiles share the same reference ground track. The following figure gives an overview of the pairs of profiles kept for this study:

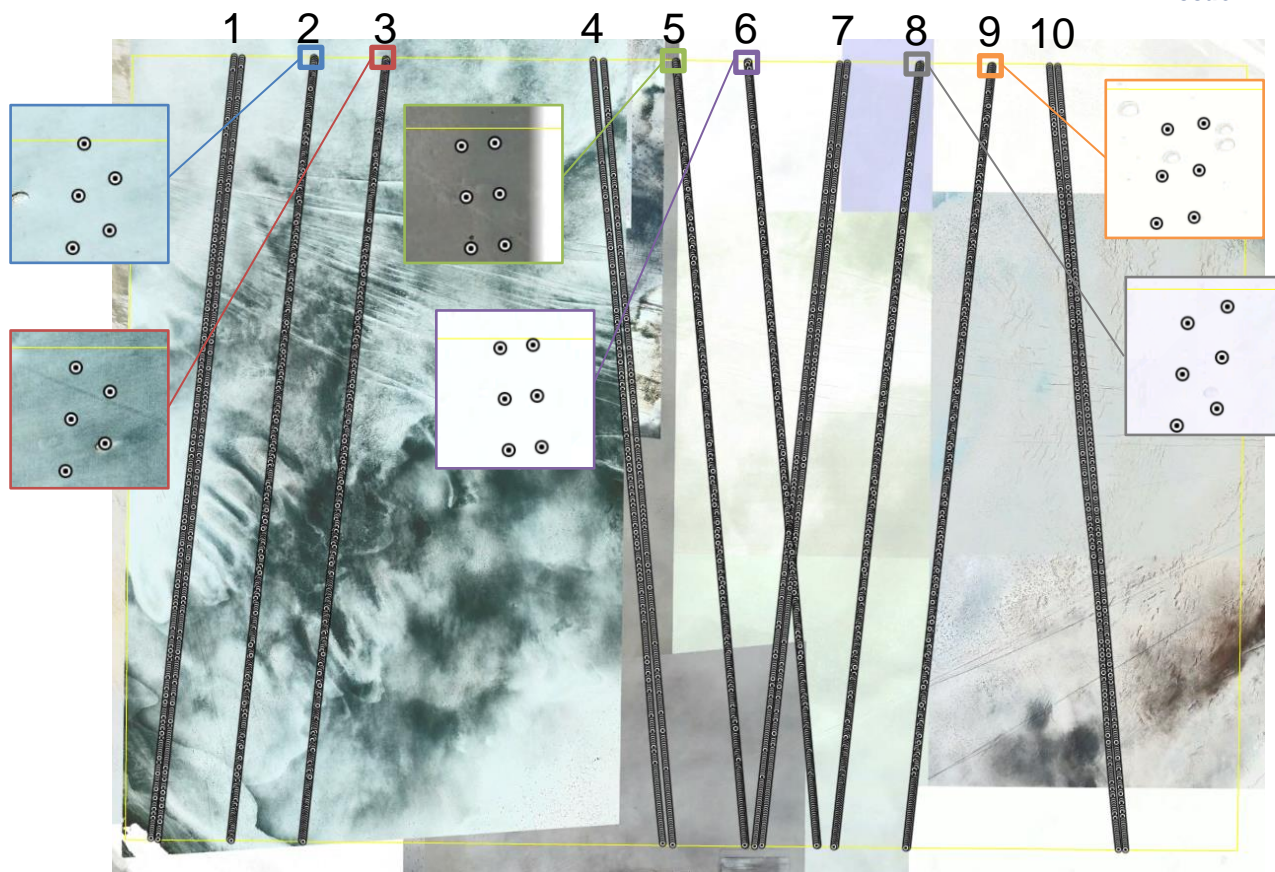


Figure 36 - Pairs of profiles considered for the ICESat-2 reliability study.

The following table gives the origin of every profile kept for this study:

Profile pair number	Product ID	Date of acquisition	Reference ground track	Laser track
1	ATL08_20200713012933_02700808_003_01.h5	13.07.2020	270	gt1l/
	ATL08_20201011210920_02700908_003_01.h5	11.10.2020	270	gt3l/
2	ATL08_20200413054946_02700708_003_01.h5	13.04.2020	270	gt3r/
	ATL08_20201011210920_02700908_003_01.h5	11.10.2020	270	gt2l/
3	ATL08_20200413054946_02700708_003_01.h5	13.04.2020	270	gt2r/
	ATL08_20201011210920_02700908_003_01.h5	11.10.2020	270	gt1l/
4	ATL08_20200617145103_12680714_003_01.h5	17.06.2020	1268	gt3l/
	ATL08_20190919035142_12680414_003_01.h5	19.09.2019	1268	gt1r/
5	ATL08_20200916103051_12680814_003_01.h5	16.09.2020	1268	gt1l/
	ATL08_20190919035142_12680414_003_01.h5	19.09.2019	1268	gt2r/
6	ATL08_20200916103051_12680814_003_01.h5	16.09.2020	1268	gt2l/

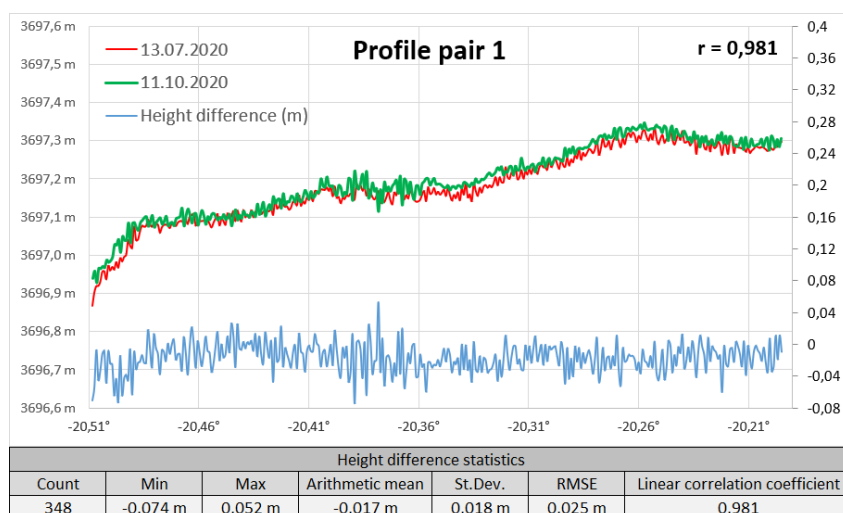
Profile pair number	Product ID	Date of acquisition	Reference ground track	Laser track
	ATL08_20190919035142_12680414_003_01.h5	19.09.2019	1268	gt3r/
7	ATL08_20200811000536_07120808_003_01.h5	11.08.2020	712	gt1l/
	ATL08_20201109194524_07120908_003_01.h5	09.11.2020	712	gt3l/
8	ATL08_20200512042551_07120708_003_01.h5	12.05.2020	712	gt3r/
	ATL08_20201109194524_07120908_003_01.h5	09.11.2020	712	gt2l/
9	ATL08_20200512042551_07120708_003_01.h5	12.05.2020	712	gt2r/
	ATL08_20201109194524_07120908_003_01.h5	09.11.2020	712	gt1l/
10	ATL08_20191018022746_03230514_003_01.h5	18.10.2019	323	gt3r/
	ATL08_20200416174719_03230714_003_01.h5	16.04.2020	323	gt1r/

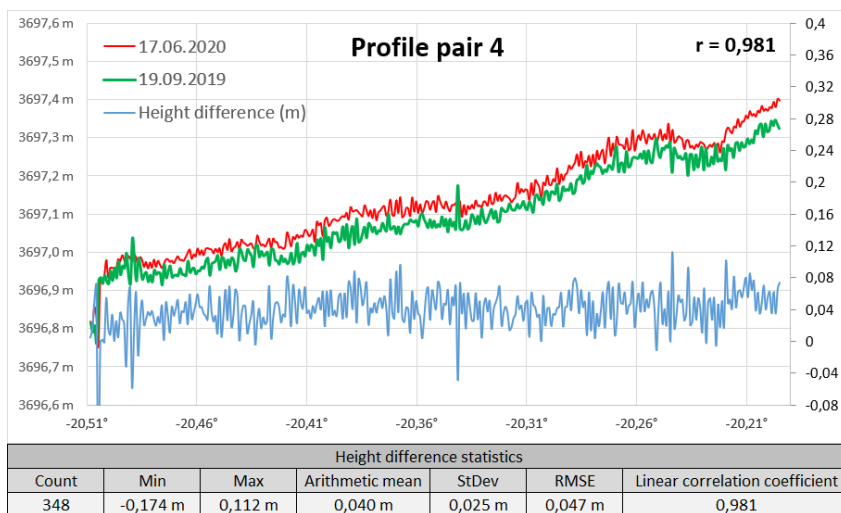
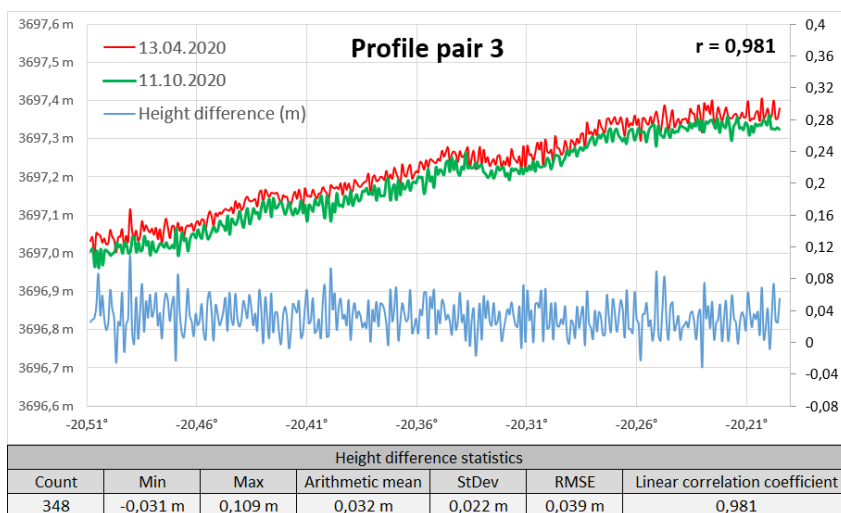
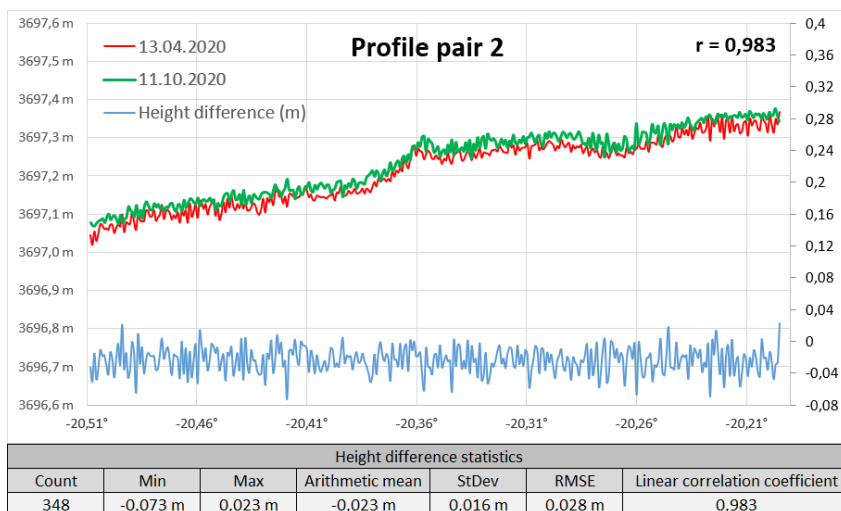
Table 17 – ICESat-2 ATL08 profile pairs origin.

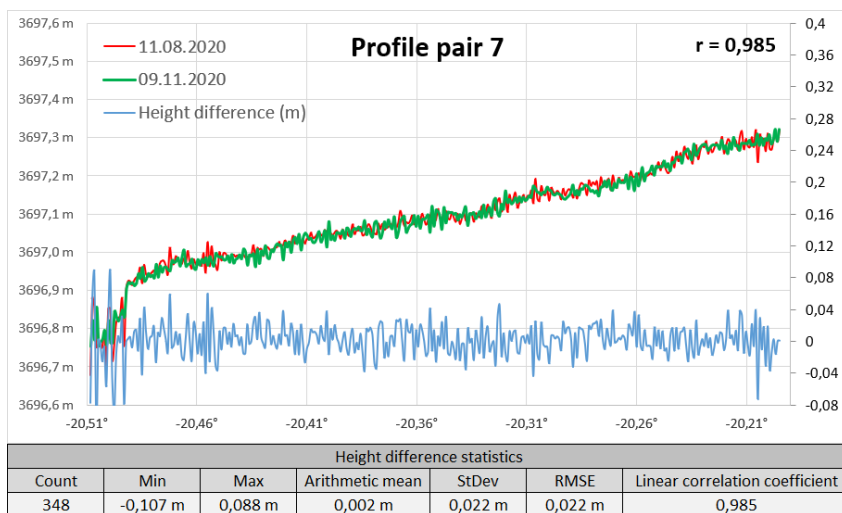
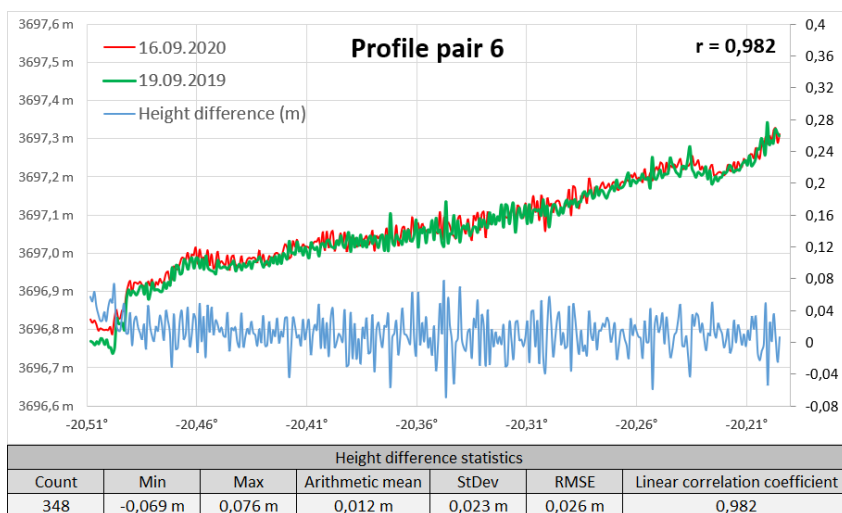
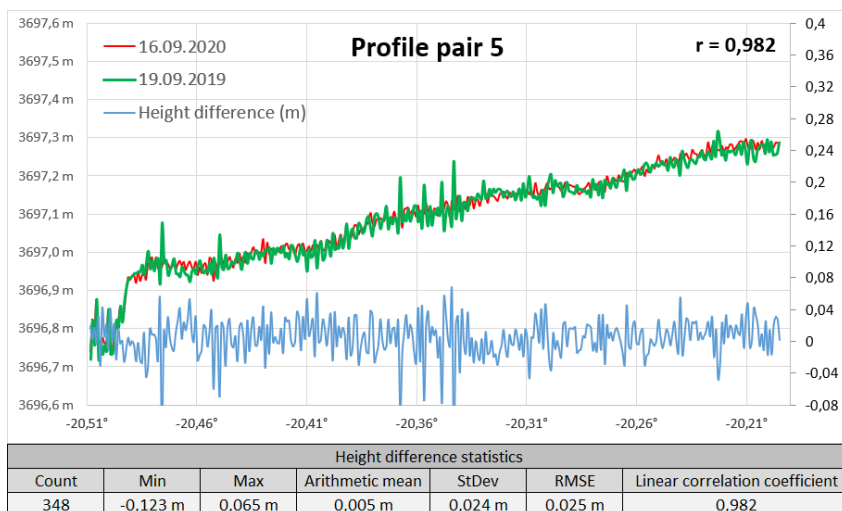
In order to compute the terrain height difference between two paired profiles, heights are linearly interpolated every 100 metres (fixed step in latitude) on every profile (see section 4.3.3.2 for equations). As the valid profiles do not contain any invalid terrain height, the number of compared interpolated heights is constant from one pair profile to another. Then, the difference between interpolated terrain heights of the same profile pair is computed at each latitude step.

4.3.3.3 Results

The following figures and tables show the height difference statistics of each profile pair:







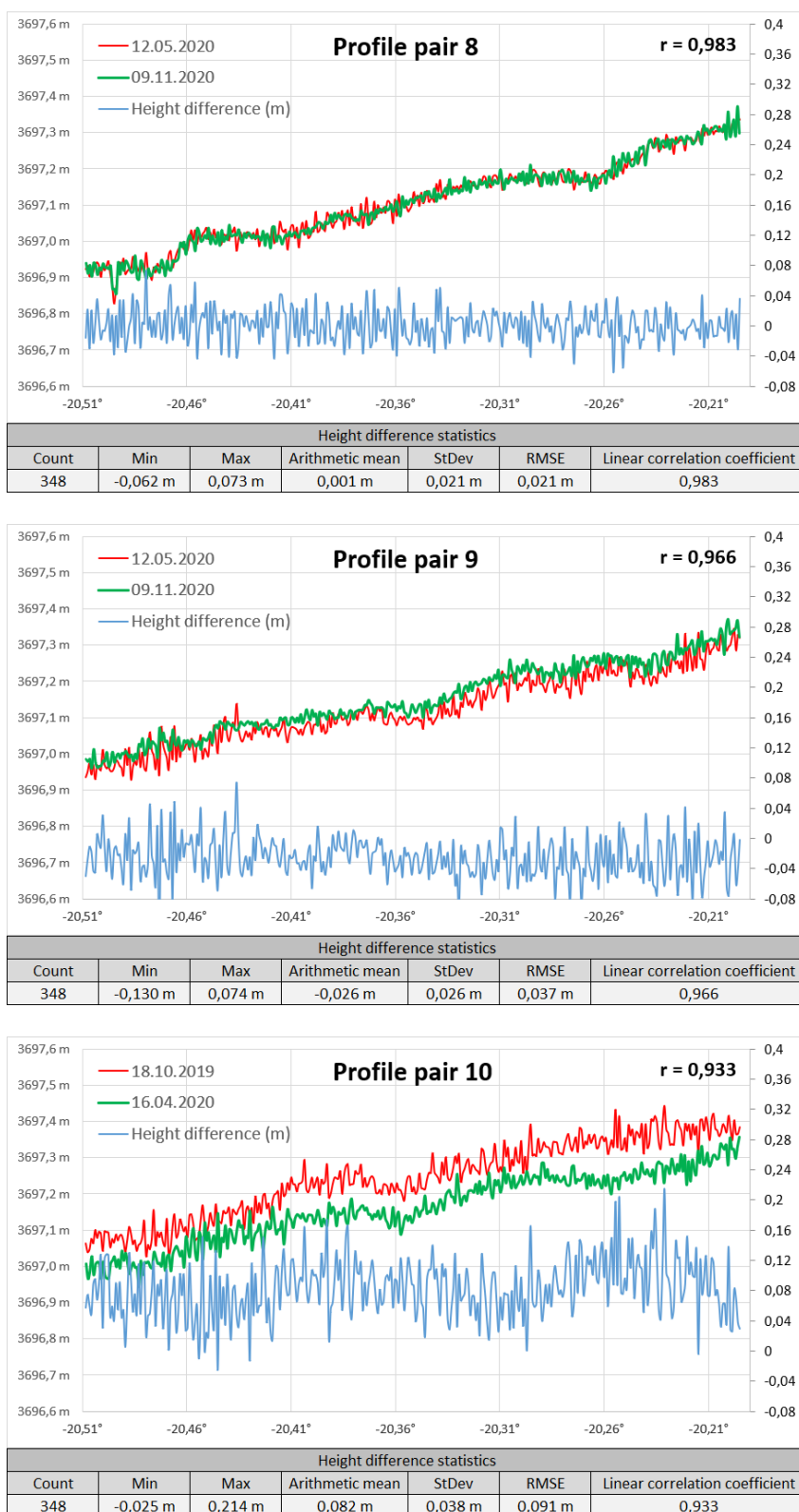


Figure 37 - Height difference statistics for every profile pair.

The height difference statistics show really good results, considering a RMSE of 0.091 m and a standard deviation of 0.038 m on profile pair 10, which are the worst results of this study.

4.3.3.4 Geographical distribution of ICESat-2 products

This study is based on **119 068** ATL08 products (**3.76 TB**), representing 9 orbit cycles of ICESat-2 data. Most of the products contain acquisitions over 1/14th of an orbit. The products are distributed all over the world as shown in the following figure.

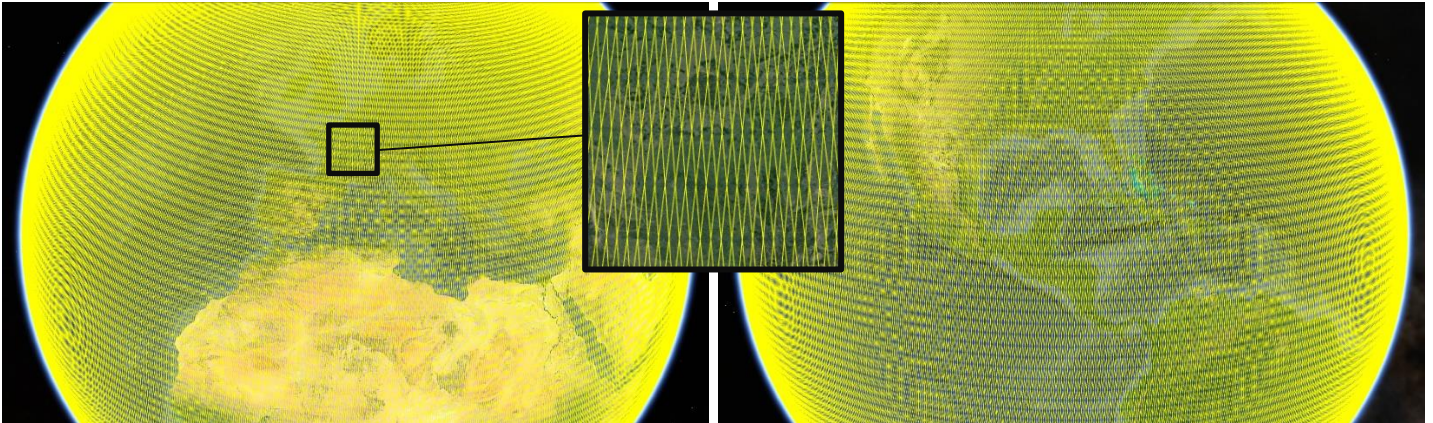


Figure 38 - Distribution of the 119 068 ATL08 products.

4.3.4 Assessment of Copernicus DEM EEA-10 from ICESat-2 / ATLAS data

This section presents the quantitative evaluation of the vertical accuracy of **Copernicus DEM EEA-10** using reference data from **ICESat-2 / ATLAS (LiDAR)**. The methods and the notations of this study are given here after (see section 4.3.4.1). The methods used to process DEM heights are the same as the ones described in section 4.2, consequently, only a summary of the steps involved in comparing the **Copernicus DEM EEA-10** to **ICESat-2 / ATLAS** data is given, referencing other sections for further details. The same methods will apply for the evaluation of **Copernicus DEM GLO-30** (section 4.3.5) and **Copernicus DEM GLO-90** (section 4.3.6) and will not be repeated.

4.3.4.1 Method and notations

4.3.4.1.1 Summary of the methods used

The ATL08 product includes terrain and canopy heights. Consequently, statistics concerning two quantitative studies are given, respectively comparing Copernicus DEM EEA-10 heights to ICESat-2 ATL08 **terrain heights only** and to ICESat-2 ATL08 **terrain heights including canopy**.

The main steps of this study are:

- Filtering bad acquisitions from ICESat-2 ATL08 products, retrieving reference ICESat-2 heights relative to the WGS84 ellipsoid,
- Interpolating Copernicus DEM EEA-10 heights at each ICESat-2 ATL08 reference height footprint location, retrieving interpolated DEM heights relative to the EGM2008 geoid,
- Convert the vertical reference system of the interpolated EGM2008 DEM heights to the WGS84 ellipsoid,
- Given ICESat-2 ATL08 heights of reference and Copernicus DEM EEA-10 heights expressed with respect to the WGS84 ellipsoid, compute height differences, both taking as reference ICESat-2 ATL08 terrain heights only and ICESat-2 ATL08 terrain with canopy heights.

Filtering ATL08 products is done using methods described in section 4.3.3.1. Consequently, only strong laser beams acquisitions of the ATL08 product have been considered, and invalid

terrain and canopy heights have been filtered. ATL08 product heights are already expressed with respect to the WGS84 ellipsoid, therefore, no vertical reference system conversion is applied to this reference data.

Bilinear interpolation is used to retrieve Copernicus DEM EEA-10 heights at each ICESat-2 strong beam footprint. Then, the interpolated heights are converted from the EGM2008 geoid to the WGS84 ellipsoid (see section 4.2.4.2.3 for more details).

From this point, the difference between Copernicus DEM EEA-10 interpolated heights and ICESat-2 ATL08 heights can be calculated, as both are expressed relative to the WGS84 ellipsoid.

4.3.4.1.2 Computing the height difference

The following equation is used to compute the height difference between Copernicus DEM EEA-10 interpolated height and ICESat-2 ATL08 **terrain height only**:

$$\Delta h = h_{DEM} - h_{ICESat-2_terrain} \quad (\text{eq. 5})$$

Where:

Δh	is the height difference between Copernicus DEM EEA-10 and ICESat-2,
$h_{ICESat-2_terrain}$	is the ICESat-2 terrain height (with respect to the WGS84 ellipsoid),
h_{DEM}	is the Copernicus DEM EEA-10 height (with respect to the WGS84 ellipsoid).

The following equation is used to compute the height difference between Copernicus DEM EEA-10 interpolated height and ICESat-2 ATL08 **terrain with canopy height**:

$$\Delta h = h_{DEM} - (h_{ICESat-2_terrain} + h_{ICESat-2_canopy_only}) \quad (\text{eq. 6})$$

Where:

Δh	is the height difference between Copernicus DEM EEA-10 and ICESat-2,
$h_{ICESat-2_terrain}$	is the ICESat-2 terrain height (with respect to the WGS84 ellipsoid),
$h_{ICESat-2_canopy_only}$	is the ICESat-2 canopy height above ICESat-2 terrain height,
h_{DEM}	is the Copernicus DEM EEA-10 height (with respect to the WGS84 ellipsoid).

4.3.4.2 Overall algorithm

The following diagram summarizes the steps involved in the comparison between the Copernicus DEM EEA-10 and ICESat-2 reference data:

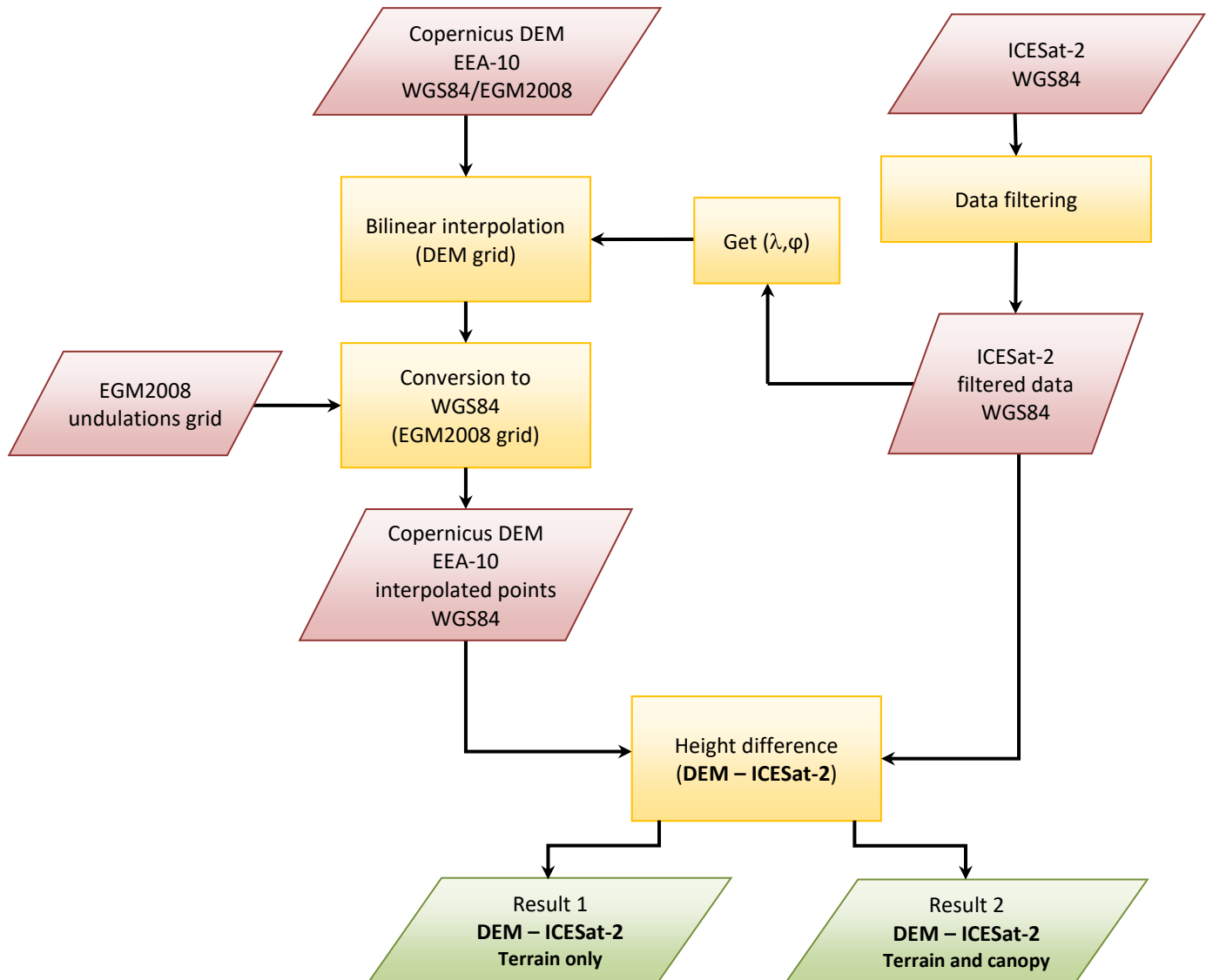


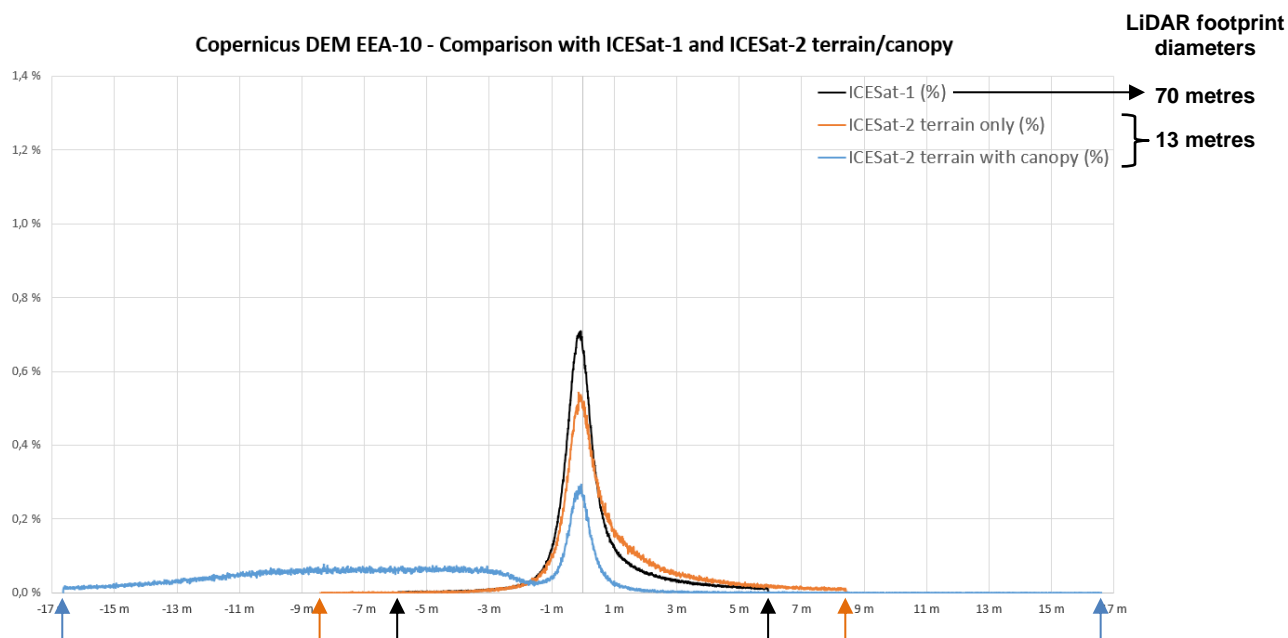
Figure 39 – Summary of the Copernicus DEM EEA-10 assessment method using ICESat-2 ATL08 as a vertical reference.

4.3.4.3 Results

Here are the results of the **Copernicus DEM EEA-10 – ICESat-2** study. The results obtained in this study are compared with results obtained in the **Copernicus DEM EEA-10 – ICESat-1** study. Statistics have been computed for two types of heights: one keeping only ICESat-2 **terrain height**, the other taking into account **canopy height** when canopy is present. All the statistics are computed with a 95% linear error (**LE95**). The following table summarizes the results of these studies:

LE95 statistics	ICESat-1	ICESat-2 (terrain only)	ICESat-2 (terrain with canopy)
Number of compared heights	1 803 551	399 179	399 179
Min	-5,924 m	-8,415 m	-16,642 m
Max	5,924 m	8,421 m	16,600 m
Mean (metres)	0,270 m	0,822 m	-5,477 m
Standard deviation (metres)	1,389 m	1,944 m	4,838 m
RMSE (metres)	1,415 m	2,111 m	7,307 m
Skewness	1,091	1,283	0,251
Kurtosis	3,797	2,823	-0,777

Table 18 - Statistics of the (Copernicus DEM EEA-10 - ICESat-2) comparison.



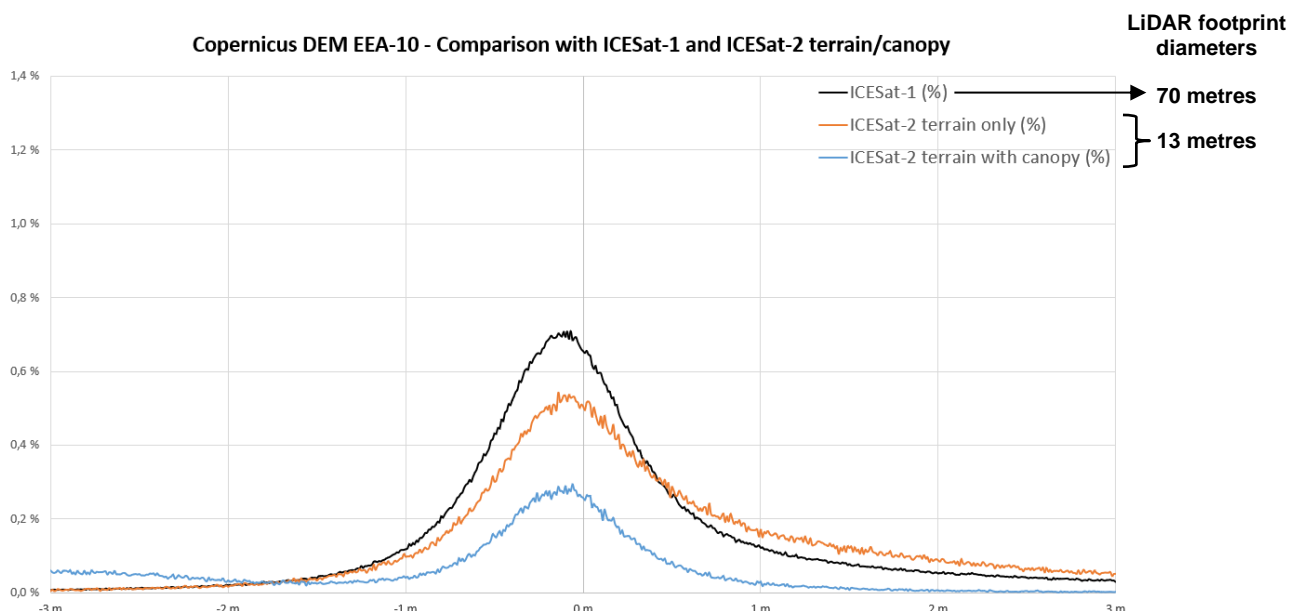


Figure 40 - Error histogram of the (Copernicus DEM EEA-10 – ICESat-2) study, comparison with previous results using ICESat-1 as vertical reference.

The histogram and the statistics show good results for both ICESat-2 terrain height only and ICESat-2 terrain with canopy height. However, the ICESat-2 terrain with canopy statistics shows worse results than the ICESat-2 terrain only statistics. Moreover, the ICESat-2 terrain with canopy histogram shows a large number of negative errors, ranging from -2 metres to -17 metres approximately. These negative errors are caused by taking into account the canopy height measured by ICESat-2. At first glance, the ICESat-2 terrain with canopy histogram might indicate that Copernicus DEM EEA-10 is not strictly a Digital Surface Model (DSM), but it must be noticed that the *h_canopy* variable of the ATL08 product is an estimation of the canopy height (see section 4.3.4.4.1). The statistics show that the (Copernicus DEM EEA-10 – ICESat-1) study gives better results than the (Copernicus DEM EEA-10 – ICESat-2) studies. The better performance of ICESat-1 could be explained by the fact that Copernicus has been validated from ICESat-1 (see RD-15). Overall, the two terrain studies show that Copernicus DEM EEA-10 is an accurate DEM.

4.3.4.4 Typical sources of elevation errors

4.3.4.4.1 ICESat-2 elevation errors

ATL08 known issues

The RD-26 document references the known issues of the ATL08 product, release 003. One major issue certainly impacting this quantitative study is the incorrect labelling of returning photons. Dense vegetation areas can cause terrain photons to be labelled as noise. The document states that in such cases “the ground height would be reported incorrectly by **approximately 3-5 m**, and the relative canopy height would be under-estimated by that same amount”.

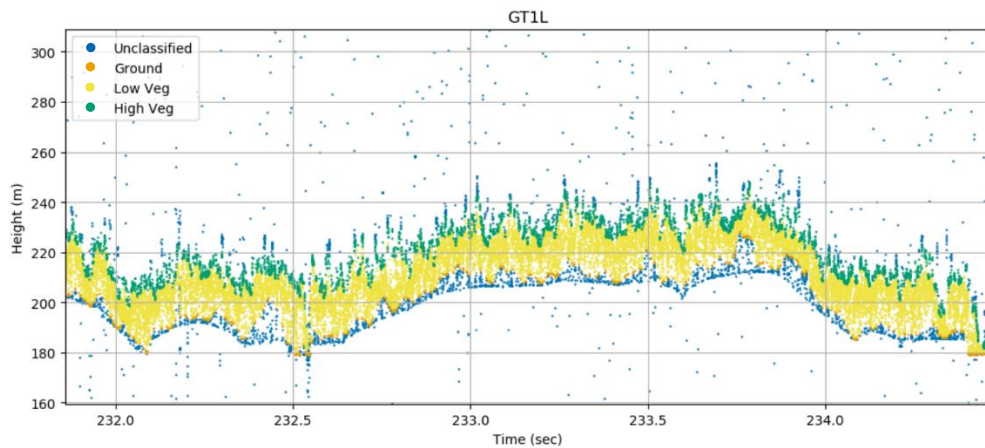


Figure 41 - Incorrect photon labelling in tropical forest (Brazil).
(extracted from RD-26)

In Figure 41, the lowest layer of photons is unclassified (blue), whereas it should be classified as ground (orange).

Such issues certainly affect the results of each Copernicus DEM instance quantitative assessment followed in this section. Other issues mentioned in the RD-26 document should not affect these studies, as they occurred in previous ATL08 product releases or describe geolocation/height errors within the geolocation and height uncertainties of this product.

h_canopy variable

The h_{canopy} variable of the ATL08 product is defined as the following: “the relative 98% height of classified canopy photon heights above the estimated terrain surface. Relative canopy heights have been computed by differencing the canopy photon height from the estimated terrain surface in the ATL08 processing. The relative canopy heights are sorted into a cumulative distribution, and the height associated with the 98% height is reported.” (see RD-23, section 2.2.6). As the retrieved canopy height is an estimation based on 100 metres worth of canopy photons, and not computed directly at the geolocation indicated in the ATL08 product, the h_{canopy} variable may introduce errors in the “Copernicus DEM EEA-10 – ICESat-2 terrain with canopy height” study, especially where the canopy height is varying.

4.3.4.4.2 Geomorphological and land use / land cover context causing elevation errors

This section aims to provide a better understanding of the sources of elevation errors by observing their repartition all over the geographical extent of Copernicus DEM EEA-10. In the figures of this section, negative height errors are depicted in blue (Copernicus DEM EEA-10 height is lower than the ICESat-2 reference height) whereas positive height errors are depicted in red (Copernicus DEM EEA-10 height is greater than the ICESat-2 reference height).

In that follow, the differences between Copernicus DEM EEA-10 and the ICESat-2 terrain (Δh_t) and the ICESat-2 terrain with canopy (Δh_c) are given at error geolocation, showing various geomorphological and/or land use / land cover contexts. Note that the footprint of ICESat-2 is not depicted (in opposite of the ICESat-1 study as illustrated in Figure 19 to Figure 27) because the elevation values are estimated from 100 metres segments of acquisition.

Canopy linked errors

As stated in 1.1.3, “The Copernicus DEM is a Digital Surface Model (DSM) which represents the surface of the Earth including buildings, infrastructure and vegetation”. Comparing Copernicus DEM EEA-10 heights relative to the top of canopy to ICESat-2 terrain heights result in positive errors, as illustrated in the case study of Figure 42.



Figure 42 - EEA-10 - ICESat-2 height differences – Case of Bois de la Mare Chantreuil near Galluis (France).

In Figure 42, an interpolated Copernicus DEM EEA-10 height is compared to a terrain height retrieved in the ATL08 product of ICESat-2. The resulting height difference is significant (+15.931 m) and highlights the major problems of comparing terrain to canopy relative heights.

Considering ICESat-2 terrain with canopy height for this comparison may be a solution for such cases, which results in a smaller but still significant height error (-8.806 m). However, the estimated canopy height is approximately equal to 25 metres, which may seem high for this case study. Bois de la Mare Chantreuil is part of the Rambouillet Forest, which has an area of 22 000 hectares. This forest is majorly known for its oak and pine trees. A reference picture of the Bois de la Mare Chantreuil have been found near the case study area of Figure 42, and is given hereafter in Figure 43.



Figure 43 - Reference picture of Bois de la Mare Chanteuil (France).

As seen in Figure 43, subfigure a, coniferous trees can be found in Bois de la Mare Chanteuil, which could reach 20 to 25 metres. As a consequence, the estimated canopy height of ICESat-2 may be accurate in this case study.

ICESat-2 canopy height estimation

Comparing Copernicus DEM EEA-10 canopy heights to ICESat-2 terrain heights can lead to important height errors, which may be reduced by considering ICESat-2 canopy heights (as seen in Figure 42). However, in some cases, this canopy height may increase errors, as the ATL08 product only provides an estimation of the canopy height based on 100 metres segments worth of canopy classified photons. The case study of Figure 44, concerning the vines of Léognan in France, is an example in which considering the canopy height estimation of ICESat-2 gives worse results than using only ICESat-2 terrain heights.



Figure 44 - EEA-10 - ICESat-2 height differences - Case of the vines of Léognan (France).

In that case study, an ICESat-2 terrain height and canopy height are retrieved over vines. Comparing Copernicus DEM EEA-10 to ICESat-2 terrain heights gives a small error of +0.497 metres. However, the height error reaches -20.041 metres when considering canopy height. The estimated canopy height seems enormous and certainly not corresponds to vines. In this case, the problem may come from the method of processing of the ATL08 product canopy height estimation, which may not be suitable for this quantitative assessment.

The ATL08 canopy height estimation is processed based on 100 metres of acquisition as follows: "The canopy heights are sorted into a cumulative distribution, and the height associated with the 98% height is reported." (see RD-23, under section 2.2.6). In this case, the estimated canopy height of the ATL08 product may depend on the height of trees surrounding the vines. As a consequence, a Copernicus DEM EEA-10 height retrieved in the vines may be compared to ICESat-2 terrain height summed with a height estimation of the surrounding canopy.

Time-varying snow ice heights

Events occurring between the acquisition periods of TanDEM-X and ICESat-2 may lead to height errors. The case study of Figure 45 highlights a positive error between Copernicus DEM EEA-10 and ICESat-2 terrain height only (+9.079 m).

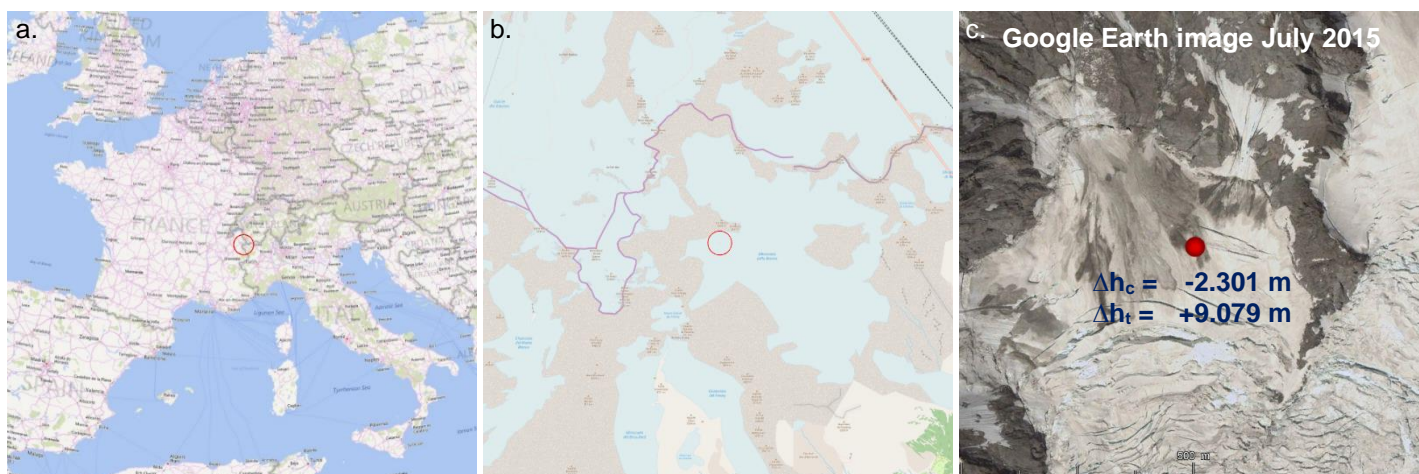


Figure 45 - EEA-10 - ICESat-2 height differences - Case of the Alps, near the Mont Blanc (Italy).

The Google Earth image used in Figure 45 was acquired on July 2015, and shows the study area partially covered by snow and ice. The Figure 46 shows another image acquired on May

2011, in which we can observe a different snow and ice repartition over the same study area. As a consequence, a cause of this error could be the snow and ice cover varying over the years.

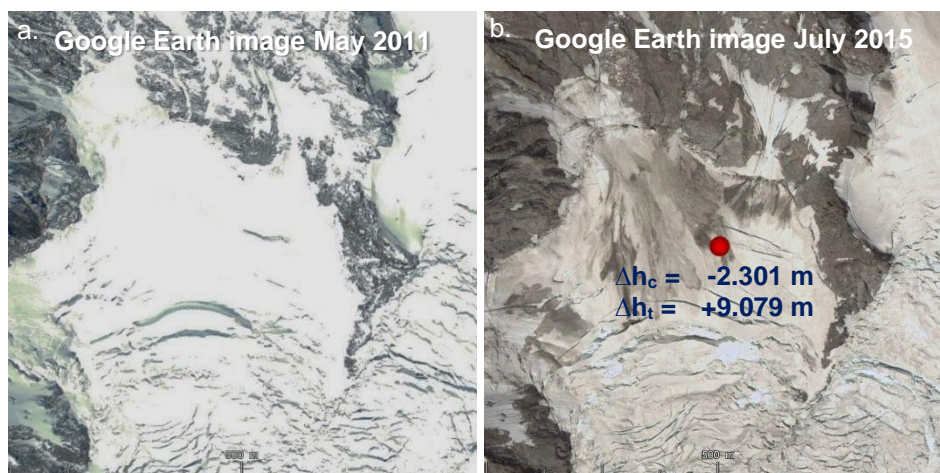


Figure 46 - EEA-10 - ICESat-2 height differences – Varying snow cover – Case of the Alps, near the Mont Blanc (Italy).

A canopy height is available for this study area, whereas no canopy is visible. The comparison of Copernicus DEM EEA-10 and ICESat-2 terrain with canopy height gives a lower absolute height error than using ICESat-2 terrain height only (only -2.301 m height error when taking into account ICESat-2 canopy estimation). As no canopy is present, the canopy estimation of ICESat-2 may be linked to terrain height, which could explain why a smaller error is obtained considering ICESat-2 terrain and canopy height than using only ICESat-2 terrain height.

Time-varying land use

Another case of time-related errors is covered in Figure 47, which highlights a negative error over an industrial building in Bergen op Zoom (Netherlands).

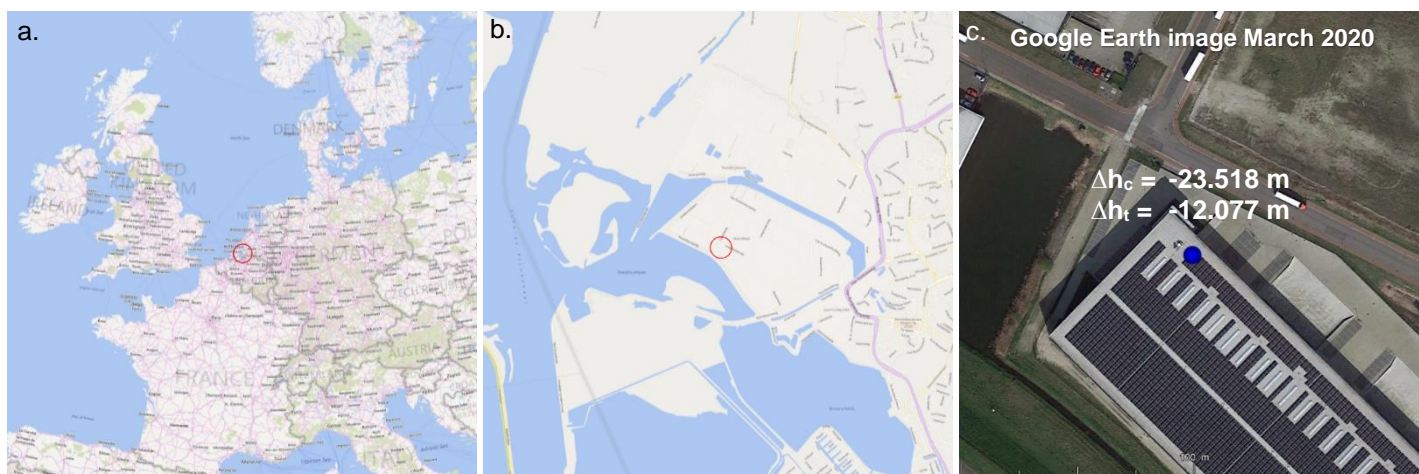


Figure 47 - EEA-10 - ICESat-2 height differences - Case of a building construction in Bergen op Zoom (Netherlands).

Here, the comparison of Copernicus DEM EEA-10 and ICESat-2 terrain height results in a negative error of -12.077 metres. The Google Earth image used in Figure 47 (subfigure c) was acquired on March 2020, and highlights the geolocation of the error over an industrial building. Figure 48 shows the same area, but acquired on July 2014 (subfigure b), where no building is visible.

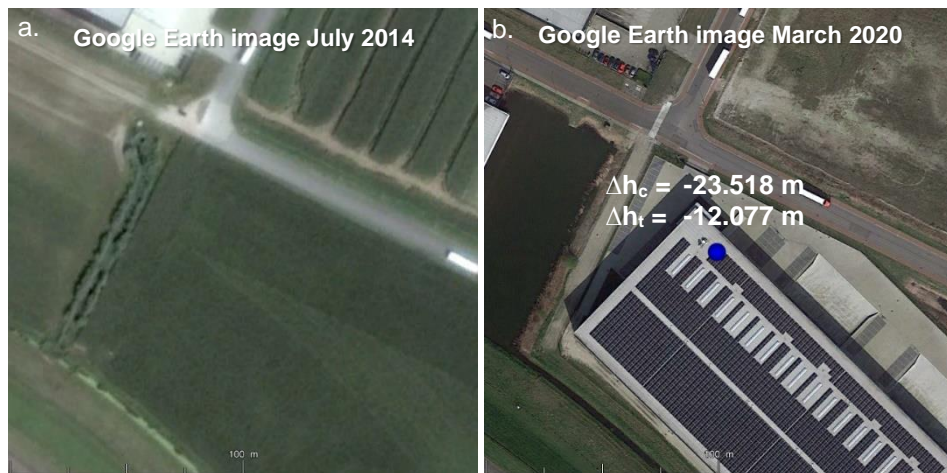


Figure 48 - EEA-10 - ICESat-2 height differences – Field before building construction in Bergen op Zoom (Netherlands).

As the building was constructed between the two acquisition periods of TanDEM-X and ICESat-2, the Copernicus DEM EEA-10 height is probably relative to the terrain, and the ICESat-2 terrain height is certainly relative to the top of the building.

In this case, a canopy height estimation is also available from ICESat-2 data, whereas no canopy is present. The comparison between the Copernicus DEM EEA-10 height and the ICESat-2 terrain with canopy height is high, almost two times higher than the results obtained using ICESat-2 terrain heights only. Given these facts, the ICESat-2 canopy height estimation may have been computed considering building heights instead of canopy heights.

4.3.5 Assessment of Copernicus DEM GLO-30 from ICESat-2 / ATLAS data

4.3.5.1 Spatial extent

Spatial extent of the Copernicus DEM GLO-30 is given in section 4.2.5.1.

As stated in section 4.2.5.1, Copernicus DEM GLO-30 is only assessed in the $[-60^\circ, 60^\circ]$ latitude interval in order to compare its results with SRTM-GL1, ASTER GDEM and ALOS World 3D. This limitation has been chosen considering the latitude limitation of SRTM-GL1 and the voids of ALOS World 3D.

4.3.5.2 Method and notations

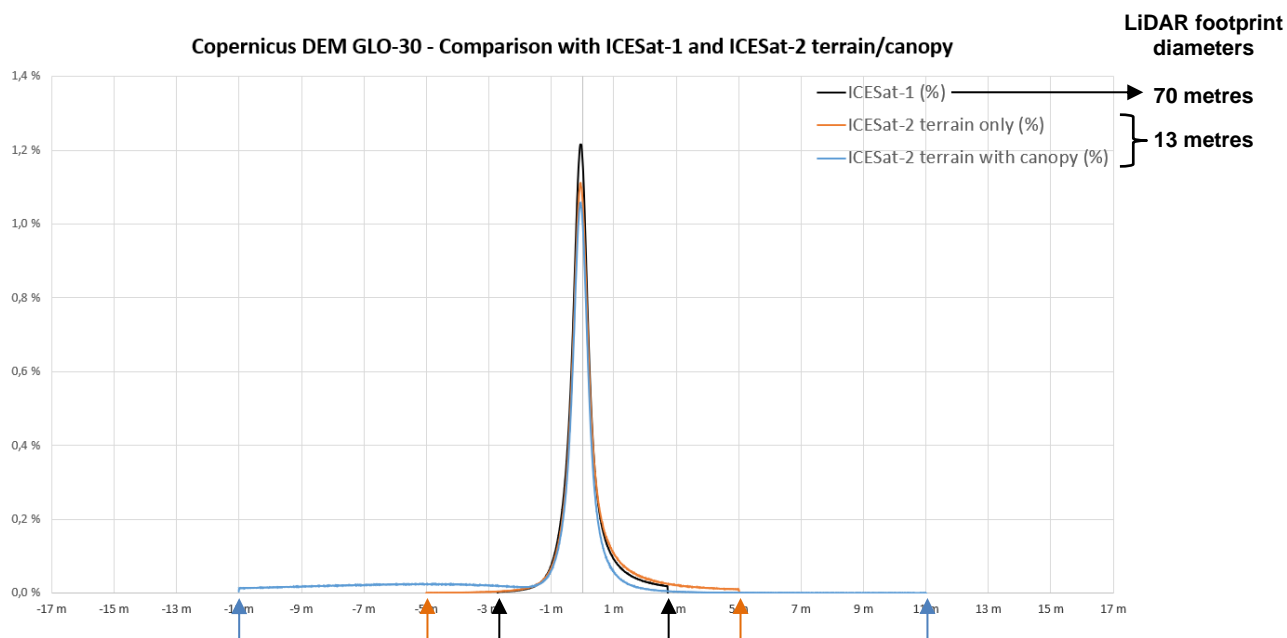
The methodology used is the same as the one for the assessment of Copernicus DEM EEA-10 from ICESat-2 (see section 4.3.4.1).

4.3.5.3 Results

Here are the results of the **Copernicus DEM GLO-30 – ICESat-2** study. The results obtained in this study are compared with results obtained in the **Copernicus DEM GLO-30 – ICESat-1** study. Statistics have been computed for two types of heights: one keeping only ICESat-2 **terrain height**, the other considering **canopy height** when canopy is present. All the statistics are computed with a 95% linear error (**LE95**). The following table summarizes the results of these studies:

LE95 statistics	ICESat-1	ICESat-2 (terrain only)	ICESat-2 (terrain with canopy)
Number of compared heights	59 319 279	13 816 724	13 816 724
Min	-2,725 m	-5,012 m	-11,008 m
Max	2,725 m	5,012 m	11,008 m
Mean (metres)	0,033 m	0,195 m	-1,124 m
Standard deviation (metres)	0,627 m	0,979 m	2,680 m
RMSE (metres)	0,628 m	0,999 m	2,907 m
Skewness	0,943	1,667	-1,953
Kurtosis	3,594	6,085	3,318

Table 19 - Statistics of the (Copernicus DEM GLO-30 – ICESat-2) comparison.



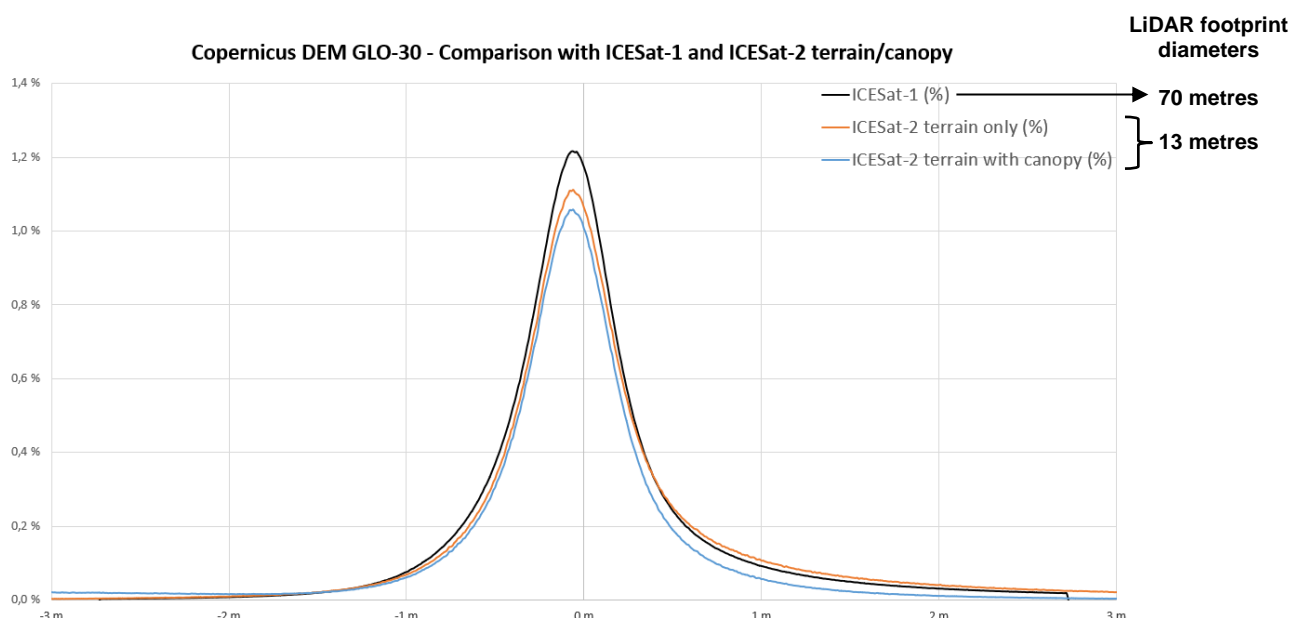


Figure 49 - Error histogram of the (Copernicus DEM GLO-30 – ICESat-2) study, comparison with previous results using ICESat-1 as vertical reference.

The histogram and the statistics show good results for both ICESat-2 terrain height only and ICESat-2 terrain with canopy height. However, the ICESat-2 terrain with canopy statistics shows worse results than the ICESat-2 terrain only statistics. At first glance, the ICESat-2 terrain with canopy histogram might indicate that Copernicus DEM GLO-30 is not strictly a Digital Surface Model (DSM), but it must be noticed that the h_{canopy} variable of the ATL08 product is an estimation of the canopy height (see section 4.3.4.4.1). The statistics show that the (Copernicus DEM GLO-30 – ICESat-1) study gives better results than the (Copernicus DEM GLO-30 – ICESat-2) studies. The better performance of ICESat-1 could be explained by the fact that Copernicus has been validated from ICESat-1 (see RD-15). Overall, the three studies show that Copernicus DEM GLO-30 is a really accurate DEM.

4.3.6 Assessment of Copernicus DEM GLO-90 from ICESat-2 / ATLAS data

4.3.6.1 Spatial extent

Spatial extent of the Copernicus DEM GLO-90 is given in section 4.2.6.1.

As stated in section 4.2.6.1, Copernicus DEM GLO-90 is only assessed in the [-60, 60] latitude interval in order to compare its results with SRTM-GL1, ASTER GDEM and ALOS World 3D. This limitation has been chosen considering the latitude limitation of SRTM-GL1 and the voids of ALOS World 3D.

4.3.6.2 Method and notations

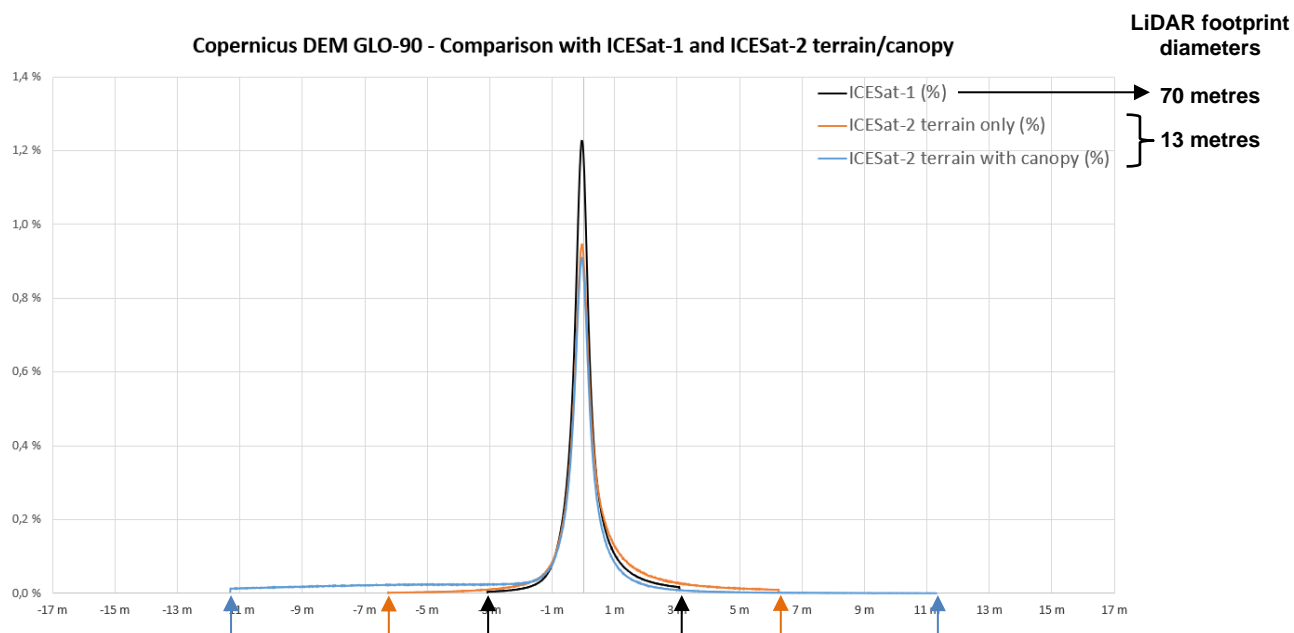
The methodology used is the same as the one for the assessment of Copernicus DEM EEA-10 from ICESat-2 (see section 4.3.4.1).

4.3.6.3 Results

Here are the results of the **Copernicus DEM GLO-90 – ICESat-2** study. The results obtained in this study are compared with results obtained in the **Copernicus DEM GLO-90 – ICESat-1** study. Statistics have been computed for two types of heights: one keeping only ICESat-2 **terrain height**, the other taking into account **canopy height** when canopy is present. All the statistics are computed with a 95% linear error (**LE95**). The following table summarizes the results of these studies:

LE95 statistics	ICESat-1	ICESat-2 (terrain only)	ICESat-2 (terrain with canopy)
Number of compared heights	59 396 074	13 838 239	13 838 239
Min	-3,015 m	-6,256 m	-11,308 m
Max	3,015 m	6,256 m	11,308 m
Mean (metres)	0,066 m	0,271 m	-1,102 m
Standard deviation (metres)	0,706 m	1,391 m	2,898 m
RMSE (metres)	0,709 m	1,417 m	3,100 m
Skewness	0,793	0,919	-1,587
Kurtosis	3,600	4,759	2,841

Table 20 - Statistics of the (Copernicus DEM GLO-90 – ICESat-2) comparison.



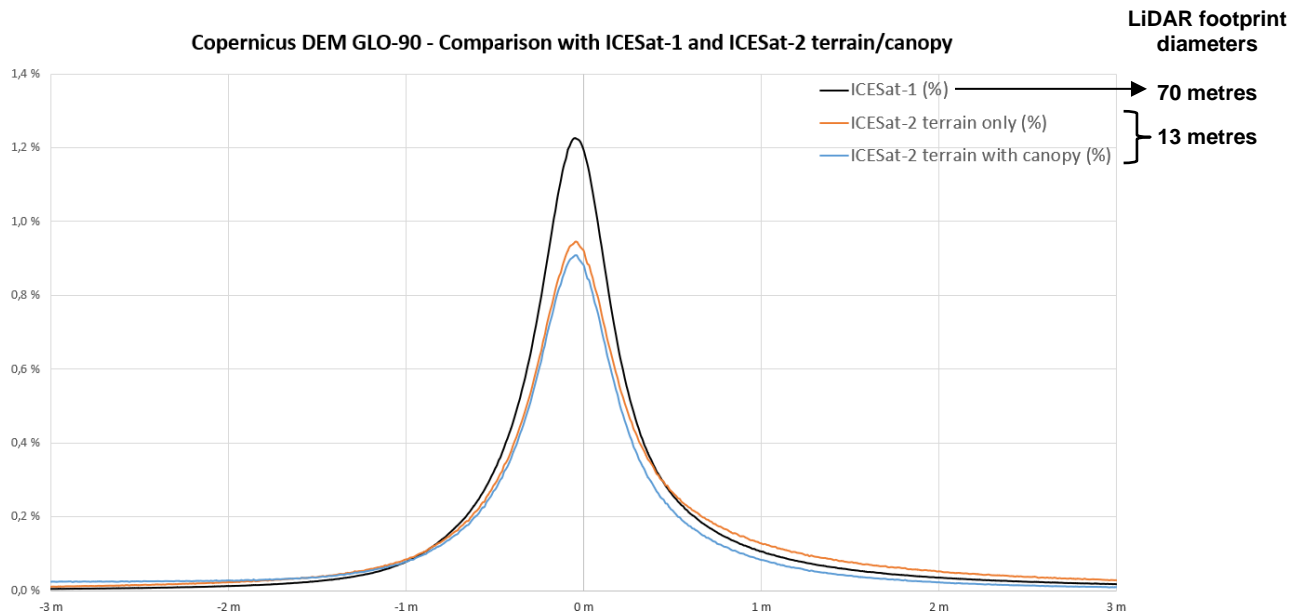


Figure 50 - Error histogram of the (Copernicus DEM GLO-90 – ICESat-2) study, comparison with previous results using ICESat-1 as vertical reference.

The histogram and the statistics show good results for both ICESat-2 terrain height only and ICESat-2 terrain with canopy height. However, the ICESat-2 terrain with canopy statistics shows worse results than the ICESat-2 terrain only statistics. At first glance, the ICESat-2 terrain with canopy histogram might indicate that Copernicus DEM GLO-90 is not strictly a Digital Surface Model (DSM), but it must be noticed that the *h_canopy* variable of the ATL08 product is an estimation of the canopy height (see section 4.3.4.4.1). The statistics show that the (Copernicus DEM GLO-90 – ICESat-1) study gives better results than the (Copernicus DEM GLO-90 – ICESat-2) studies. Once again, the better performance of ICESat-1 could be explained by the fact that Copernicus has been validated from ICESat-1 (see RD-15). Overall, the three studies show that Copernicus DEM GLO-90 is a really accurate DEM.

4.4 Elevation assessment from GEDI LiDAR – Quantitative assessment

4.4.1 History of GEDI

GEDI (Global Ecosystem Dynamics Investigation) was a mission led by the University of Maryland in collaboration with NASA Goddard Space Flight Center (GSFC). The GEDI instrument is a LiDAR launched to the ISS (International Space Station) on the 5th of December 2018. This LiDAR acquired data from March 2019 to March 2021. The main goal of this mission was to measure how deforestation has contributed to atmospheric CO₂ concentrations.

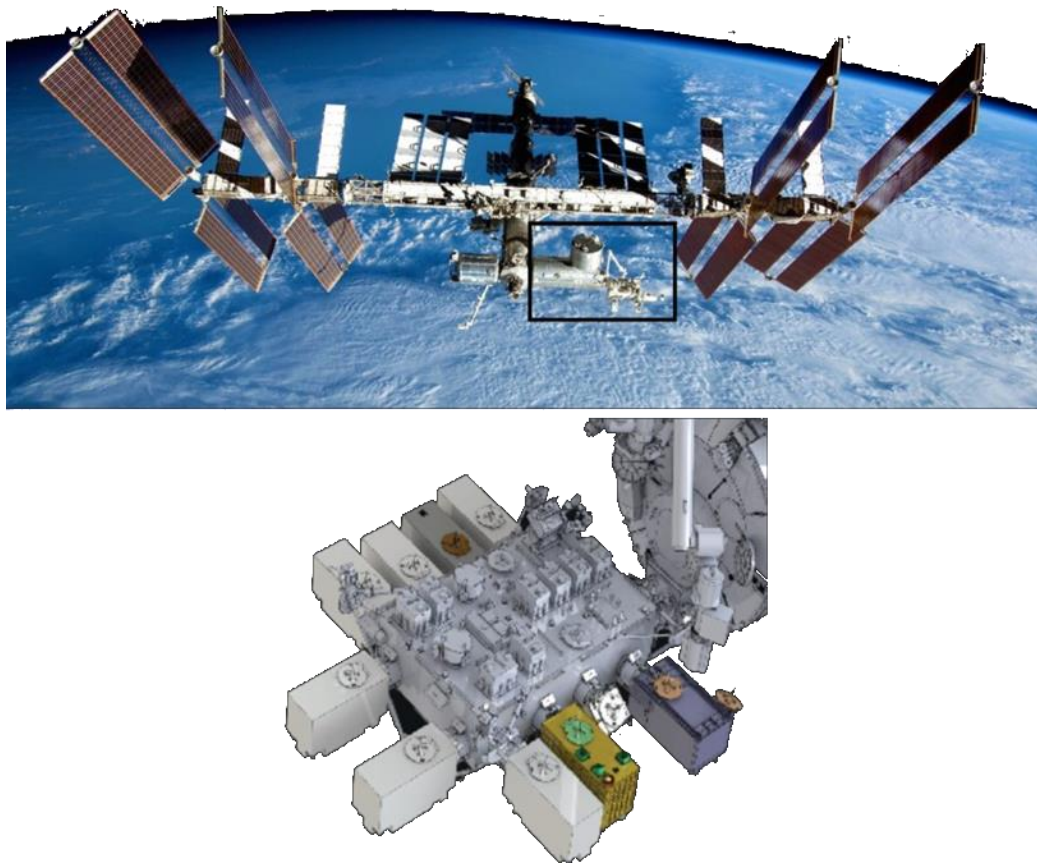


Figure 51 - GEDI onboard the ISS.
(<https://gedi.umd.edu/instrument/instrument-overview/>)

4.4.2 Technical specifications

Onboard the ISS, the GEDI instrument fires laser pulses at the frequency of **242 Hz**. This instrument acquires data over 8 ground tracks, as illustrated in the following figure.

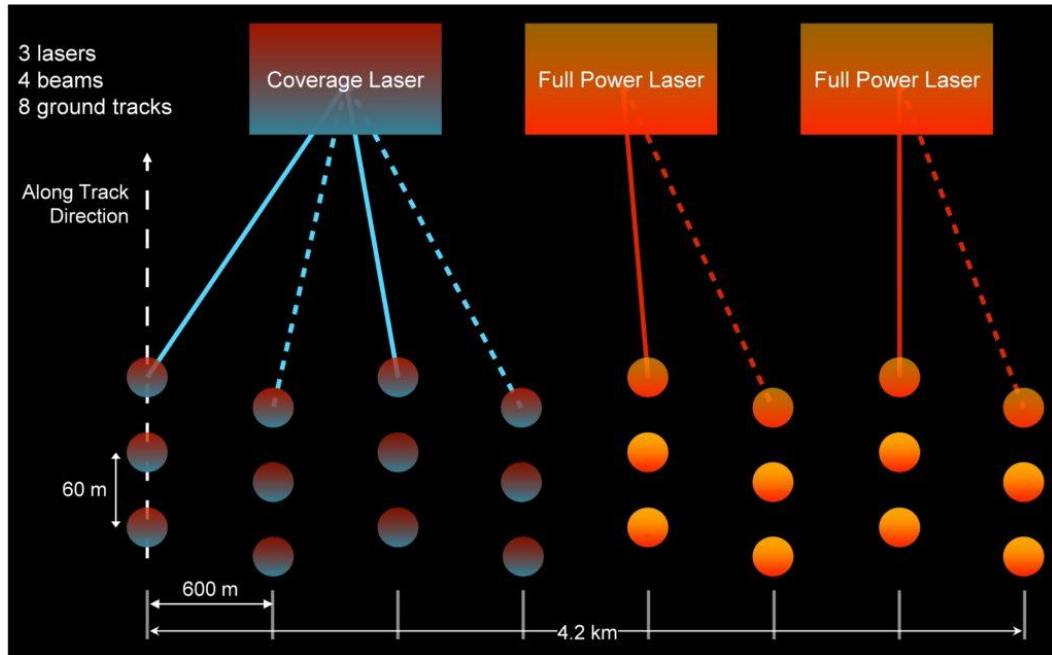


Figure 52 - GEDI lasers, beams and ground tracks.
(<https://gedi.umd.edu/instrument/specifications/>)

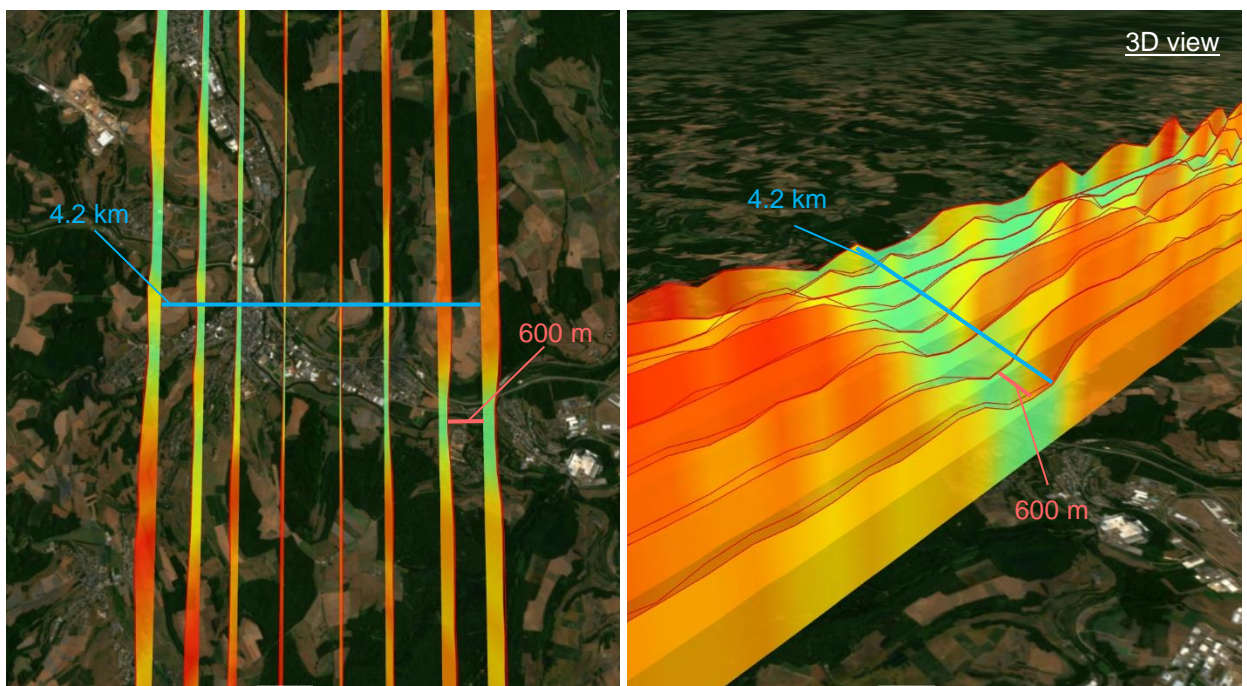


Figure 53 - GEDI height profiles over Luxembourg (near Diekirch, 2019.04.18).

As illustrated, the GEDI instrument is composed of three lasers (one coverage laser and two full power lasers). The coverage laser is split into two beams, whereas the two full power lasers fire a unique beam, resulting in four laser beams fired simultaneously. Each laser beam

alternates between two ground tracks, giving the eight ground tracks covered by the GEDI instrument.

The following table summarizes the characteristics of the GEDI instrument.

Technical specification	Value
Instrument name	Global Ecosystem Dynamics Investigation (GEDI)
First acquisition date	25.03.2019
Last acquisition date	Ongoing
Acquisition frequency	242 Hz
Ground sampling distance	~60 m (along track)
Central wavelength	1064 nm (near infrared)
Number of beams	8
Inter-beams distance	600 m
Repeat cycle	No repeat cycle
Footprint diameter	~25 m

Table 21 – GEDI technical specifications.

4.4.3 Assessment of GEDI measurement reliability

4.4.3.1 GEDI02_A product

4.4.3.1.1 Product organisation

The GEDI02_A product provides both waveform related variables and heights processed from the GEDI01_B product (geolocated waveforms). This product includes the ground elevation (elev_lowestmode) and the top of canopy height (elev_highestreturn). This product is available in the HDF5 format, which is composed of a hierarchical data structure (containing groups of variables). The root groups of these products are shown in Figure 54.

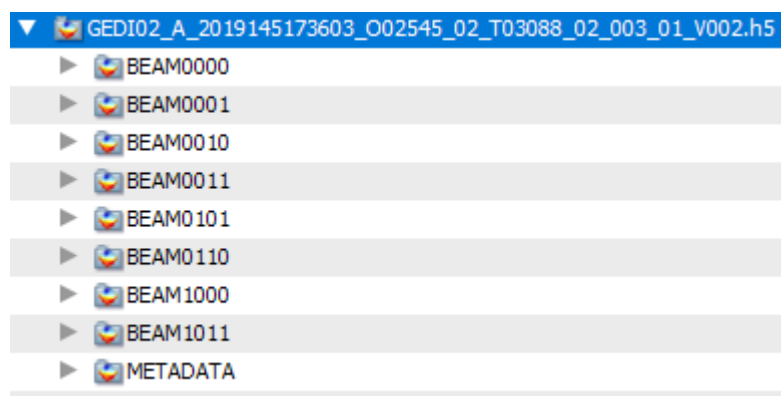


Figure 54 – Root group of GEDI02_A products.

All of these groups contain variables relative to one laser beam (except for the METADATA group, which contains dataset related metadata). The **BEAM0000**, **BEAM0001**, **BEAM0010**

and **BEAM0011** groups contain acquisitions of the four coverage beams of GEDI, whereas the **BEAM0101**, **BEAM0110**, **BEAM1000** and **BEAM1011** groups contain acquisitions of the four full-power beams.

In each group, two height acquisitions are retrieved:

- **elev_lowestmode** - elevation of centre of lowest mode relative to reference ellipsoid,
- **elev_highestreturn** - elevation of highest detected return relative to reference ellipsoid.

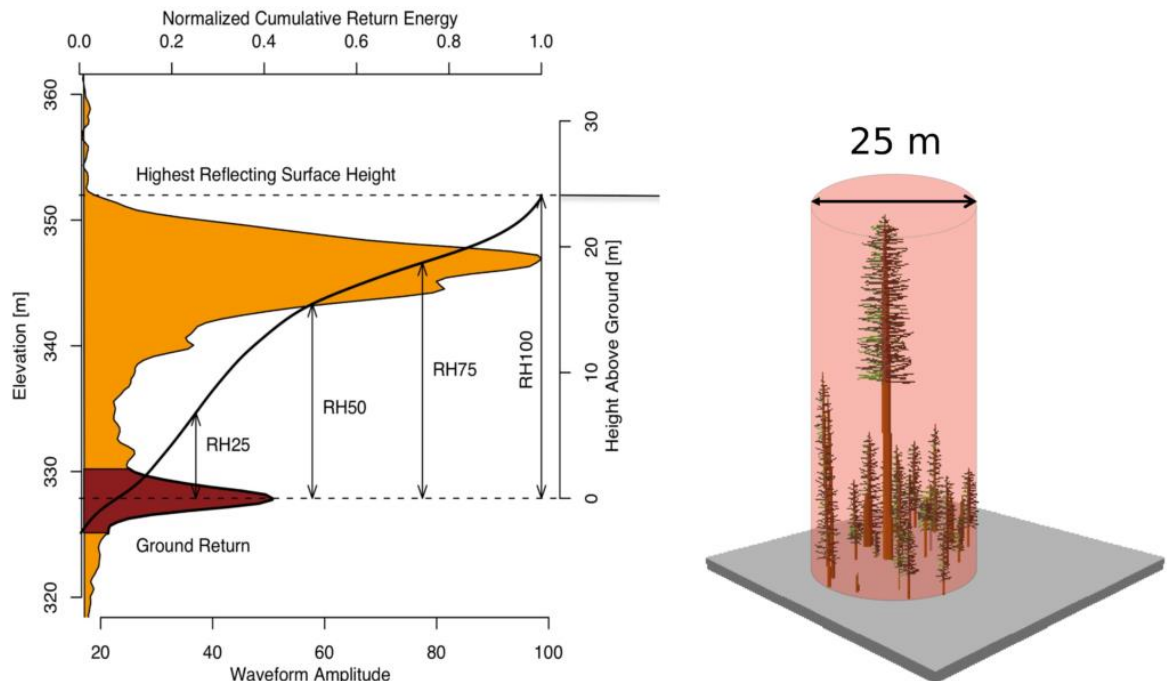


Figure 55 – GEDI return waveform and footprint.

As illustrated in Figure 55, when canopy is present, the **elev_lowestmode** and **elev_highestreturn** variables respectively correspond to the ground and the top of canopy elevations (labelled “Ground Return” and “Highest Reflecting Surface Height” in Figure 55). These elevations are given relative to the WGS84 ellipsoid.

The following histogram highlights the difference between the lowest mode and highest return elevations of the GEDI02_A product (acquisitions from 2019.04.18 to 2019.05.18). Outliers have been filtered using the **surface_flag** of the GEDI02_A product (equal to 1).

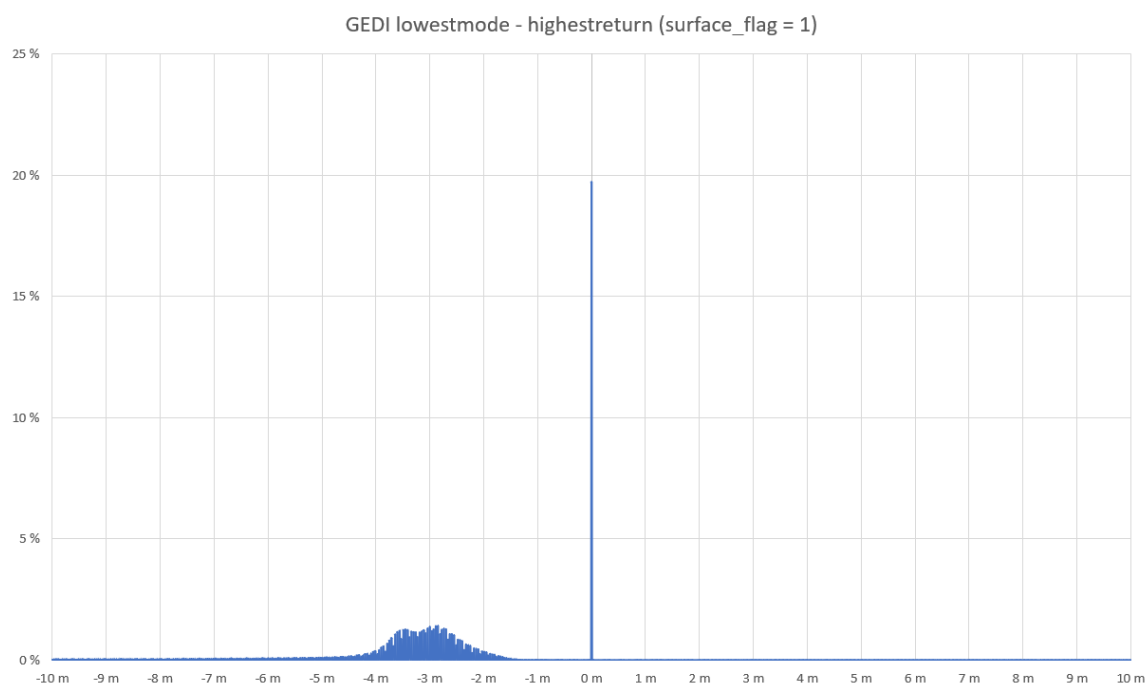


Figure 56 – Histogram of the difference between GEDI lowest mode and highest return, filtered using surface_flag.

As illustrated in Figure 56, for nearly 20% of GEDI acquisitions from 2019.04.18 to 2019.05.18, the lowest mode and highest return elevations are equal. Most of the differences (54.24%) between those elevations are included in the [-4 m, -2 m] interval.

4.4.3.1.2 Data filtering

Considering valid reference data requires GEDI02_A products to be filtered. Hereafter, three instances of the same GEDI02_A height profile are compared using different filtering techniques.

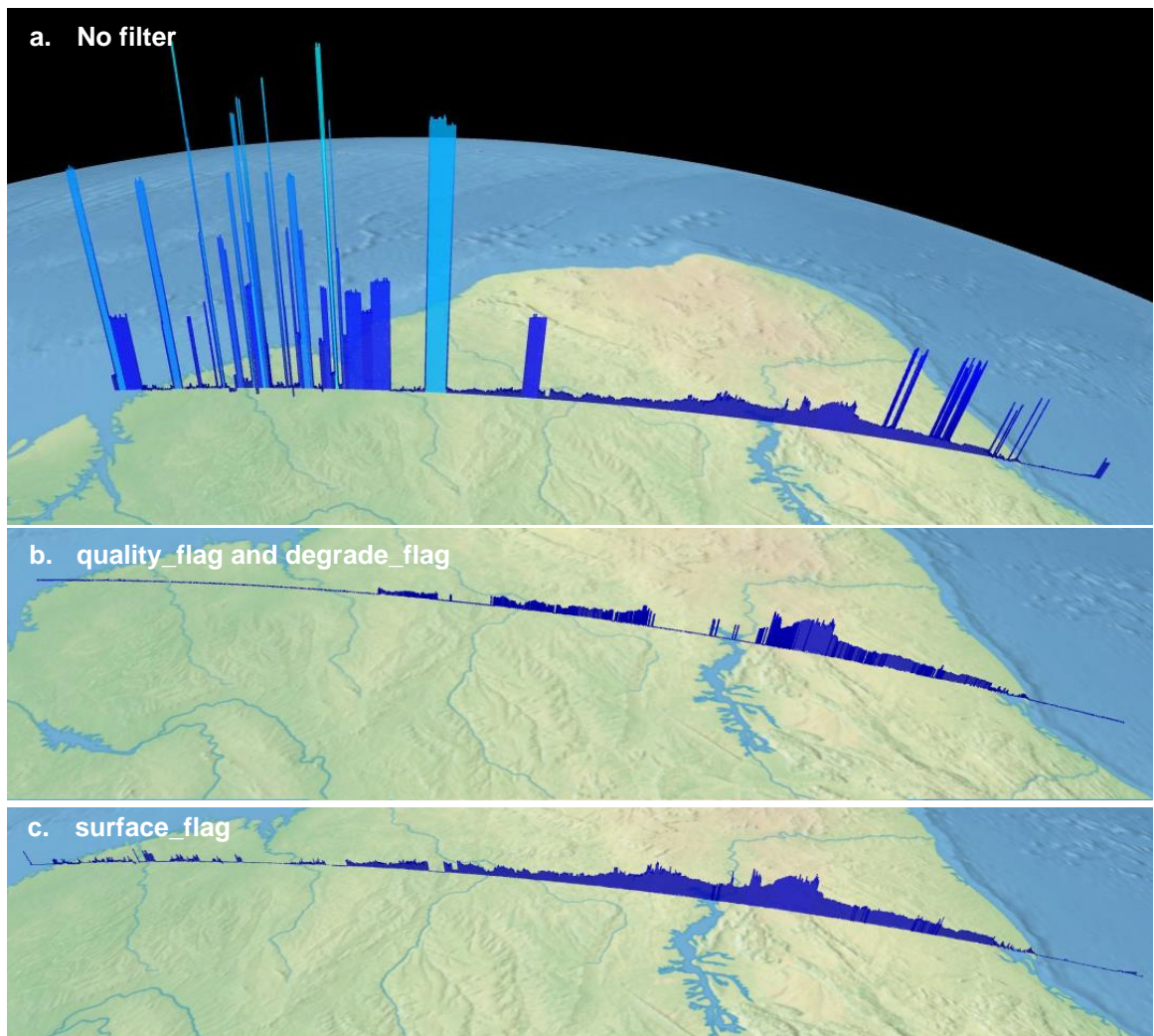


Figure 57 – GEDI02_A BEAM0000 height filtering over Brazil (2019.04.19).

The three instances of the same GEDI profile are retrieved with the following methods:

- No filtering is applied to the data (subfigure a),
- quality_flag and degrade_flag are used to filter bad quality data (subfigure b),
- surface_flag is used to filter outliers (subfigure c).

Only removing outliers using the surface_flag (subfigure c) is a good approach for visualization purposes. Using the quality_flag and degrade_flag is more suitable for quality assessments, as the majority of bad quality data is removed (subfigure b).

For this assessment, the filtering method depicted in Figure 57, subfigure b is used to consider valid GEDI02_A data. The filtering conditions are described in the following table.

Flag	Condition	Meaning
quality_flag	= 1	Valid acquisition (based on energy, sensitivity, amplitude, real-time surface tracking quality)
degrade_flag	= 0	No degraded orbit (geolocation errors)

Table 22 – GEDI02_A product height validity conditions.

However, using these quality flags filter the acquisitions for which GEDI lowest mode and highest return elevation are equal (which is not the case using the surface_flag, see Figure 56). The difference between GEDI lowest mode and highest return elevations is illustrated by the following histogram (filtered with quality_flag and degrade_flag).

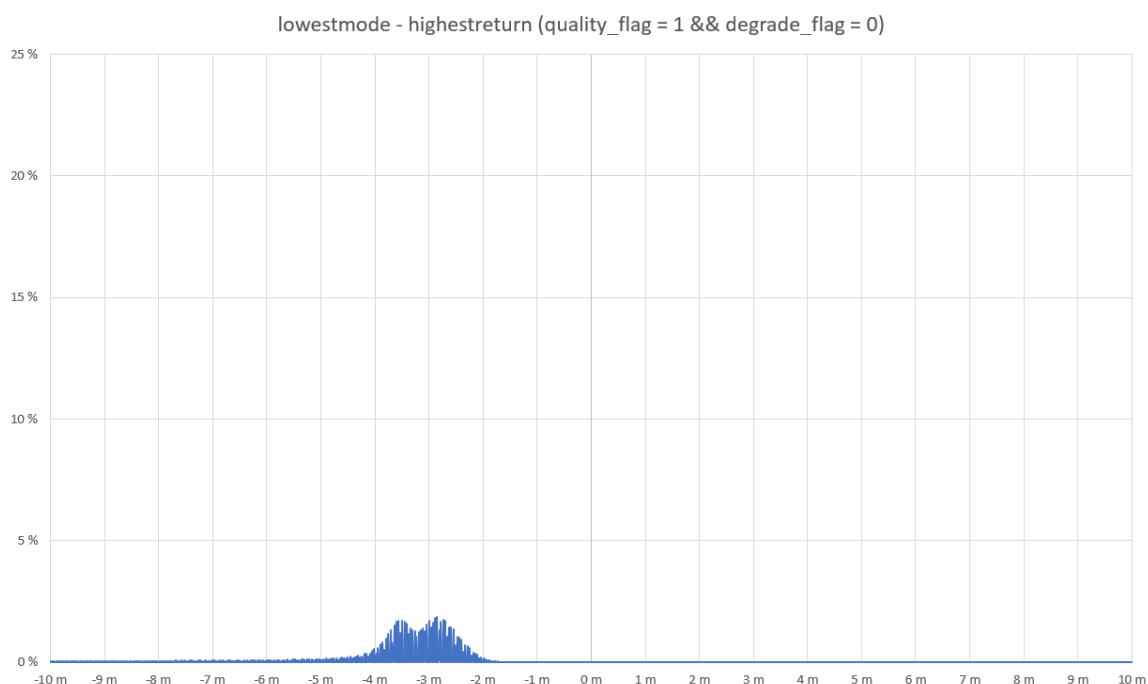


Figure 58 - Histogram of the difference between GEDI lowest mode and highest return, filtered using quality_flag and degrade_flag.

As illustrated in Figure 58, for the majority of GEDI acquisitions, the difference between lowest mode and highest return elevations is included in the [-4 m, -2 m] interval.

These filtered heights are both used to assess the accuracy of GEDI02_A heights (see section 0) and to assess the quality of Copernicus DEM EEA-10 (see section 4.4.4), Copernicus DEM GLO-30 (see section 4.4.5) and Copernicus DEM GLO-90 (see section 4.4.6).

4.4.3.2 Sampling of GEDI data

Sampling method (linear interpolation) used for GEDI data do not differ from the one used in the ICESat-1 / GLAS study. Please refer to section 4.2.3.2 for further details.

4.4.3.3 Height comparison with ICESat-1 and ICESat-2

4.4.3.3.1 Scope

In sections 4.2.3 and 4.3.3, ICESat-1 and ICESat-2 heights are compared on the same orbit over multiple revolutions to assess their constancy. Unfortunately, the ISS has no specific orbit repeat cycle, which prevents a similar study to be followed for the GEDI instrument.

As an alternative, this section presents multiple comparisons between GEDI (GEDI02_A) heights and ICESat-1 (GLAH14) / ICESat-2 (ATL08) heights over the Salt Lake Salar de Uyuni in Bolivia. This Salt Lake is known to be particularly flat and surrounded by mountains. Height comparisons are computed both on flat and mountainous areas, giving an overview of the similarities and differences between each LiDAR retrieved heights.

4.4.3.3.2 Method

The RD-41 presents multiple height comparisons over profile intersections between GEDI (GEDI02_A product) and ICESat-1/ICESat-2 (GLAH14 and ATL08 products) height profiles. The following figure highlights the study area and the intersecting height profiles.

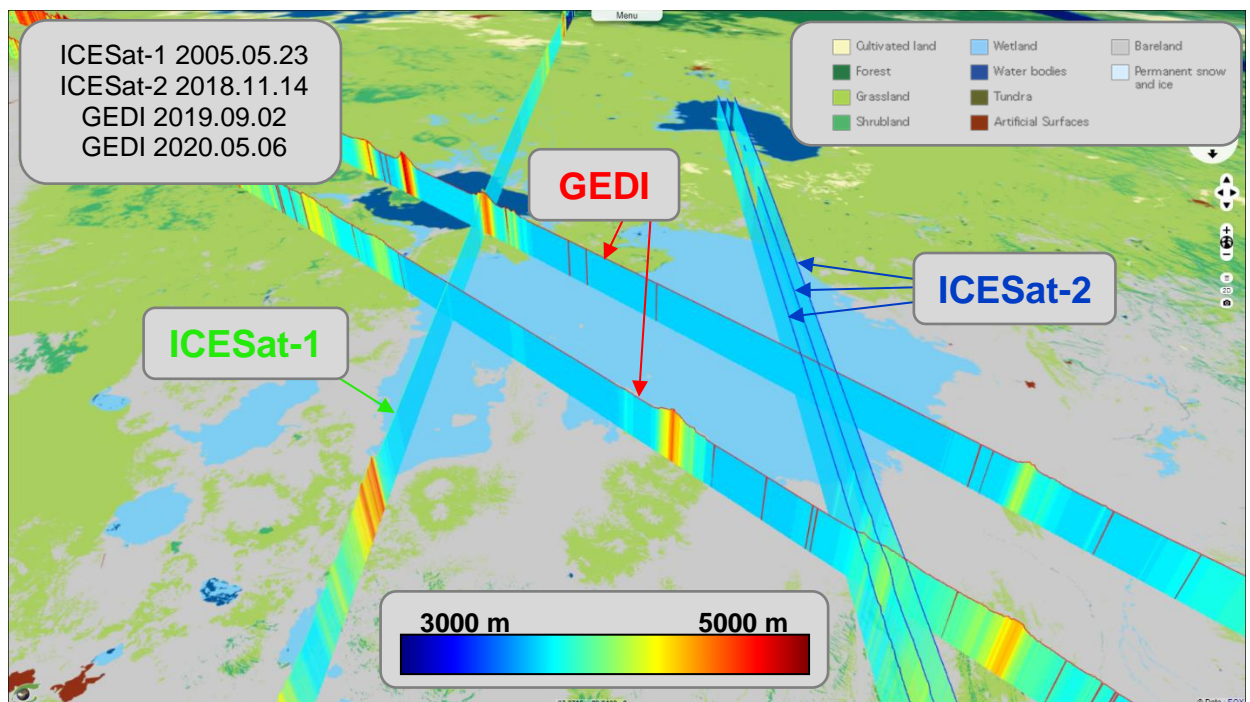


Figure 59 – Intersection of GEDI and ICESat-1 / ICESat-2 height profiles over Salar de Uyuni.

Heights are interpolated on GEDI lowest mode, ICESat-1 and ICESat-2 terrain profiles at each intersection location. Then, the differences between the interpolated heights of GEDI and ICESat-1 / ICESat-2 is computed, named Δh in the following figures.

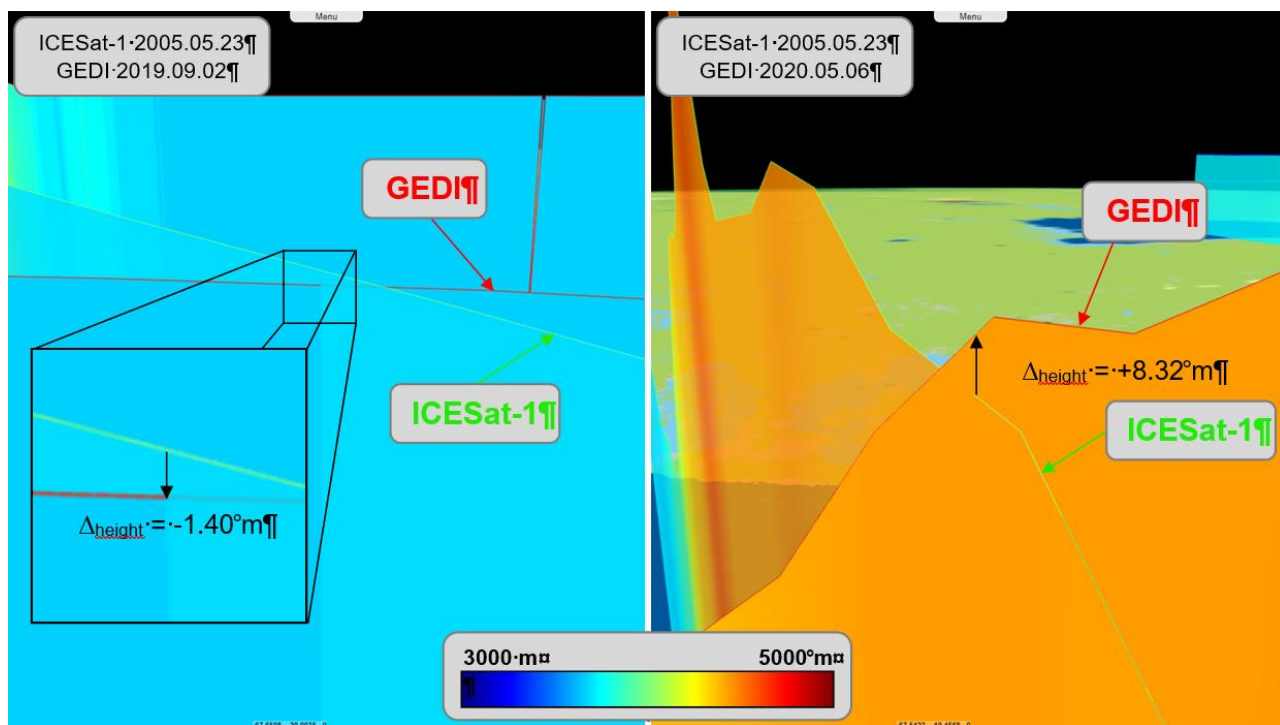


Figure 60 – Intersections between GEDI and ICESat-1 over Salar de Uyuni (left), outside of Salar de Uyuni (right).

As illustrated in Figure 60, a relatively important height difference is observed over the Salar de Uyuni (-1.40 metres); a smaller error may have been expected due to the flatness of this area. An even bigger height difference is observed on mountainous areas around the Salar de Uyuni (+8.32 metres).

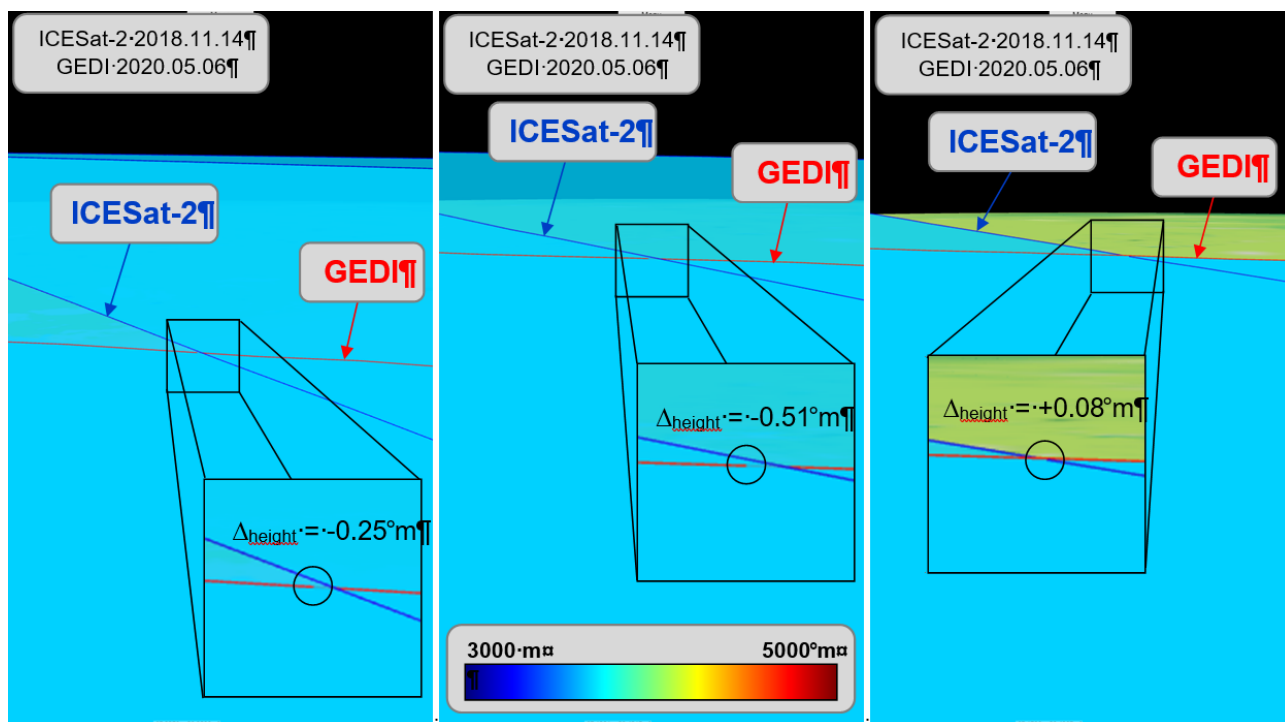


Figure 61 – Intersections between GEDI and ICESat-2 over Salar de Uyuni.

As illustrated in Figure 61, small elevation differences may be observed when comparing GEDI lowest mode to ICESat-2 terrain heights. The differences between GEDI and ICESat-2 look smaller than those observed between GEDI and ICESat-1.

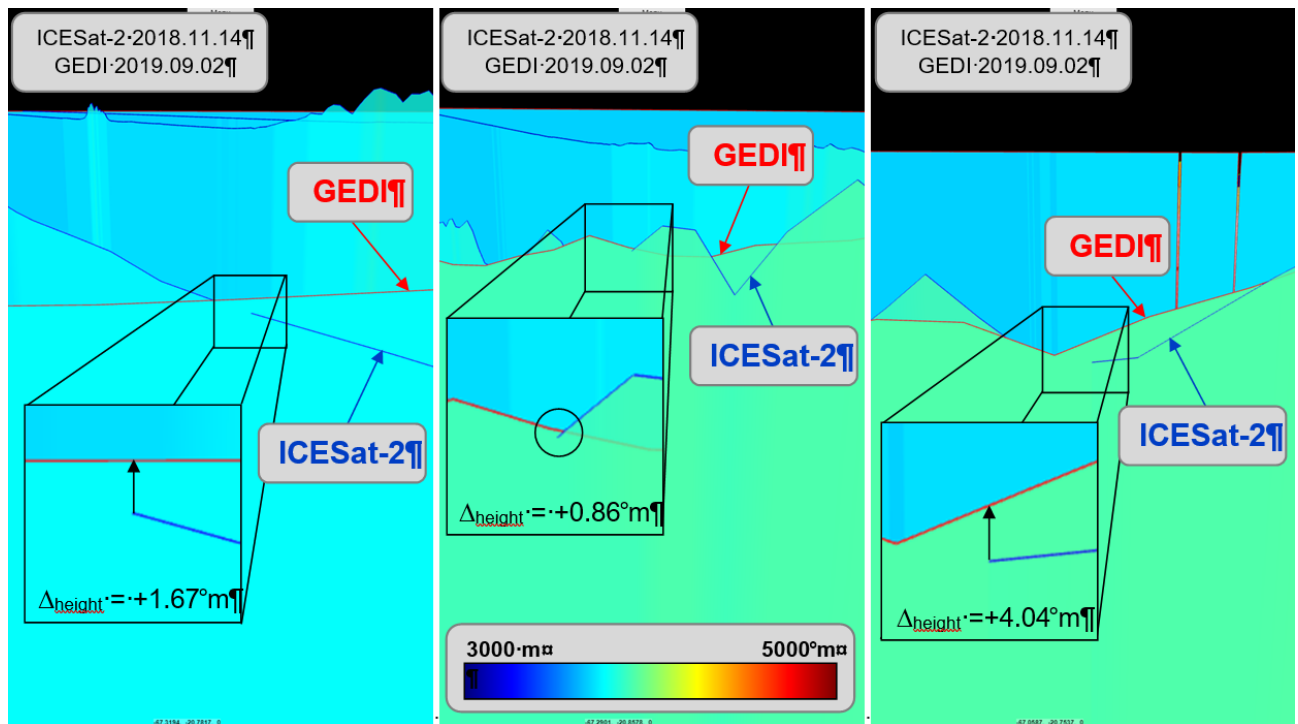


Figure 62 – Intersections between GEDI and ICESat-2 around Salar de Uyuni.

On the opposite of the small height differences observed in the Salar (see Figure 61), these differences are much larger in the mountainous areas around the Salar (see Figure 62).

This study is only performed on a few examples. The intercomparison of multiple LiDAR acquisitions should be performed on a more representative number of samples.

4.4.3.4 Geographical distribution of GEDI products

This study is based on **1628** GEDI02_A products (**2.44 TB**), representing one month of GEDI data (2019.04.18 to 2019.05.18). The products contain acquisitions up to 1/4th of an orbit. GEDI acquisitions are limited to the $[-51.6^\circ, +51.6^\circ]$ latitude interval, as shown in the following figure.

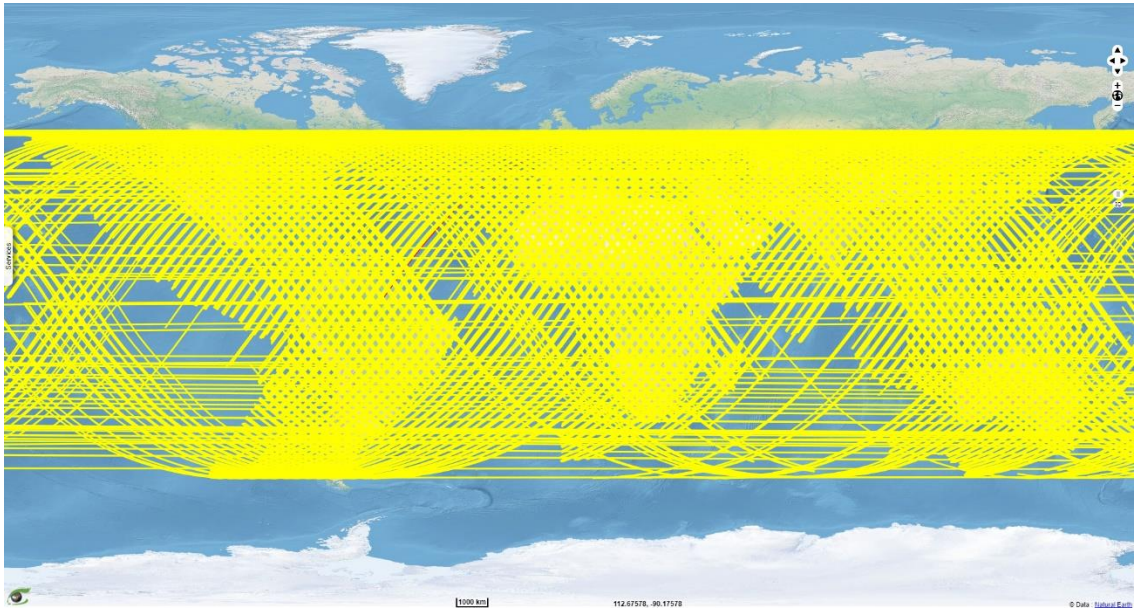


Figure 63 - Distribution of the 1628 used GEDI02_A products.

4.4.4 Assessment of Copernicus DEM EEA-10 from GEDI data

This section presents the quantitative evaluation of the vertical accuracy of **Copernicus DEM EEA-10** using reference data from **GEDI (LiDAR)**. The methods and the notations of this study are given here after (see section 4.4.4.1). The methods used to process DEM heights are the same as the ones described in section 4.2, consequently, only a summary of the steps involved in comparing the **Copernicus DEM EEA-10** to **GEDI** data is given, referencing other sections for further details. The same methods will apply for the evaluation of **Copernicus DEM GLO-30** (section 4.4.5) and **Copernicus DEM GLO-90** (section 4.4.6) and will not be repeated.

4.4.4.1 Method and notations

4.4.4.1.1 Summary of the methods used

The GEDI02_A product includes two distinct elevations: the lowest mode elevation and the highest return elevation. Consequently, statistics concerning two quantitative studies are given, respectively comparing Copernicus DEM EEA-10 heights to GEDI02_A **lowest mode elevation** and to GEDI02_A **highest return elevation**.

The main steps of this study are:

- Filtering bad acquisitions from GEDI02_A products, retrieving reference GEDI heights relative to the WGS84 ellipsoid,
- Interpolating Copernicus DEM EEA-10 heights at each GEDI02_A reference height footprint location, retrieving interpolated DEM heights relative to the EGM2008 geoid,
- Convert the vertical reference system of the interpolated EGM2008 DEM heights to the WGS84 ellipsoid,
- Given GEDI02_A heights of reference and Copernicus DEM EEA-10 heights expressed with respect to the WGS84 ellipsoid, compute height differences, both taking as reference GEDI02_A lowest mode elevations and GEDI02_A highest return elevations.

Filtering GEDI02_A products is done using methods described in section 4.4.3.1. GEDI02_A product heights are already expressed with respect to the WGS84 ellipsoid. Therefore, no vertical reference system conversion is applied to this reference data.

Bilinear interpolation is used to retrieve Copernicus DEM EEA-10 heights at each GEDI acquisition footprint. Then, the interpolated heights are converted from the EGM2008 geoid to the WGS84 ellipsoid (see section 4.2.4.2.3 for more details).

From this point, the difference between Copernicus DEM EEA-10 and GEDI02_A heights can be calculated, as both are expressed relative to the WGS84 ellipsoid.

4.4.4.1.2 Computing the height difference

The following equation is used to compute the height difference between Copernicus DEM EEA-10 interpolated height and GEDI02_A **lowest mode**:

$$\Delta h = h_{DEM} - h_{GEDI_{lm}} \quad (\text{eq. 7})$$

Where:

Δh	is the height difference between Copernicus DEM EEA-10 and ICESat-2,
$h_{GEDI_{lm}}$	is the GEDI02_A lowest mode height (with respect to the WGS84 ellipsoid),
h_{DEM}	is the Copernicus DEM EEA-10 height (with respect to the WGS84 ellipsoid).

The following equation is used to compute the height difference between Copernicus DEM EEA-10 interpolated height and GEDI02_A **highest return**:

$$\Delta h = h_{DEM} - h_{GEDI_{hr}} \quad (\text{eq. 8})$$

Where:

Δh	is the height difference between Copernicus DEM EEA-10 and ICESat-2,
$h_{GEDI_{hr}}$	is the GEDI highest return height (with respect to the WGS84 ellipsoid),
h_{DEM}	is the Copernicus DEM EEA-10 height (with respect to the WGS84 ellipsoid).

4.4.4.2 Overall algorithm

The following diagram summarizes the steps involved in the comparison between the Copernicus DEM EEA-10 and GEDI reference data:

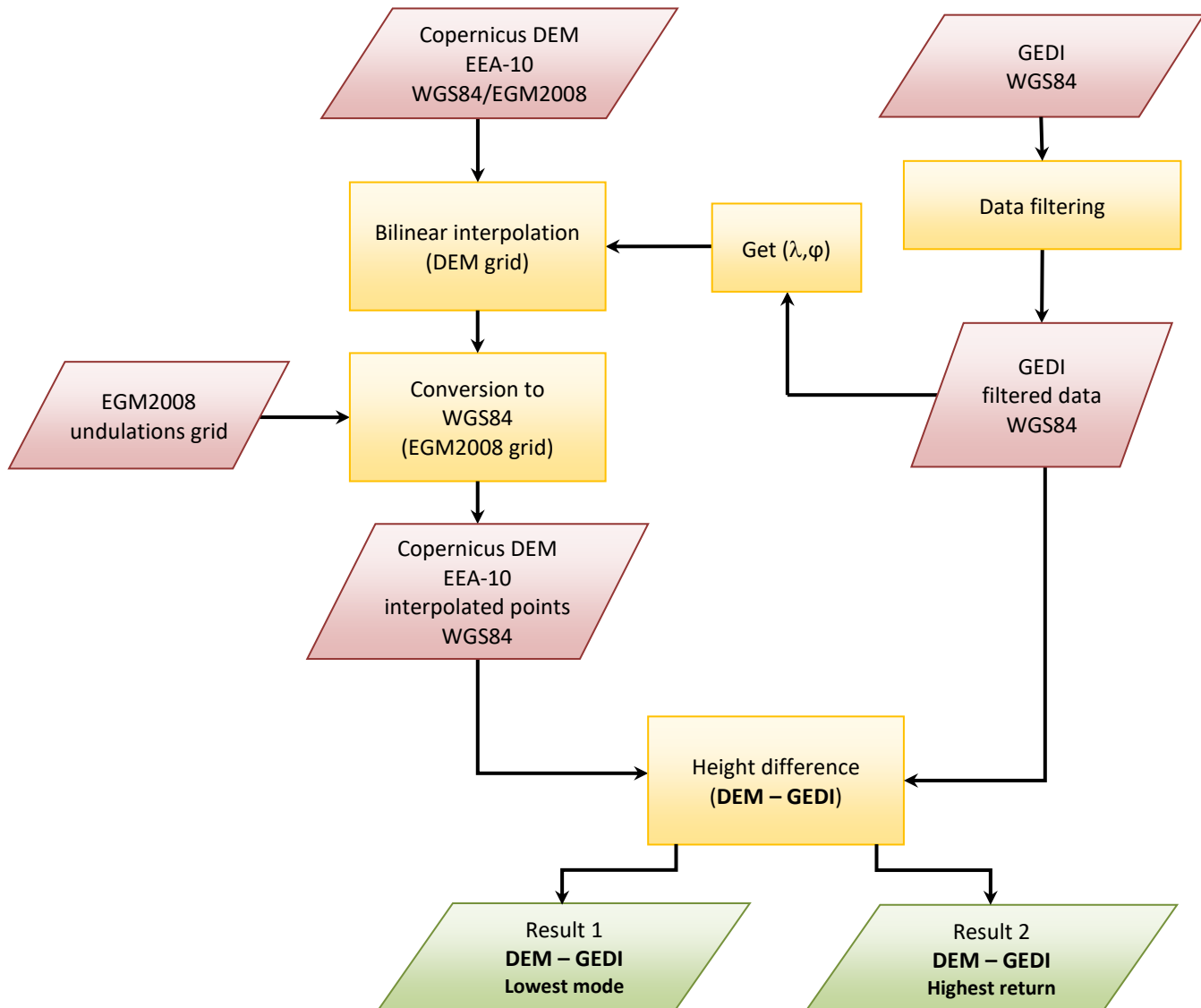


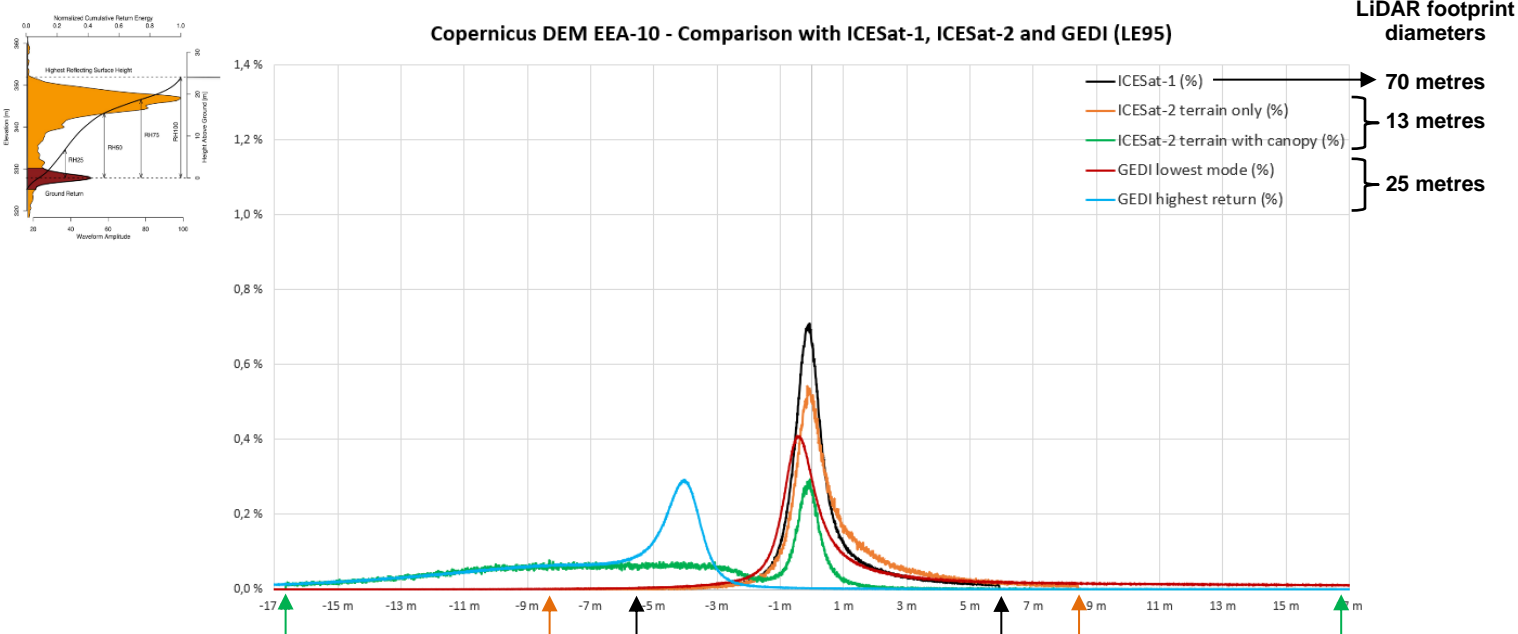
Figure 64 – Summary of the Copernicus DEM EEA-10 assessment method using GEDI as a vertical reference.

4.4.4.3 Results

Here are the results of the **Copernicus DEM EEA-10 – GEDI** study. The results obtained in this study are compared with results obtained in the **Copernicus DEM EEA-10 – ICESat-1** and **Copernicus DEM EEA-10 – ICESat-2** studies. Statistics have been computed for two types of heights, respectively considering the lowest mode and highest return elevations of GEDI02_A products. All the statistics are computed with a 95% linear error (**LE95**). The following table summarizes the results of these studies:

LE95 statistics	ICESat-1	ICESat-2 (terrain only)	ICESat-2 (terrain with canopy)	GEDI (lowest mode)	GEDI (highest return)
Number of compared heights	1 803 551	399 179	399 179	11 263 632	11 263 634
Min	-5,924 m	-8,415 m	-16,642 m	-20,090 m	-17,780 m
Max	5,924 m	8,421 m	16,600 m	20,150 m	17,600 m
Mean (metres)	0,270 m	0,822 m	-5,477 m	2,363 m	-6,916 m
Standard deviation (metres)	1,389 m	1,944 m	4,838 m	5,277 m	3,968 m
RMSE (metres)	1,415 m	2,111 m	7,307 m	5,782 m	7,973 m
Skewness	1,091	1,283	0,251	1,610	-0,218
Kurtosis	3,797	2,823	-0,777	2,031	2,017

Table 23 - Error statistics of the (Copernicus DEM EEA-10 - GEDI) study, comparison with previous results using ICESat-1 and ICESat-2 as vertical references.



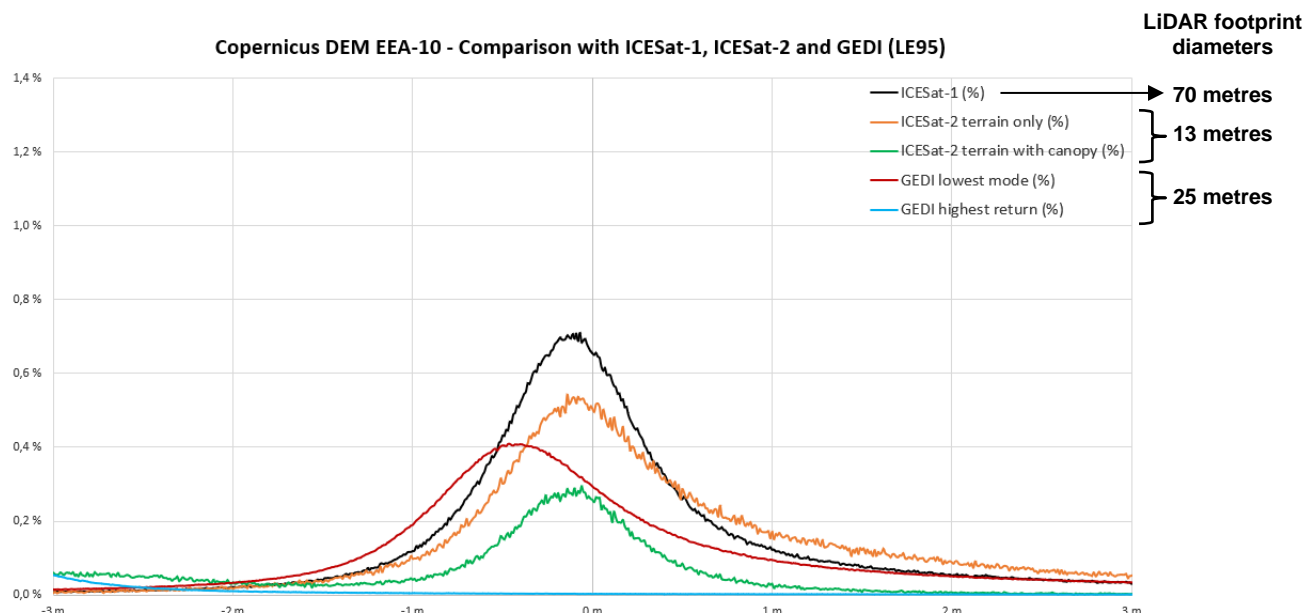


Figure 65 - Error histogram of the (Copernicus DEM EEA-10 - GEDI) study, comparison with previous results using ICESat-1 and ICESat-2 as vertical references.

The histogram and the statistics show better results using GEDI lowest mode than using GEDI highest return as a vertical reference. As a consequence, Copernicus DEM EEA-10 heights are closer to GEDI lowest mode (ground return) than to GEDI highest return (top of canopy return). Here, a difference of a few metres can be observed (algebraic mean difference of 9.279 m) between the modes of the (Copernicus DEM EEA-10 – GEDI lowest mode) and the (Copernicus DEM EEA-10 – GEDI highest return). This difference is linked to the GEDI02_A product, for which every valid acquisition has a different lowest mode and highest return elevations (see section 4.4.3.1.2 for further details). Considering ICESat-1 reference data still gives the best results, retrieving a mean, standard deviation and RMSE of respectively 0.270 metres, 1.389 metres and 1.415 metres. Considering GEDI highest return reference data gives the worst results for both mean height error and RMSE, respectively reaching -6.916 metres and 7.973 metres. The worst standard deviation is obtained using GEDI lowest mode as reference data, reaching 5.277 metres.

4.4.4.4 Typical sources of elevation errors

4.4.4.4.1 GEDI elevation errors

Section 8 of RD-28 references known issues for GEDI02_A and GEDI02_B products. Concerning the GEDI02_A product, the following issues are mentioned:

- **Orbit degradation periods:** periods when the orbit is degraded may impact the quality of the geolocation. This issue is fixed by considering the `degrade_flag` of the GEDI02_A product, which indicates a non-degraded orbit.
- **Retrieval algorithms:** six different algorithm settings can be used to compute `elev_lowestmode` (ground height), `elev_highestreturn` (top of canopy elevation) as well as their respective geolocations. GEDI02_A geolocations and heights are retrieved from the algorithm settings giving the best global product performance. Locally, other algorithm settings may give better results. For this study, the algorithm giving the best global performance has been considered.
- **Surface flag:** The `surface_flag` may incorrectly be set to 0 in high elevation areas, causing the filtering of good acquisitions over these areas.
- **BEAM0000/BEAM0001:** RD-28 references a known bias affecting the BEAM0000 and BEAM0001 absolute heights (up to 60 centimetres of error). This issue was already fixed in the L1B products version 2 and does not occur in this study.

- **Degrade flag:** some elevation errors are stated not to be identified by the “\\ade” flag (supposedly the “degrade” flag). Users are encouraged to use the “degrade_flag” and to consider the difference between GEDI and DEM heights to filter bad acquisitions. In the case of this study, the “quality_flag” already considers this difference to filter bad acquisitions.

4.4.4.4.2 Geomorphological and land use / land cover context causing elevation errors

This section aims to provide a better understanding of the sources of Copernicus DEM EEA-10 height errors by observing their repartition all over the geographical extent of this study. In the figures of this section, negative height errors are depicted in blue (Copernicus DEM EEA-10 height is lower than the GEDI reference height) whereas positive height errors are depicted in red (Copernicus DEM EEA-10 height is greater than the GEDI reference height).

In the following examples, the differences between Copernicus DEM EEA-10 and the GEDI lowest mode (Δh_{lm}) and the GEDI highest return (Δh_{hr}) are given at error geolocation, showing various geomorphological and/or land use / land cover contexts.

DSM heights vs. terrain heights

As stated in 1.1.3, “The Copernicus DEM is a Digital Surface Model (DSM) which represents the surface of the Earth including buildings, infrastructure and vegetation”. Comparing Copernicus DEM EEA-10 heights relative to the top of canopy to GEDI lowest mode heights (ground return) result in positive errors, as illustrated in the case study of Figure 66.

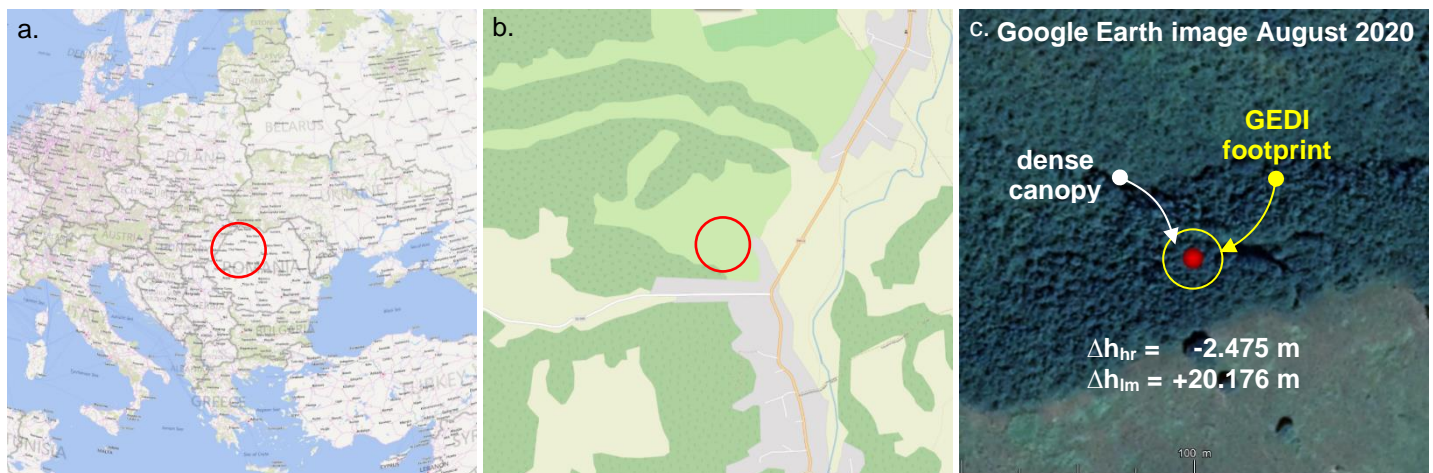


Figure 66 - EEA-10 - GEDI height differences – Case of dense forests near Chendrea (Romania).

In Figure 66, an interpolated Copernicus DEM EEA-10 height is compared to a lowest mode elevation retrieved in a GEDI02_A product. The resulting height difference is significant (+20.176 m) and highlights the major problems of comparing terrain to canopy heights.

Considering the GEDI02_A highest return elevation for this comparison may be a solution for such cases, which results in a smaller error (-2.475 m).

Sparse canopy

In this case study, GEDI02_A lowest mode and highest return elevations are retrieved from an acquisition over a small cluster of trees.



Figure 67 - EEA-10 - GEDI height differences – Case of sparse canopy near fields of Centro Tre Denari (Italy).

As shown in Figure 67, the Copernicus DEM EEA-10 height is really close to the lowest mode elevation of GEDI, retrieving a small height error (-0.131 m). On the opposite, a high error is retrieved when using the highest return elevation of GEDI (-24.980 m).

Excavations

In this case study, a Copernicus DEM EEA-10 height and GEDI02_A elevations are compared over the Tagebau Nochten mine in Germany.

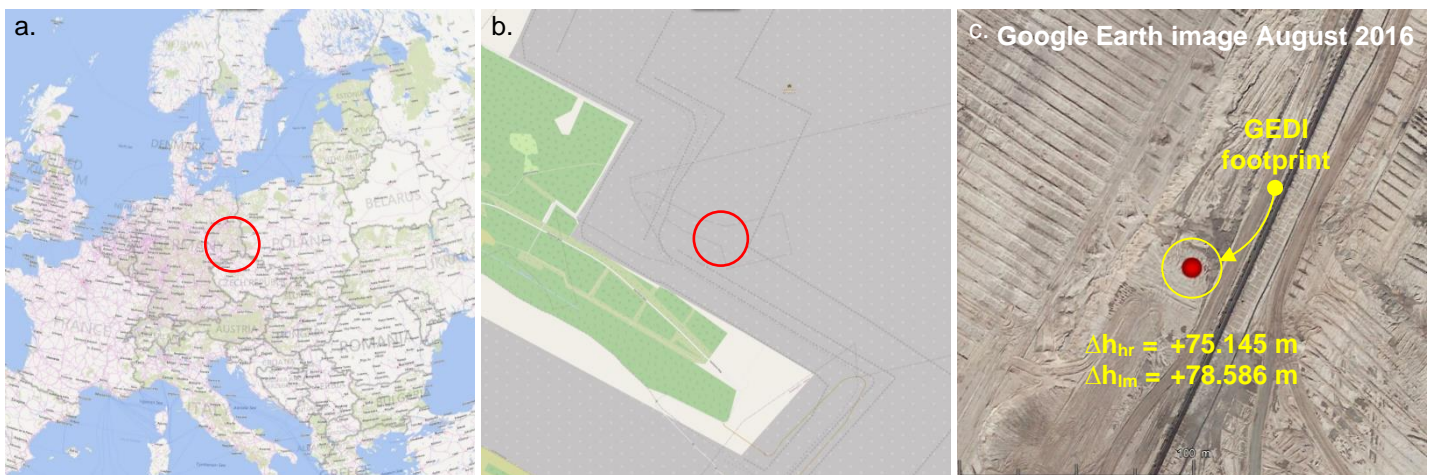


Figure 68 - EEA-10 - GEDI height differences – Case of the Tagebau Nochten mine (Germany).

Excavations such as the Tagebau Nochten mine can lead to high height errors from one acquisition to another. Figure 69 highlights the evolution of the Tagebau Nochten mine from September 2014 to August 2016.



Figure 69 - EEA-10 - GEDI height differences – Evolution of the Tagebau Nochten mine (Germany).

As seen in Figure 69, the Tagebau Nochten mine have expanded from 2014 to 2016. The Copernicus DEM EEA-10 heights are retrieved from 2010 to 2015 TanDEM-X acquisitions, whereas the reference GEDI heights are retrieved from 2019 acquisitions. As a consequence, important height errors highlighted in Figure 68 (respectively +75.145 m and +78.586 m for highest return and lowest mode) are certainly linked to the activity of the Tagebau Nochten mine.

Buildings

In this case study, Copernicus DEM EEA-10 and GEDI heights are compared close to a building in Striesa (Germany).

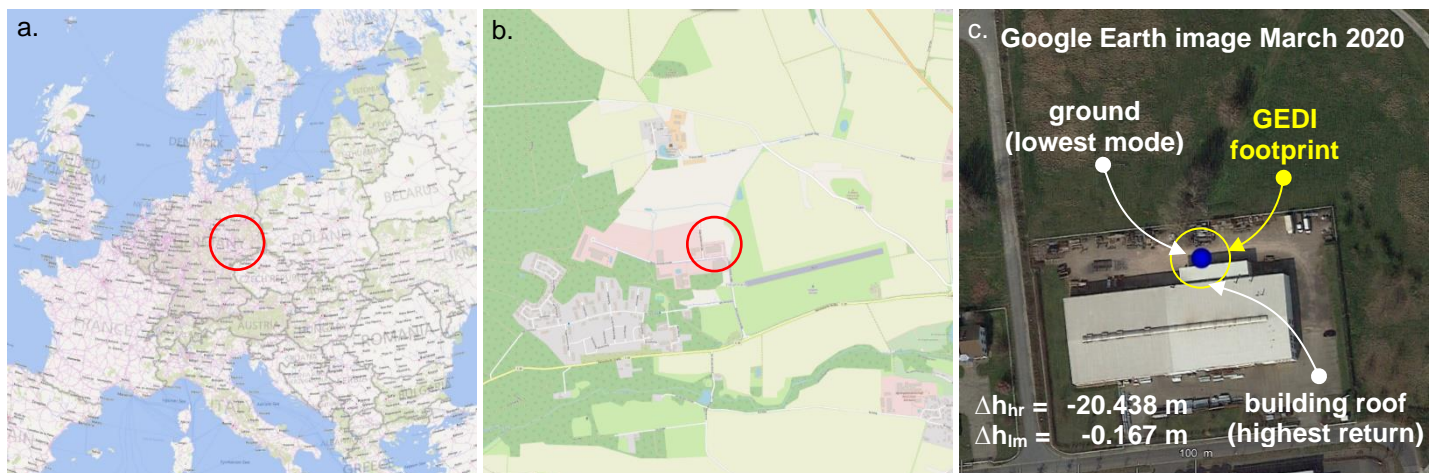


Figure 70 - EEA-10 - GEDI height differences – Case of an industrial building in Striesa (Germany).

As illustrated in Figure 70, the footprint of the GEDI acquisition covers both ground and the roof of a building. As a consequence, the GEDI lowest mode and highest return elevations highly differ. In this case, the Copernicus DEM EEA-10 height is closer to the lowest mode elevation (-0.167 metres of difference) than to the highest return of GEDI (-20.438 metres of difference).

4.4.5 Assessment of Copernicus DEM GLO-30 from GEDI data

4.4.5.1 Spatial extent

Spatial extent of the Copernicus DEM GLO-30 is given in section 4.2.5.1.

Copernicus DEM GLO-30 is only assessed in the $[-51.6^\circ, 51.6^\circ]$ latitude interval, as GEDI acquisitions are restricted to this geographical extent due to the orbit of the ISS.

4.4.5.2 Method and notations

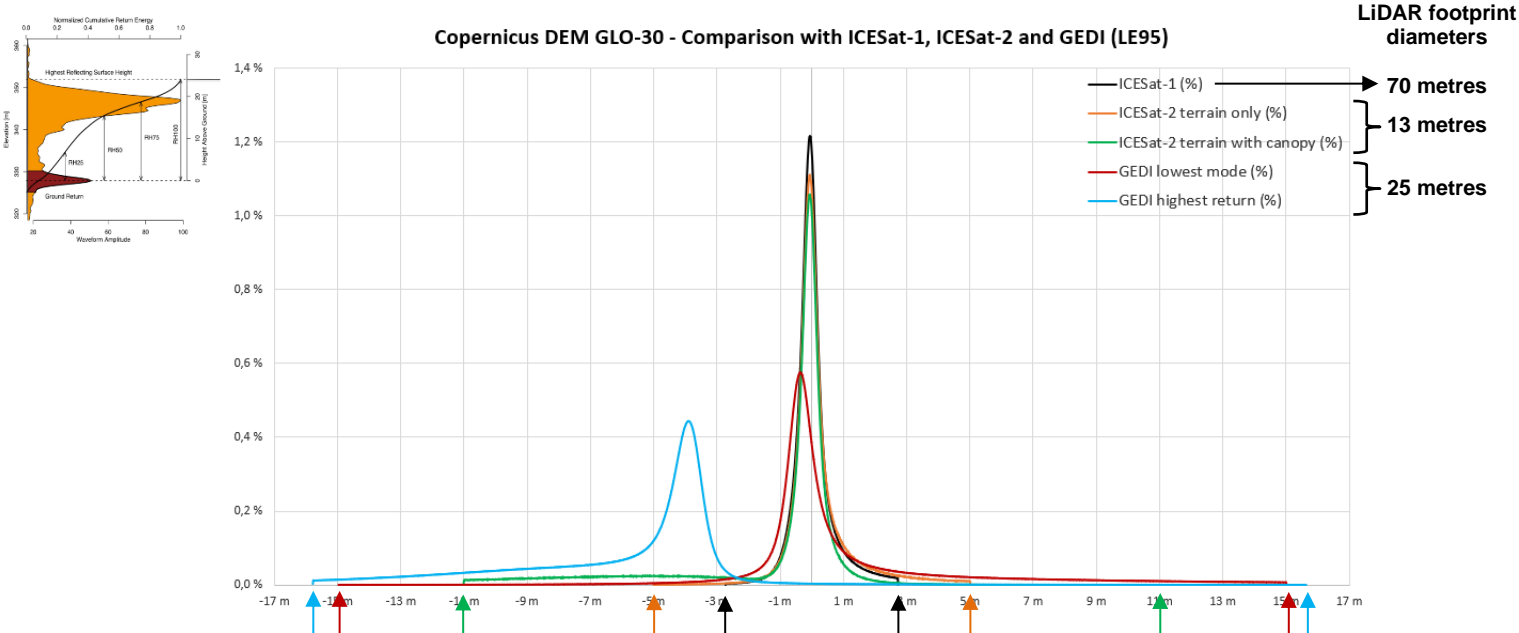
The methodology used is the same as the one for the assessment of Copernicus DEM EEA-10 from GEDI (see section 4.4.4.1).

4.4.5.3 Results

Here are the results of the **Copernicus DEM GLO-30 – GEDI** study. The results obtained in this study are compared with results obtained in the **Copernicus DEM GLO-30 – ICESat-1** and **Copernicus DEM GLO-30 – ICESat-2** studies. Statistics have been computed for two types of heights, respectively considering the lowest mode and highest return elevations of GEDI02_A products. All the statistics are computed with a 95% linear error (**LE95**). The following table summarizes the results of these studies:

LE95 statistics	ICESat-1	ICESat-2 (terrain only)	ICESat-2 (terrain with canopy)	GEDI (lowest mode)	GEDI (highest return)
Number of compared heights	59 319 279	13 816 724	13 816 724	208 487 940	208 487 940
Min	-2,725 m	-5,012 m	-11,008 m	-14,970 m	-15,780 m
Max	2,725 m	5,012 m	11,008 m	15,010 m	15,640 m
Mean (metres)	0,033 m	0,195 m	-1,124 m	1,088 m	-5,840 m
Standard deviation (metres)	0,627 m	0,979 m	2,680 m	3,472 m	3,304 m
RMSE (metres)	0,628 m	0,999 m	2,907 m	3,639 m	6,710 m
Skewness	0,943	1,667	-1,953	1,759	-0,663
Kurtosis	3,594	6,085	3,318	3,937	2,147

Table 24 - Error statistics of the (Copernicus DEM GLO-30 - GEDI) study, comparison with previous results using ICESat-1 and ICESat-2 as vertical references.



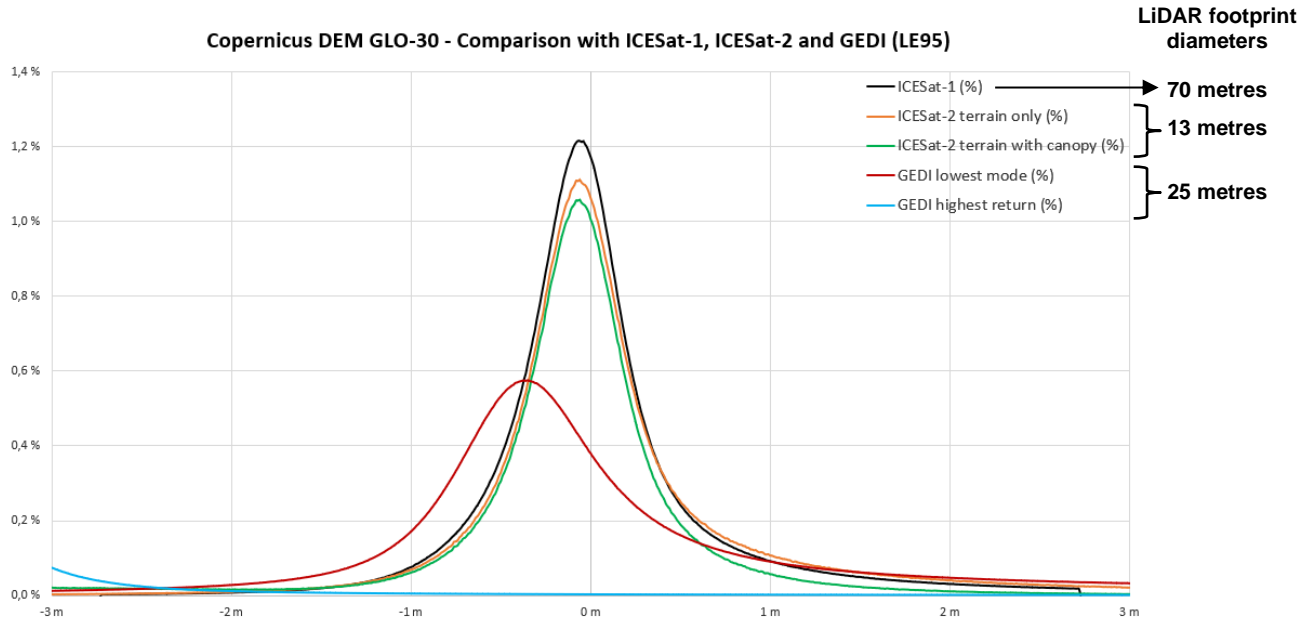


Figure 71 - Error histogram of the (Copernicus DEM GLO-30 - GEDI) study, comparison with previous results using ICESat-1 and ICESat-2 as vertical references.

The histogram and the statistics show better results using GEDI lowest mode than using GEDI highest return as a vertical reference. As a consequence, Copernicus DEM GLO-30 heights are closer to GEDI lowest mode (ground return) than to GEDI highest return (top of canopy return). Here, a difference of a few metres (algebraic mean difference of 6.928 m) can be observed between the modes of the Copernicus DEM GLO-30 – GEDI lowest mode and the Copernicus DEM GLO-30 – GEDI highest return modes. This difference is linked to the GEDI02_A product, for which every valid acquisition has a different lowest mode and highest return elevations (see section 4.4.3.1.2 for further details). Considering ICESat-1 reference data still gives the best results, retrieving a mean, standard deviation and RMSE of respectively 0.033 metres, 0.627 metres and 0.628 metres. Considering GEDI highest return reference data gives the worst results for both mean height error and RMSE, respectively reaching -5.840 metres and 6.710 metres. The worst standard deviation is obtained using GEDI lowest mode as reference data, reaching 3.472 metres.

4.4.6 Assessment of Copernicus DEM GLO-90 from GEDI data

4.4.6.1 Spatial extent

Spatial extent of the Copernicus DEM GLO-90 is given in section 4.2.6.1.

Copernicus DEM GLO-90 is only assessed in the $[-51.6^\circ, 51.6^\circ]$ latitude interval, as GEDI acquisitions are restricted to this geographical extent due to the orbit of the ISS.

4.4.6.2 Method and notations

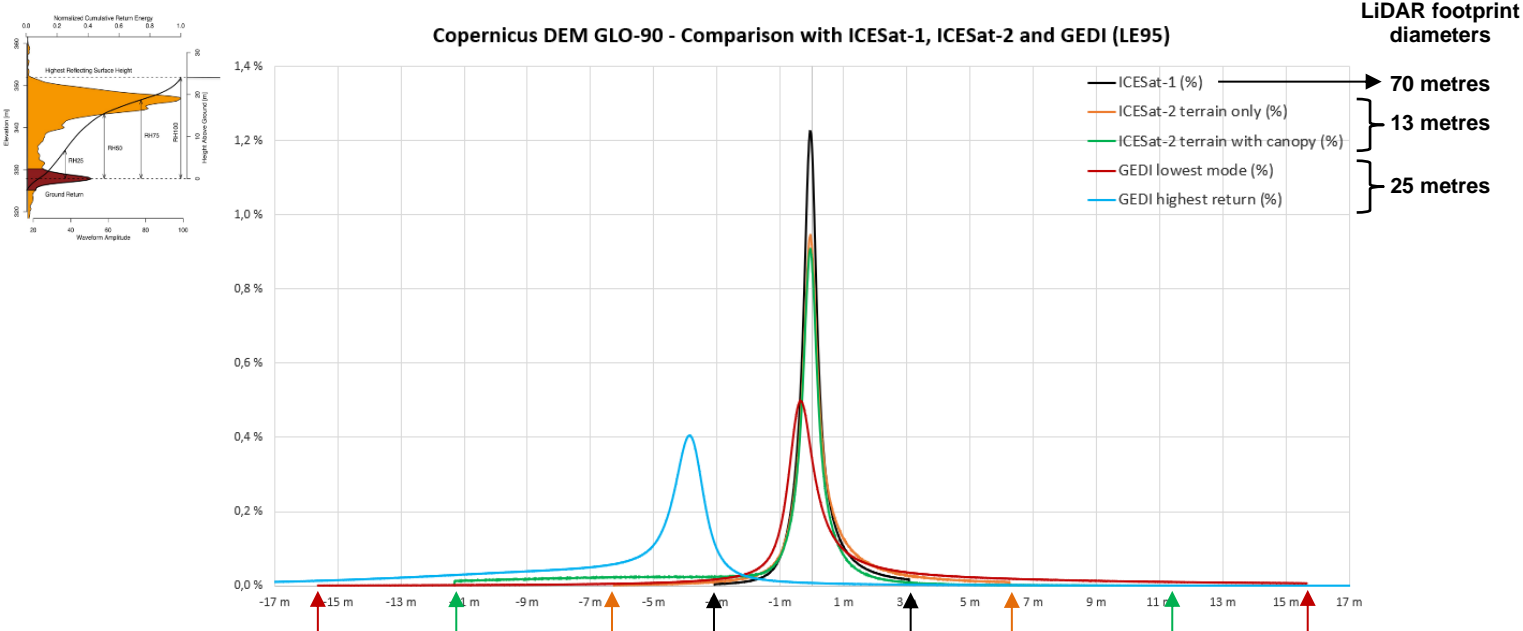
The methodology used is the same as the one for the assessment of Copernicus DEM EEA-10 from GEDI (see section 4.3.4.1).

4.4.6.3 Results

Here are the results of the **Copernicus DEM GLO-90 – GEDI** study. The results obtained in this study are compared with results obtained in the **Copernicus DEM GLO-90 – ICESat-1** and **Copernicus DEM GLO-90 – ICESat-2** studies. Statistics have been computed for two types of heights, respectively considering the lowest mode and highest return elevations of GEDI02_A products. All the statistics are computed with a 95% linear error (**LE95**). The following table summarizes the results of these studies:

LE95 statistics	ICESat-1	ICESat-2 (terrain only)	ICESat-2 (terrain with canopy)	GEDI (lowest mode)	GEDI (highest return)
Number of compared heights	59 396 074	13 838 239	13 838 239	208 436 657	208 436 657
Min	-3,015 m	-6,256 m	-11,308 m	-15,630 m	-17,200 m
Max	3,015 m	6,256 m	11,308 m	15,660 m	17,060 m
Mean (metres)	0,066 m	0,271 m	-1,102 m	1,098 m	-5,748 m
Standard deviation (metres)	0,706 m	1,391 m	2,898 m	3,881 m	3,793 m
RMSE (metres)	0,709 m	1,417 m	3,100 m	4,034 m	6,887 m
Skewness	0,793	0,919	-1,587	1,198	-0,503
Kurtosis	3,600	4,759	2,841	3,325	2,294

Table 25 - Error statistics of the (Copernicus DEM GLO-90 - GEDI) study, comparison with previous results using ICESat-1 and ICESat-2 as vertical references.



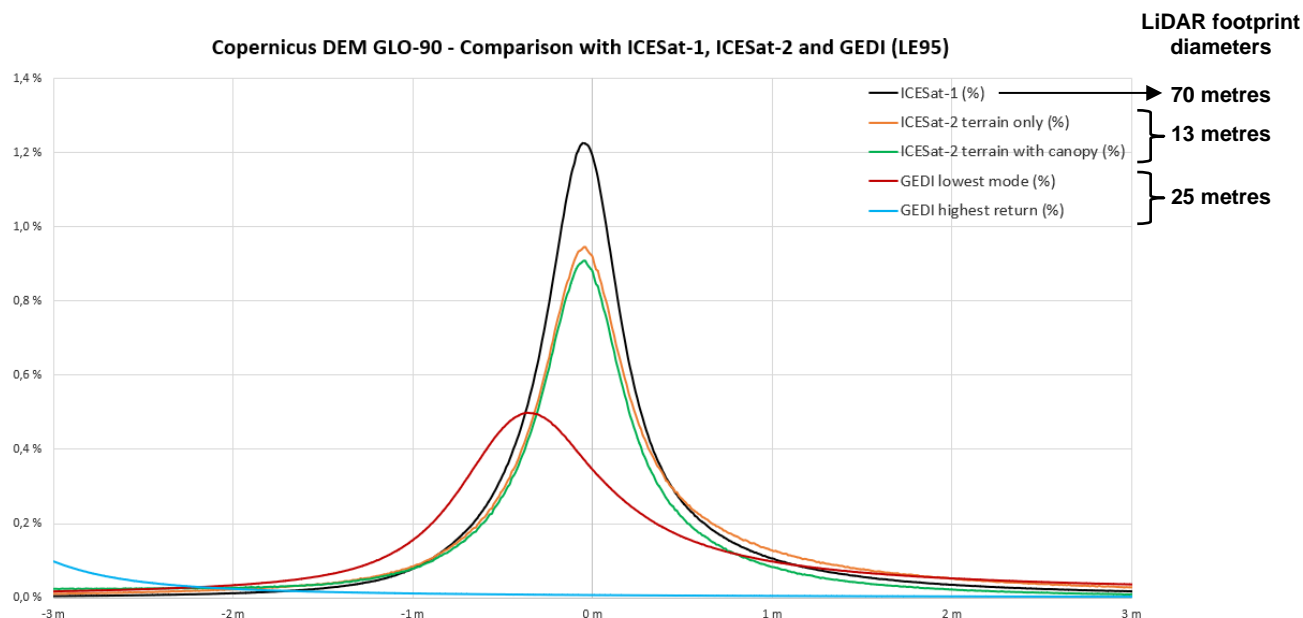


Figure 72 - Error histogram of the (Copernicus DEM GLO-90 - GEDI) study, comparison with previous results using ICESat-1 and ICESat-2 as vertical references.

The histogram and the statistics show better results using GEDI lowest mode than using GEDI highest return as a vertical reference. As a consequence, Copernicus DEM GLO-90 heights are closer to GEDI lowest mode (ground return) than to GEDI highest return (top of canopy return). Here, a difference of a few metres (algebraic mean difference of 6.846 m) can be observed between the modes of the Copernicus DEM GLO-90 – GEDI lowest mode and the Copernicus DEM GLO-90 – GEDI highest return modes. This difference is linked to the GEDI02_A product, for which every valid acquisition has a different lowest mode and highest return elevations (see section 4.4.3.1.2 for further details). Considering ICESat-1 reference data still gives the best results, retrieving a mean, standard deviation and RMSE of respectively 0.066 metres, 0.706 metres and 0.709 metres. Considering GEDI highest return reference data gives the worst results for both mean height error and RMSE, respectively reaching -5.748 metres and 6.887 metres. The worst standard deviation is obtained using GEDI lowest mode as reference data, reaching 3.881 metres.

5. CONCLUSIONS

5.1 Mission / product assessment overview

5.1.1 Comparing the “FAIR”

As indicated in section 3.2.1, VisioTerra has introduced an individual notation of the four FAIR principles to assess a global notation more traceable. Table below summarizes these notations comparing the capabilities of Copernicus DEMs with those of the other global DEMs.

	Findable /4	Accessible /3	Interoperable /3	Reusable /4	FAIR /14
SRTM	3	3	1.5	3	10.5
ASTER GDEM	3	3	2	3	11
ALOS World 3D	4	3	1.5	4	12.5
Copernicus DEMs	4	3	3	4	14

Table 26 - Comparison of the detailed FAIR notations.

The Copernicus DEMs fully meet the FAIR principles and are given the best FAIR note among tested DEMs.

5.1.2 Features of Copernicus DEMs compared to other global DEMs

Copernicus DEMs and the three other DEMs have many common features:

- **CRS** - they are expressed in the same “Geographic CRS” that sacrifices the deformations at higher latitudes but is simple to describe.
- **GSD** – the ground sampling distance (size of pixels) is 1” (1 arc-second) matching approximately 30 metres along equator but tending to 0 metres of width when getting closer to the poles.
- **VRS** – the vertical reference system is a geoid model and not an ellipsoid. This is certainly due to the fact that sea-level altitudes have a value 0 above the geoid and this is that users are expecting. One may nevertheless deplore the fact that EGM96 has been chosen and not a more recent Earth gravity model like EGM2008 for the latest versions of the geoid.

DEM	version	mode ⁽¹⁾	observation interval	CRS ⁽²⁾	GSD ⁽³⁾	extents	VRS ⁽⁴⁾
SRTM GL1	3.0 (2015)	IF	11 Feb.2000 - 22 Feb.2000	Geo.	1”	56°S – 60°N	EGM96
ASTER GDEM	2.0 (2011)	PG	Dec.1999 - Feb.2011	Geo.	1”	Global	EGM96
ALOS World 3D	2.2 (Apr.2019)	PG	2006 - 2011	Geo.	1”	Global	EGM96
Copernicus DEMs	2019 v1	IF	2010 - 2015	Geo.	0.4” 1” 3”	Europe Global	EGM2008

- (1) mode IF: interferometry – PG: photogrammetry
 (2) CRS Coordinates Reference System – “Geo” for Geographic ([EPSPG:4326](https://epsg.org/EPSPG:4326)).
 (3) GSD Ground Sampling Distance (size of the pixel)
 (4) VRS Vertical Reference System – EGM: Earth Gravity Model (or geoid).

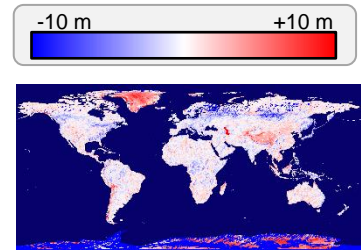
Table 27 - DEM features.

5.2 Detailed assessment

5.2.1 Intercomparison of DEMs (qualitative assessment)

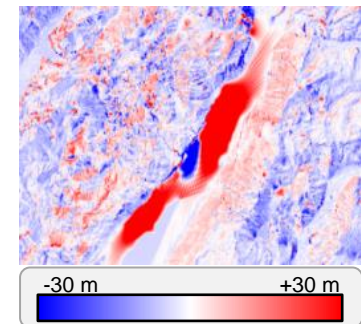
By computing on-the-fly the difference between two DEMs, one may perform a qualitative assessment to very easily detect defects both at global scale and at large scale:

- **Global scale** - comparison between “ALOS World 3D” (best DEM against SRTMGL1 and ASTER GDEM) and “Copernicus DEM GLO-30” shows defects at high latitudes and along the mountainous chains...
- **Large scale** – local differences are observed that could be due to the difference of ice or snow heights between the acquisition dates, or change of mine depths, or changes of land covers, landslides...



By computing on-the-fly the difference between two DEMs at any scale, one may immediately detect artefacts in few views. The sign and magnitude of the difference often enables to guess which DEM contains the artefact.

Depending on the scales, the height variations (roughness) of the landscapes change. For low-scale views (large extents of a region), the relief is smoothed by the pyramidal organisation of the layer and the rendering shall be strongly stretched (for example in the range [-10m;+10m] in the upper attached figure). At high-scale (small extent or zoomed view), variations are more apparent and the stretching may be released (for example in the range [-30m;+30m] as shown in the lower attached figure).



5.2.2 Copernicus DEMs height comparison with ICESat-1, ICESat-2 and GEDI (quantitative assessment)

Five quantitative studies are performed in order to assess the quality of the three Copernicus DEMs, respectively using ICESat-1, ICESat-2 terrain heights only, ICESat-2 terrain with canopy heights, GEDI lowest mode elevation and GEDI highest return elevation. This section provides a summary of the results obtained in the quantitative assessments of this technical note.

5.2.2.1 ICESat-1, ICESat-2 and GEDI: technical specifications

The Copernicus DEMs are assessed using reference heights from ICESat-1, ICESat-2 and GEDI missions. The characteristics of these missions are compared and summarized in the following table.

Technical specification	ICESat-1	ICESat-2	GEDI
Instrument name	Geoscience Laser Altimeter System (GLAS)	Advanced Topographic Laser Altimeter System (ATLAS)	Global Ecosystem Dynamics Investigation (GEDI)
First acquisition date	02.20.2003	13.10.2018	25.03.2019
Last acquisition date	11.10.2009	Ongoing	Ongoing
Acquisition frequency	40 Hz	10 KHz	242 Hz
Ground sampling distance	~170 m	~0.7 m	~60 m
Central wavelength	532 nm (green) / 1064 nm (near infrared)	532 nm (green)	1064 nm (near infrared)
Number of beams	1	6	8
Repeat cycle	Phase 1 – 8 days – [20/02/2003; 04/10/2003] Phase 2 – 91 days – [04/10/2003; 11/10/2009]	91 days	No repeat cycle
Footprint diameter	~70 m	~13 m	~25 m

Table 28 - Technical specifications of ICESat-1, ICESat-2 and GEDI missions.

The GLAH14 product of the ICESat-1 mission, the ATL08 product of the ICESat-2 mission and the GEDI02_A product of the GEDI mission are used as vertical references in the quantitative studies. The results of the quantitative studies considering ICESat-1, ICESat-2 and GEDI products as vertical references are shown and discussed hereafter in next section 5.2.2.2.

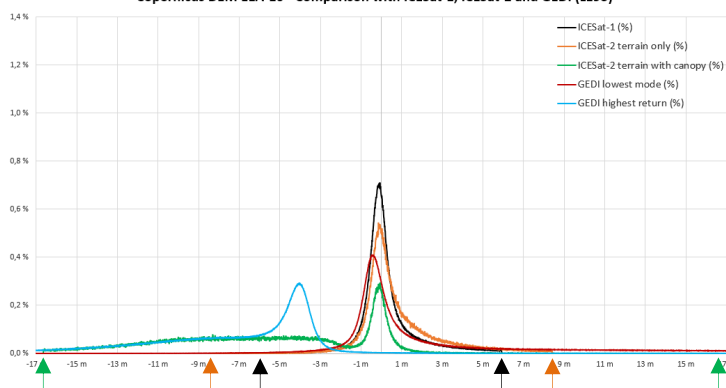
5.2.2.2 Results of the EEA-10, GLO-30 and GLO-90 quantitative assessments

The LE95 height error statistics of Copernicus DEM EEA-10, Copernicus DEM GLO-30 and Copernicus DEM GLO-90 are summarized in the following table and histograms.

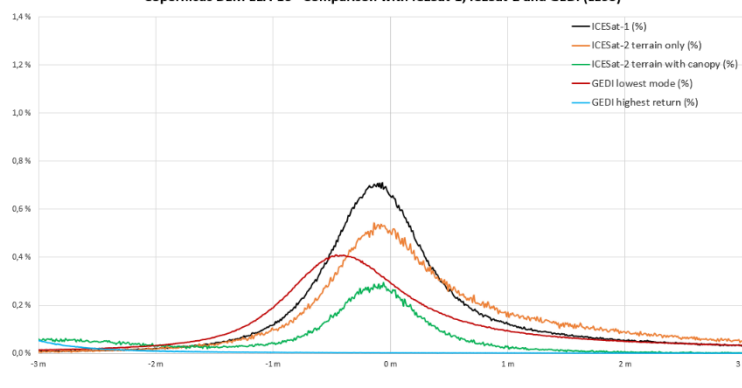
Copernicus DEM instance	Reference heights	Count	Min	Max	Mean	Standard Deviation	RMSE	Skewness	Kurtosis
EEA-10	ICESat-1	1 803 551	-5,924 m	5,924 m	0,270 m	1,389 m	1,415 m	1,091	3,797
	ICESat-2 terrain only	399 179	-8,415 m	8,421 m	0,822 m	1,944 m	2,111 m	1,283	2,823
	ICESat-2 terrain with canopy	399 179	-16,642 m	16,600 m	-5,477 m	4,838 m	7,307 m	0,251	-0,777
	GEDI lowest mode	11 263 632	-20,090 m	20,150 m	2,363 m	5,277 m	5,782 m	1,610	2,031
	GEDI highest return	11 263 634	-17,780 m	17,600 m	-6,916 m	3,968 m	7,973 m	-0,218	2,017
GLO-30	ICESat-1	59 319 279	-2,725 m	2,725 m	0,033 m	0,627 m	0,628 m	0,943	3,594
	ICESat-2 terrain only	13 816 724	-5,012 m	5,012 m	0,195 m	0,979 m	0,999 m	1,667	6,085
	ICESat-2 terrain with canopy	13 816 724	-11,008 m	11,008 m	-1,124 m	2,680 m	2,907 m	-1,953	3,318
	GEDI lowest mode	208 487 940	-14,970 m	15,010 m	1,088 m	3,472 m	3,639 m	1,759	3,937
	GEDI highest return	208 487 940	-15,780 m	15,640 m	-5,840 m	3,304 m	6,710 m	-0,663	2,147
GLO-90	ICESat-1	59 396 074	-3,015 m	3,015 m	0,066 m	0,706 m	0,709 m	0,793	3,600
	ICESat-2 terrain only	13 838 239	-6,256 m	6,256 m	0,271 m	1,391 m	1,417 m	0,919	4,759
	ICESat-2 terrain with canopy	13 838 239	-11,308 m	11,308 m	-1,102 m	2,898 m	3,100 m	-1,587	2,841
	GEDI lowest mode	208 436 657	-15,630 m	15,660 m	1,098 m	3,881 m	4,034 m	1,198	3,325
	GEDI highest return	208 436 657	-17,200 m	17,060 m	-5,748 m	3,793 m	6,887 m	-0,503	2,294

Table 29 - Copernicus DEM EEA-10, GLO-30 and GLO-90 LE95 height errors statistics.

Copernicus DEM EEA-10 - Comparison with ICESat-1, ICESat-2 and GEDI (LE95)

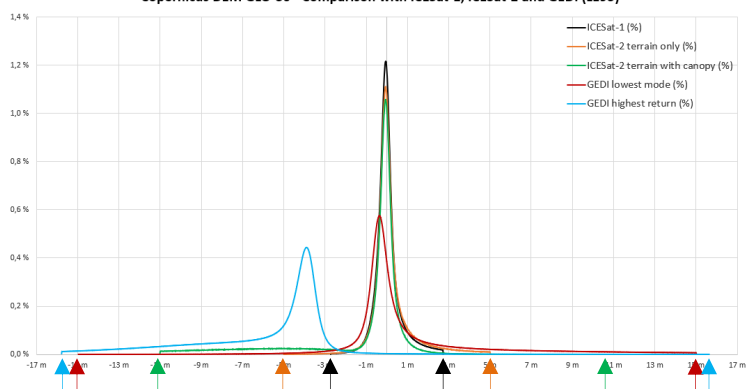


Copernicus DEM EEA-10 - Comparison with ICESat-1, ICESat-2 and GEDI (LE95)



**Figure 73 - Copernicus DEM EEA-10 height error histogram
from -17 m to 17 m (left) – from -3 m to 3 m (right).**

Copernicus DEM GLO-30 - Comparison with ICESat-1, ICESat-2 and GEDI (LE95)



Copernicus DEM GLO-30 - Comparison with ICESat-1, ICESat-2 and GEDI (LE95)

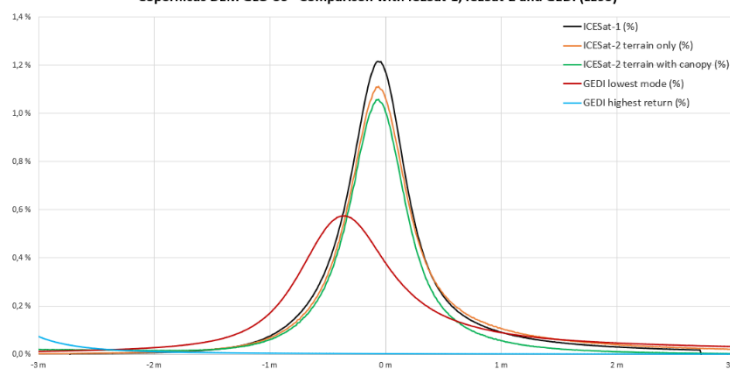
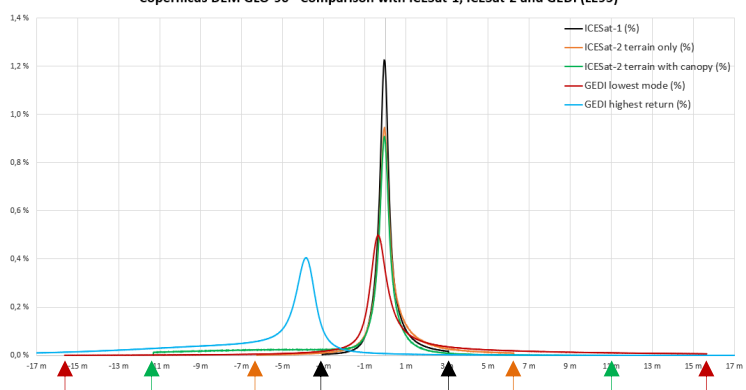


**Figure 74 - Copernicus DEM GLO-30 height error histogram
from -17 m to 17 m (left) – from -3 m to 3 m (right).**

Copernicus DEM GLO-90 - Comparison with ICESat-1, ICESat-2 and GEDI (LE95)



Copernicus DEM GLO-90 - Comparison with ICESat-1, ICESat-2 and GEDI (LE95)

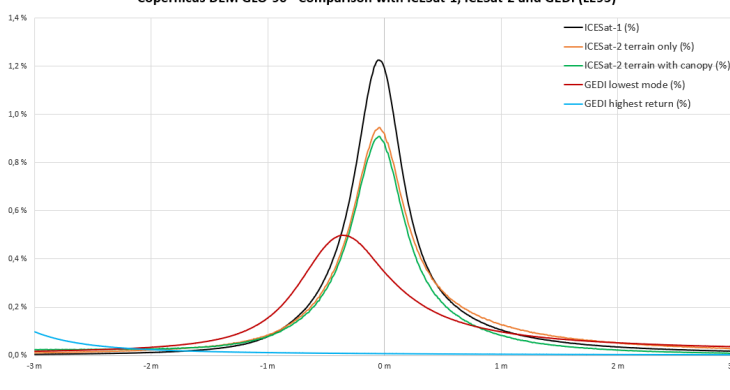


**Figure 75 - Copernicus DEM GLO-90 height error histogram
from -17 m to 17 m (left) – from -3 m to 3 m (right).**

The height error statistics of Table 23 show that the Copernicus DEM GLO-30 has the lowest mean (0.033 metres), standard deviation (0.627 metres) and RMSE (0.628 metres) of all the quantitative studies (ICESat-1 quantitative study). The Copernicus DEM GLO-90 shows similar height error statistics, with a mean of 0.066 metres, a standard deviation of 0.706 m and a RMSE of 0.709 metres (ICESat-1 quantitative study). The worst results are obtained with Copernicus DEM EEA-10, for which the height error statistics result in a mean of 0.270 metres, a standard deviation of 1.389 metres and a RMSE of 1.415 metres (ICESat-1 quantitative study). These results are also visible on the height error histograms, for which the Copernicus DEM GLO-30 and Copernicus DEM GLO-90 obtain similar distributions with a low standard deviation. The Copernicus DEM EEA-10 height error histogram

differs from this distribution, with a lower mode and a greater standard deviation. The same ranking applies for the ICESat-2 terrain only, ICESat-2 terrain with canopy, GEDI lowest mode and GEDI highest return quantitative studies. Among the three DEMs, according to these quantitative studies, **Copernicus DEM GLO-30** obtains the best statistics. Further studies are followed in section 5.2.2.3, for which Copernicus DEM EEA-10, GLO-30 and GLO-90 are compared over the EEA-10 geographical extent.

The height error statistics also show that using ICESat-1 as a vertical reference gives the best results for every instance of the Copernicus DEM assessed. Relatively similar results are obtained with ICESat-2 terrain heights only. Worse results are obtained considering ICESat-2 terrain with canopy, which is depicted in the histogram by a large number of negative errors. The height error may increase accounting ICESat-2 canopy heights, as these canopy heights are only estimations (see sections 4.3.4.4.1 and 4.3.4.4.2 for further explanations). For the three DEMs, GEDI lowest mode obtains the highest height error standard deviation, and GEDI highest return obtains the highest absolute mean and RMSE. As a consequence, the recommended reference data is the **GLAH14 product of ICESat-1**, which gives the best results for all the quantitative studies. Such conclusion could be due to the fact that Copernicus DEM has been validated from ICESat-1 data (see RD-15).

5.2.2.3 Comparison of EEA-10, GLO-30 and GLO-90 over Europe

In this section, the EEA-10, GLO-30 and GLO-90 DEMs height error statistics are compared (linear error at 95% statistics). These height errors are computed using ICESat-1 data as a reference (see section 4.2). The goal of this study is to compare the EEA-10, GLO-30 and GLO-90 products on the EEA-10 product's geographical extent (Europe continent and worldwide European islands).

The following statistics show the results of this study.

	EEA-10 – ICESat-1	GLO-30 – ICESat-1	GLO-90 – ICESat-1
Number of heights compared	1 803 551		
Min	-5,924 m	-5,460 m	-5,289 m
Max	5,924 m	5,460 m	5,289 m
Arithmetic mean (metres)	0.270°m	0.297°m	0.351°m
Standard deviation (metres)	1.389°m	1.264°m	1.339 m
RMSE (metres)	1.415 m	1.298 m	1.384 m

Table 30 - Copernicus DEM EEA-10, GLO-30 and GLO-90 height errors statistics over Europe.

In section 4.2, EEA-10, GLO-30 and GLO-90 were compared to ICESat-1 data over their respective geographical extent (whole globe for GLO-30 and GLO-90, only Europe for EEA-10). Despite having a better spatial resolution, the EEA-10 product has shown worse height error statistics than the GLO-30 and GLO-90 products (see Table 10, Table 11, and Table 9). Height error statistics of each DEM over Europe are really close. Consequently, EEA-10 height errors statistics are worse than the global statistics of GLO-30 and GLO-90 mostly because of its geographical extent.

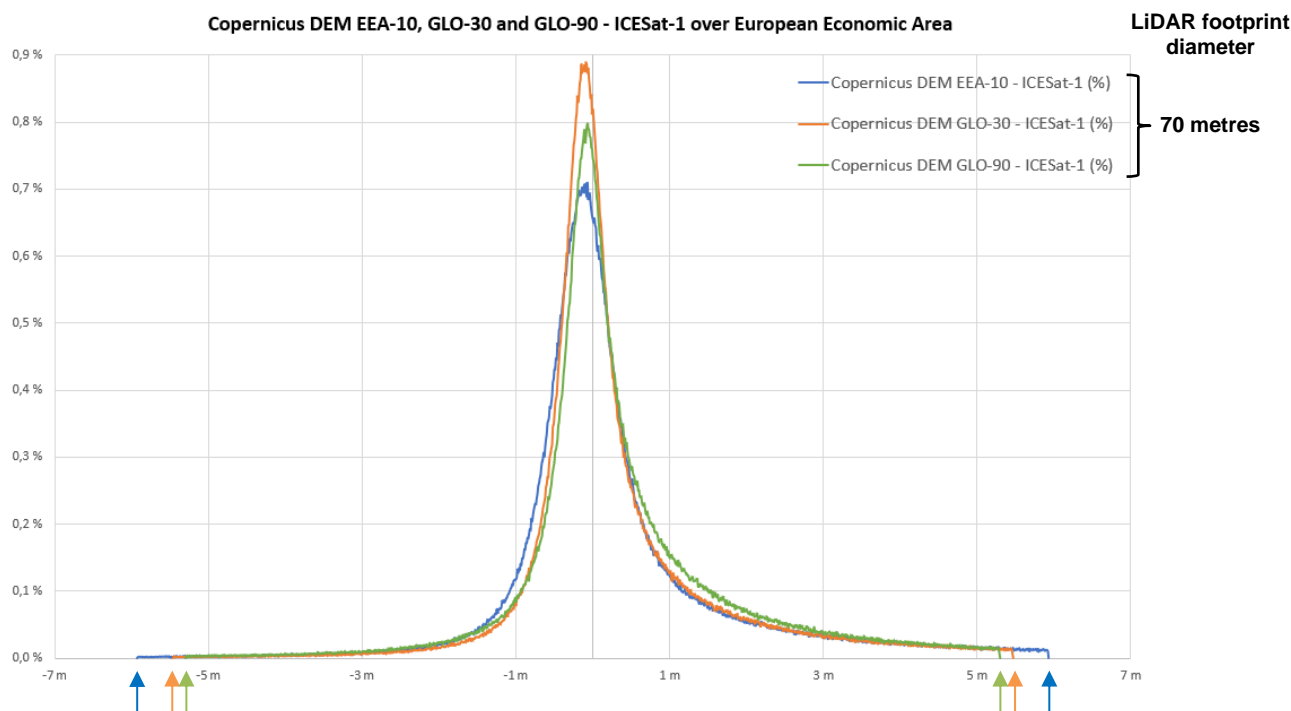


Figure 76 - Copernicus DEM EEA-10, GLO-30 and GLO-90 height errors histogram over Europe.

The height error histogram of the EEA-10, GLO-30 and GLO-90 products also show similar error distributions. It must be noticed that the EEA-10 product still performs worse than GLO-30 and GLO-90. This difference may be linked to ICESat-1's footprint diameter of 70 m, which is 7 times the 10 metres resolution of Copernicus DEM EEA-10 at equator.

5.2.2.4 Comparison of GLO-30 vs. SRTM, ASTER-GDEM and ALOS World 3D

In this section, the Copernicus DEM GLO-30 error statistics are compared to other global DEM statistics. The table here after sums up the quantitative assessment of the GLO-30 DEM, SRTM, ASTER GDEM and ALOS World 3D with regard to the ICESat-1 and ICESat-2 reference data (LE95).

LE95 statistics	Reference data	Number of heights compared	Arithmetic mean (metres)	Standard deviation (metres)	RMSE (metres)	Median (metres)
SRTMGL1	ICESat-1	57 152 763	-0.561 m	2.491 m	2.554 m	-0.60 m
ASTER GDEM	ICESat-1	88 267 823	-2.709 m	7.432 m	7.911 m	-2.62 m
ALOS World 3D	ICESat-1	57 968 266	-0.151 m	1.653 m	1.660 m	-0.15 m
Copernicus DEM GLO-30	ICESat-1	59 319 279	<u>0.033 m</u>	<u>0.627°m</u>	<u>0.628°m</u>	0.04 m
	ICESat-2 terrain only	13 816 724	0.195 m	0.979 m	0.999 m	<u>-0.01 m</u>
	ICESat-2 terrain with canopy	13 816 724	-1.124 m	2.680 m	2.907 m	0.14 m
	GEDI lowest mode	208 487 940	1,088 m	3,472 m	3,639 m	-0.10 m
	GEDI highest return	208 487 940	-5,840 m	3,304 m	6,710 m	-4.51 m

Table 31 - Quantitative assessment of GLO-30 compared to other global DEMs.

The statistics tend to show that Copernicus DEM GLO-30 is the most accurate DEM among those being assessed. This is also highlighted by comparing the height error histograms of each DEM.

The following histogram shows the distribution of the four qualified DEMs in percentage of occurrence (LE95). One can see the distribution of:

- **SRTMGL1 – ICESat-1** in orange,
- **ASTER GDEM – ICESat-1** in blue,
- **ALOS World 3D – ICESat-1** in purple,
- **Copernicus DEM GLO-30 – ICESat-1** in black,
- **Copernicus DEM GLO-30 – ICESat-2 terrain only** in yellow,
- **Copernicus DEM GLO-30 – ICESat-2 terrain with canopy** in green,
- **Copernicus DEM GLO-30 – GEDI lowest mode** in red,
- **Copernicus DEM GLO-30 – GEDI highest return** in cyan.

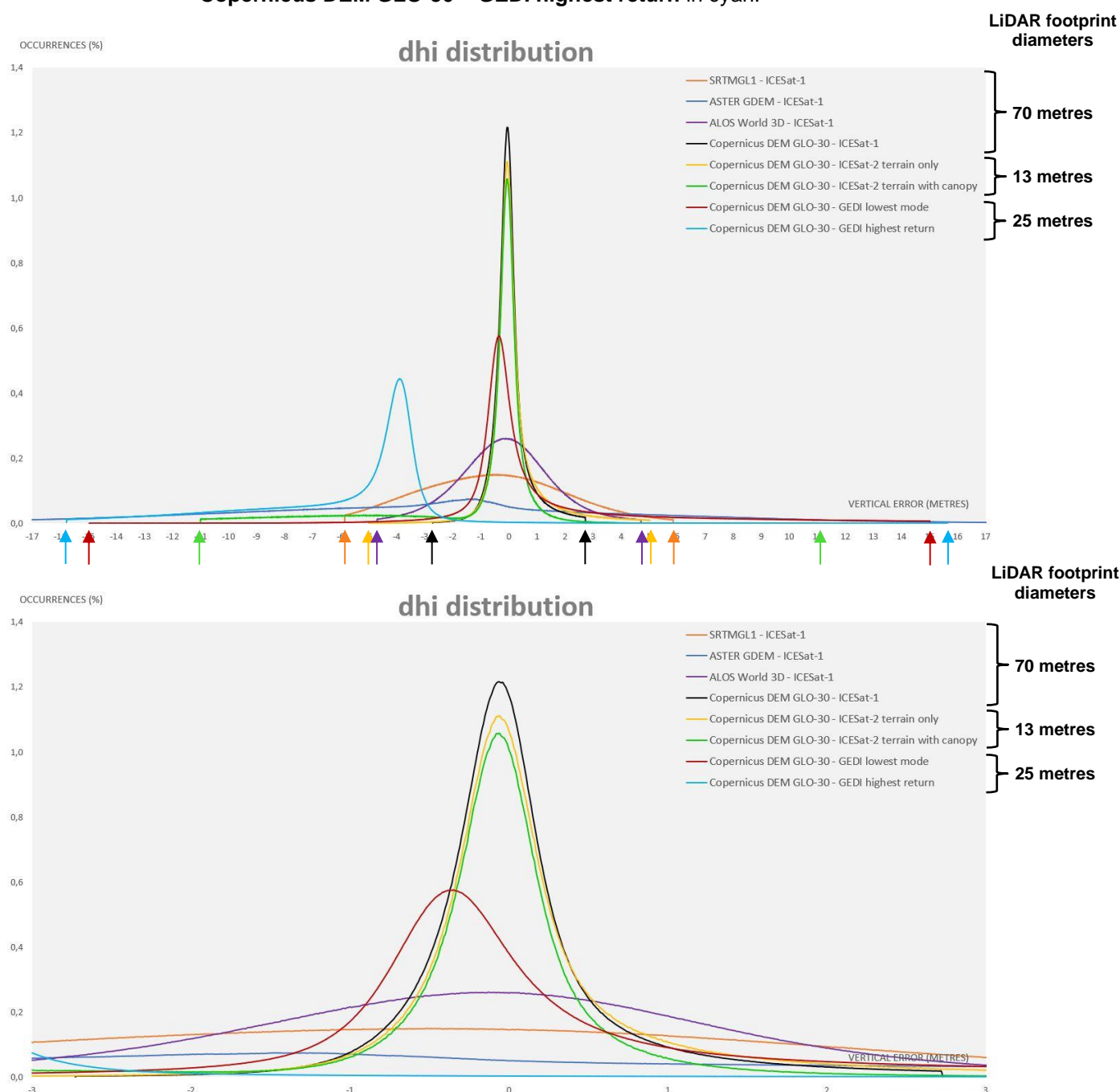


Figure 77 - Histogram of height differences between ICESat-1/ICESat-2 and global DEMs (LE95).

The height error histograms of the (Copernicus DEM GLO-30 – ICESat-1) and (Copernicus DEM GLO-30 – ICESat-2 terrain only) quantitative studies show that Copernicus DEM GLO-30 significantly outperforms SRTMGL1, ASTER GDEM and ALOS World 3D in terms of **precision**. Even for the (Copernicus DEM GLO-30 – GEDI lowest mode) histogram, one may observe a higher mode than those of the other global DEMs. The (Copernicus DEM GLO-30 – ICESat-2 terrain with canopy) errors seems to follow the distribution of the other Copernicus DEM GLO-30 studies, but the tail of distribution is longer due to the introduction of the ICESat-2 estimated canopy height. Most of the (Copernicus DEM GLO-30 – GEDI highest return) errors are negative, showing that Copernicus DEM GLO-30 is closer to GEDI lowest mode (ground return) than to GEDI highest return (top of canopy return).

According to this study, **Copernicus DEM GLO-30** shows the best **accuracy** with the lowest arithmetic mean (0.033°m). The same applies for the best standard deviation (0.627°m) and RMSE (0.628°m) when compared to ICESat-1 reference data.